

**An Integrated DNA Selection in Micro-flow Reactors as an Approach
for Molecular Computation and Diagnostics**

Scientific book

by

Robert Dimitrov Penchovsky

based on his doctoral thesis from the University of Cologne, Germany

Sofia, Bulgaria

2019

An Integrated DNA Selection in Micro-flow Reactors as an Approach for Molecular Computation and Diagnostics

by Robert D. Penchovsky

Copyright © 2019 Robert D. Penchovsky. All rights reserved.

ISBN (online): 978-619-91360-0-1

Editor: Prof. Dr. Jonathan Howard

Reviewers: Prof. Dr. Jonathan Howard

Prof. Dr. Diethard Tautz

Prof. Dr. Hans-Günter Schmalz

all from Cologne University, Germany

To my mother: many thanks.

In memory of my recently dead grandfather who managed to outlive the Bulgarian Communism.

Let all things be done decently and in order. Bible, I Corinthians 14:40.

Acknowledgments

I would like to thank Prof. Dr. Jonathan Howard for the constant support, editing the text, and for many helpful discussions, including very helpful proposals upon choosing of buffering solutions for the DNA hybridisation transfer under isothermal conditions.

I also wish to thank Dr. Eckhard Birch-Hirschfeld for helpful discussions on DNA immobilisation chemistry and Dr. Jorg Ackermann for helpful discussions on the DNA library design.

ABSTRACT

As a result of Adleman's original work in 1994, the floodgates of DNA computing were released. Since then, a few insightful researchers are working to bridge the gap between molecular biology and computing theory in order to build a practical DNA or RNA based computer. The research undertaken on the feasibility of DNA and RNA based computers provoked a critical evaluation of the currently available tools of molecular biology for their potential for molecular computation. Thus, an opportunity arose for a new insight into some of the essential bio-molecular processes such as DNA selection, ligation, amplification, and self-assembly. The developing of on-chip biotechnology is a shared ground between DNA and RNA based diagnostics and computing. This is because owing both applications require a high degree of automation and integration of a great number of molecular processes in parallel.

In this thesis, the results are reported of the development of a novel approach to an automated and integrated multi-step DNA selection employing micro-fluidic bead-based selection modules. The approach is based on a proposed novel micro-fluidic design, and a novel reversible chemistry for multi-step DNA hybridisation transfer under isothermal conditions. The micro-fluidic design allows a programmed attachment in parallel of different DNA oligomers (or other bio-molecules) to beads incorporated in cascably connected micro-reactors, by separated delivery of the DNA oligomers and cross-linking reagent. The use of an inhibition step (by a pH change) of the DNA immobilisation upon mixing in crossing micro-channels guarantees a high level of specificity in addressing beads placed in cascably connected chambers with different DNA sequences. The pH-reversible approach to sequence-specific DNA transfer allows a multi-step selection from a complex pool of different DNA molecules in cascably connected micro-flow reactors, achieved either by a pH change of the pumped solutions or, in steady flow conditions, by moving magnetic beads through solutions with a different pH. Performing the whole selection procedure under a constant temperature allows potentially the integration of many selection modules on a single wafer. The method avails of the fast DNA hybridisation kinetics on beads under flow conditions, and of the small sample values needed. The efficiency and fidelity of the DNA hybridisation transfer are demonstrated between two micro-fluidic selection modules. The approach is suitable for integrated applications in the fields of DNA computation and diagnostics. A twelve-bit DNA library, designed according to thermodynamic constraints, is experimentally constructed and tested using molecular biology tools. The results demonstrate a high level of specific hybridisation achieved with all library bits under identical conditions.

CONTENTS

Berichterstatter	ii
Dedications	iii
Acknowledgements	iv
Abstract	v
List of Figures	ix
List of Tables	xii
1 Introduction	1
1.1 Molecular computation and evolution	2
1.2 Molecular based diagnostics	6
1.3 Microfluidics as a common ground between DNA based computation and diagnostics.....	8
1.4 Research goals	11
2 Materials and Methods	12
2.1 Materials	12
2.1.1 Chemicals, enzymes and solutions	12
2.1.2 Nucleic acids and paramagnetic beads	14
2.1.3 Micro-flow reactors	16
2.2 Methods	19
2.2.1 Synthesis of DNA library	20
2.2.2 DNA immobilisation procedures	20
2.2.2.1 Immobilisation of amino-modified synthetic DNA to carboxyl-coated beads and inhibition of the immobilisation reaction by a pI-change	20
2.2.2.2 Cascadable DNA immobilisation to carboxyl beads placed in micro-chambers	21
2.2.2.3 Immobilisation of thiol-modified DNA to carboxyl-coated beads	22
2.2.2.4 Photo-dependent immobilisation of amino-modified DNA to amino-coated beads	23
2.2.2.5 Immobilisation of biotin-labelled DNA to streptavidin-coated beads	25
2.2.3 DNA hybridisation, denaturation and sequence specific transfer	25

2.2.3.1 DNA hybridisation analyses in solutions using a quenching system	25
2.2.3.2 DNA hybridisation and denaturation on beads in eppendorf tubes	26
2.2.3.3 DNA hybridisation and denaturation on beads under flow conditions	26
2.2.3.4 Sequence-specific DNA transfer between micro-reactor selection modules under isothermal conditions	26
2.2.4 DNA ligation, amplification and melting temperature estimation	27
2.2.5 DNA isolation, purification and concentration	28
2.2.6 DNA detection, quantification and fluorescence imaging set-up	29
2.2.6.1 DNA quantification	29
2.2.6.2 Fluorescence imaging set-up for DNA detection in micro-flow reactors	30
2.2.7 Flow stability and bead movement in micro-flow reactors	30
2.2.8 Algorithm used for DNA library design.....	32
3 Results and discussions	35
3.1 DNA immobilisation to beads	35
3.1.1 Immobilisation of amino-modified synthetic DNA to carboxyl-coated beads and inhibition of the immobilisation reaction by a pI-change. Non-specific DNA attachment	35
3.1.2 pH-dependent immobilisation of amino-modified DNA to carboxyl-coated beads placed in cascably connected micro-fluidic chambers	38
3.1.3 Immobilisation of thiol-modified DNA to carboxyl-coated beads	45
3.1.4 Photo-dependent immobilisation of synthetic DNA to amino-coated beads	47
3.1.5 Discussion	49
3.2 Fidelity of DNA hybridisation	53
3.2.1 Fidelity of DNA hybridisation in different solutions	53
3.2.2 Fidelity of DNA hybridisation on beads. Non-specific DNA attachment to beads	58
3.2.3 Discussion	66
3.3 DNA/DNA hybridisation and denaturation kinetics on beads under flow conditions	67
3.3.1 DNA/DNA hybridisation kinetics on beads under flow conditions	67
3.3.2 Kinetics and efficiency of DNA/DNA denaturation on beads	69

3.3.3 Discussion	72
3.4 Multistep DNA hybridisation transfer between micro-reactor selection modules under isothermal conditions. An integrated and automated micro-fluidic chip for bio-molecular analyses	74
3.4.1 Reversible chemistry for multi-step DNA hybridisation transfer under isothermal conditions by a pH change	74
3.4.2 Efficiency of cascable hybridisation DNA transfer between micro-reactor selection modules by a pH neutralization	76
3.4.3 DNA hybridisation transfer by moving beads in micro-chambers	81
3.4.4 An integrated and automated micro-fluidic chip for bio-molecular analyses	84
3.4.5 Discussion	90
3.5 DNA library for molecular computation in micro-flow reactors	92
3.5.1 DNA library design criteria	95
3.5.2 Assembly and amplification of the DNA library	100
3.5.3 Testing integrity and fidelity of the DNA library	102
3.5.4 Discussion	108
4 Conclusions	112
4.1 Summary of the achieved research goals	112
4.2 Applicability of micro-fluidics for molecular based computation and diagnostics	115
5 Appendix	118
5.1 Statistical analysis of experimental data	118
5.2 Abbreviations used	124
5.3 Equipment and software used	126
5.4 Deutsche Zusammenfassung	128
5.5 Erkldrung	130
5.6 Lebenslauf	131
6 References	133

LIST OF FIGURES

1 Schematic presentation of the complexity classes and their presumed relationships	3
2 Multi-step bio-molecular processing in cascadably connected selection modules	9
3 Scheme of the micro-flow reactor presenting one strand transfer module (STM) used for a single strand DNA transfer by moving beads under steady flow conditions	16
4 Scheme of the micro-flow reactor used in photo-dependent DNA immobilisation experiments	17
5 Scheme of the micro-flow reactor used in the DNA hybridisation transfer and immobilisation experiments	18
6 Synthesis of the DNA library	19
7 Scheme of immobilisation of amino-modified DNA to carboxyl-coated bead	21
8 Immobilisation scheme of thiol-modified synthetic DNA to carboxyl — coated beads by using of a heterobifunctional cross-linking reagent PDPH	23
9 Overall scheme of photo-dependent DNA immobilisation	24
10 A standard titration curve for quantification of 5' Rhodamine 6G labelled DNA	30
11 Scheme of two different set-ups for a fluorescence image acquisition in micro-flow reactors		31
12 Hybridisation analyses of 5' amino-labelled DNA immobilisation to carboxyl-coated beads		40
13 Hybridisation analyses of 5' amino-labelled DNA immobilisation to carboxyl-coated beads by sodium hydroxide and temperature denaturing	41
14 A picture of two cascadably connected micro-chambers	42
15 Inhibition of the DNA immobilisation upon mixing in cascadably connected micro-reactor chambers. Hybridisation analyses	43
16 Specific immobilisation by separate delivery of the DNA oligomer and the cross-linking reagent in cascadably connected micro-reactor chambers. Hybridisation analyses	44
17 Specific DNA immobilisation by a reversible pH change in cascadably connected micro-reactor chambers. Hybridisation analyses	45
18 DNA/DNA hybridisation analysis on 5' thiol immobilised DNA to carboxyl-coated beads		46
19 Light-dependent DNA immobilisation to beads in micro-flow reactor channels	48

20 Micro-fluidic architecture for spatially defined parallel bio-molecular immobilisation to beads incorporated in cascadably connected micro-reactor chambers or to their surfaces	50
21 Quenching efficiency of QSY-7 towards TAMRA	54
22 Estimation of DNA/DNA hybridisation yields in different buffer solutions by using of a quenching system	55
23 Estimation of hybridisation yield of DNA hybrid with two mismatches over length of 21 by using of a quenching system	56
24 A standard titration curve for quantification of 3' TAMRA labelled DNA	57
25 Scheme of DNA/DNA hybridisation fidelity analyses on beads	59
26 DNA/DNA hybridisation fidelity analyses on beads	60
27 Testing stability of the fluorescence signal of rhodamine 6G in 100 mM NaON	61
28 DNA hybridisation fidelity analyses on beads placed in a micro-flow reactor under flow conditions	62
29 Scheme of DNA/DNA hybridisation fidelity analyses on beads under flow conditions	63
30 DNA/DNA hybridisation fidelity analyses on beads placed in micro-chambers under flow conditions without washing	64
31 Scheme of DNA/DNA hybridisation analyses on beads placed in micro-chambers under flow conditions	65
32 DNA/DNA hybridisation fidelity analyses on beads placed in micro-chambers after washing	65
33 DNA/DNA hybridisation kinetics on beads under high flow rate conditions	68
34 DNA/DNA hybridisation kinetics on beads under low flow conditions rate	69
35 DNA/DNA hybridisation/denaturation cycles on beads	70
36 DNA/DNA denaturation kinetics on beads under flow conditions	71
37 Reversible chemistry for a multi-step DNA hybridisation transfer under isothermal by a pH change	74
38 Schemes of two coupled modules for automated, multi-step DNA selection under isothermal conditions based on moving magnetic beads in spatially separated laminar flows	75
39 DNA Hybridisation transfer between micro-reactors selection modules under isothermal conditions at a high flow rate	77

40 Quantitative analysis of DNA hybridisation transfer from beads in one module to those in a second module at a high flow rate	78
41 Mixing efficiency in the micro-flow reactor used for a DNA hybridisation transfer under isothermal conditions at a low flow rate	79
42 DNA hybridisation transfer between micro-reactors selection modules under isothermal conditions at a low flow rate	80
43 Quantitative analysis of DNA hybridisation transfer from beads in one module to those in a second module at a low flow rate	81
44 Fluorescence images of steady flow patterns in strand transfer modules	82
45 DNA hybridisation transfer in STM under steady flow conditions	83
46 Scheme of integrated, automated, programmable and reusable micro-fluidic device for a parallel, multi-step, sequence-specific DNA selection under isothermal conditions by using of valves	85
47 Micro-fluidic mixers and crossing channels	87
48 Scheme of an automated, programmable and reusable micro-fluidic device for a multi-step, sequence-specific DNA selection under isothermal conditions by using of valves	88
49 Schematic presentation of the partition function for perfectly matching DNA strands	93
50 Schematic presentation of partition function for non-perfectly matching DNA strands	94
51 Assembly of DNA library	100
52 PCR amplification of the DNA library	101
53 Single-strand purification of the DNA library	102
54 Testing the integrity and the fidelity of the library by PCR amplifications with 'zero' capture probes	103
55 Testing the integrity and the fidelity of the library by PCR amplifications with 'one' capture probes	104
56 Finding the origin of the wrong library amplification signal with capture probe V7	105
57 Testing the library sequences for a hybridisation and a secondary structure formation.....	106
58 PCR readout of the DNA library on 4% agarose gel after one selection step on beads with the capture probe V4	107

LIST OF TABLES

1 The DNA library words (bits) and their complimentary sequences (capture probes)	14
2 Four individual library sequences with 111111111111, 000000000000, 101010101010, and 010101010101 bit values, representing all ligation sites among the DNA words (bits)	15
3 DNA sequences used in different hybridisation experiments	15
4 The properties of the paramagnetic beads used as specified by the manufacturer	16
5 The properties of the magnetic stand used as specified by the manufacturer	17
6 Quantification of DNA oligomers by a UV absorbance	29
7 Quantification of 5' end amino-modified DNA immobilisation to carboxyl-coated beads for two hours	36
8 Quantification of 5' amino-modified DNA immobilisation to carboxyl-coated beads for twelve hours	36
9 Quantification of non-specific DNA attachment to carboxyl-coated beads for two hours	37
10 Quantification of non-specific DNA attachment to carboxyl-coated beads for twelve hours	37
11 Quantification of 5' amino-modified DNA immobilisation to carboxyl-coated beads for two hours under pH reversible conditions	38
12 Inhibition of 5' amino-modified DNA immobilisation to carboxyl-coated beads by pH change	39
13 Quantification of 5' end thiol-modified DNA immobilisation to carboxyl-coated bead	46
14 Average fluorescence intensity signal (integrated pick 560-600 nm) plotted in Figure 22	55
15 DNA melting points in different buffer solutions	58
16 Unified nearest-neighbour thermodynamic parameters for DNA helix formation in 1 M NaCl	97
17 Thermodynamic properties of DNA word sequences (bits) and their capture probes used in the constriction of the presented DNA library	98
18 Slide matches (SC) and reverse complementary slide matches (SR) for all 24 words to the library sequences 111111111111, 000000000000, 101010101010, and 010101010101	99
19 Four sequences representing all ligation subsequences in the library 111111111111.000000000000, 101010101010, and 010101010101	99
20 Thermodynamic properties of DNA word sequences (bits) and their capture probes used in the constriction of a DNA library published by van Noort et al.	109

21 First half of the experimental data of 5' R6G labelled synthetic DNA titration curve presented in Figure 10	118
22 Second half of the experimental data of 5' R6G labelled synthetic DNA titration curve presented in Figure 10	118
23 Complete experimental data of DNA/DNA hybridisation experiments on beads presented in Figure 12	118
24 Complete experimental data of DNA/DNA hybridisation experiments on beads presented in Figure 13	118
25 Complete experimental data of DNA/DNA hybridisation experiments on beads presented in Figure 18	119
26 Complete experimental data of DNA/DNA hybridisation experiments in solution by using of a quenching system presented in Figure 21	119
27 Complete experimental data of DNA/DNA hybridisation experiments with two mismatches in solution using a quenching system presented in Figure 22 and Table 14	119
28 Complete experimental data of DNA/DNA hybridisation experiments with three mismatches in a solution by using a quenching system presented in Figure 22 and Table 14	120
29 Complete experimental data of DNA/DNA hybridisation experiments with five mismatches in a solution by using of a quenching system presented in Figure 22 and Table 14	120
30 Complete experimental data of DNA/DNA hybridisation experiments in a solution without any mismatches by using of a quenching system presented in Figure 22 and Table 14	120
31 Complete experimental data of 5' TAMRA-labelled DNA in a solution presented in Figure 22 and Table 14	121
32 Complete experimental data of DNA/DNA hybridisation experiments in a 1-IEPES solution by using of a quenching system, presented in Figure 23	121
33 Complete experimental data of DNA/DNA hybridisation experiments in a Tris solution by using of a quenching system, presented in Figure 23	121
34 Complete experimental data of 5' TAMRA DNA titration curve presented in Figure 24	122
35 Complete experimental data of DNA/DNA hybridisation experiments on beads presented in Figure 26	122
36 Complete experimental data of DNA/DNA hybridisation experiments on beads presented in Figure 27	122
37 Complete experimental data of DNA/DNA hybridisation experiments on beads presented in Figure 35	123
38 Complete experimental data of DNA/DNA hybridisation experiments on beads presented in Figure 58	123

1 INTRODUCTION

...I see this sort of like Columbus taking off from Spain. He was looking for India, and he smacked into America - the New World. That is what I think we are really doing. We are taking off, trying to build a practical molecular computer. But I think we are really taking off into the unknown world of biology and mathematics and computer science....

Leonard Adleman speaking on the future of the DNA computing, August 1996.

“How often have I said that when you eliminate the impossible, whatever remains, however improbable, must be true?” said Mr. Holmes¹. Reaching the true one by eliminating all false solutions is a very old and very labour consuming idea. Recently that idea acquired a novel implementation in the emerging field of DNA computing. Most of the DNA computing strategies implemented up to now are based on two major steps. In the first step, all possible solutions of a computational path search problem are encoded in binary form using DNA or RNA molecules. In the second step, the generated pool of nucleic acids undergoes numerous selection steps via the process of nucleic acid hybridisation. As a result, certain types of DNA sequences, representing the right solutions of the computational problem, are finally obtained, while all other types of DNA sequences are eliminated. Applying that basic strategy, a DNA computer has found the right solution from an initial pool of 2^{20} (over one million different DNA sequences) solutions. This is the largest computational problem solved by non-electronic tools up to now. Nevertheless, that ‘brute computation power’ approach raised a lot of questions concerning its feasibility. How could we design large sets of modular DNA molecules maintaining a high level of specific hybridisation? How could we automate and scale up the multi-step selection process in such a complex pool of different DNA molecules? How could we achieve a high level of programmability in such a procedure? Those questions are not only relevant to the DNA computing field, where the ‘brute computation power’ approach has some obvious limitations owing to the exponential number of different molecules needed, but also to many areas of contemporary molecular biology and biotechnology. Today, it seems that a productive interaction between DNA based computing and diagnostics is taking place in the shared field of DNA-chip technology. In the present work I am investigating the potential applications of microfluidic technology in the field of the so-called

‘computationally inspired biotechnology’. That is a type of biotechnology which is applicable in both fields of DNA based computing and diagnostics.

1.1 MOLECULAR COMPUTATION AND EVOLUTION

A process which led from amoeba to man appeared to philosophers to be obviously a progress, though whether the amoeba would agree with this opinion is not known.

B. Russell.

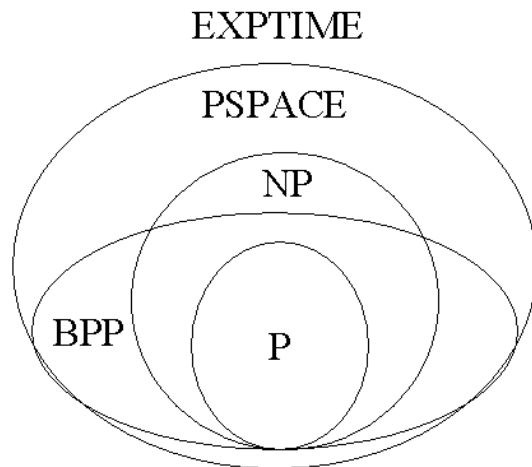
The exponential growth of information technology in the last fifty years is based theoretically on the serial programmable computer architecture, proposed by John von Neumann. As Gordon Moore observed, the enormous growth in information technology has become possible in practice because the electronic industry has managed to roughly double the density of transistors integrated on one chip every 18-24 months. The number of transistors on board chip has grown from 2,300 on the Intel 4004 in 1971 to more than 42 million on the Pentium 4 today. The key question now is how to maintain exponential growth in the future.

Moore expected his vision to hold until the chips will have become to be 0.25 microns across. The current chips have already surpassed this threshold and use 0.18 micron components. Intel claims to have found a way to manufacture components which are only 0.07 microns across. A processor made with such small components would have 400 million transistors on board and would be 10 times as powerful as the best chips available today. However, the fundamental question is what the physical limits of the computation are. If we extrapolate Moore's Law to the future, computers should be built of devices on molecule, atom, or quantum level. Today, it is an open question, how Moore's Law is going to play out, but it indisputably opens new avenues for novel research in the emerging fields of molecular and quantum computing.

Computing at the molecular level is not an idea of the last ten years. In 1959, Richard Feynman gave a lecture called, "There is Plenty of Room at the Bottom"ⁱⁱ. He speculated that if we were ever able to write one bit of information per an atom, we could store every bit of information ever generated by the entire human race in something smaller than a grain of sand. The computer that is capable of using such atom-size memory should be sub-microscopic. It is Bennett who associated the Turing Machine and the DNA replication by DNA polymerase. As the Turing Machineⁱⁱⁱ is a universal but not very efficient computer in terms of computing speed, Bennett imagined the DNA polymerase as an enzymatic machine capable of performing universal

computation with low energy consumptions^{iv}. In 1994, Leonard Adleman, using the tools of molecular biology, resolved the instance of the directed Hamiltonian path problem encoding small six-node graph in DNA molecules^v. This is how the field of nucleic acid-based computation came

into existence.



Soon after the Adleman's experiment the search for the most suitable and useful application ('the killer application') of DNA computing has begun.

Figure 1 Schematic presentation of the complexity classes and their presumed relationships.

Computational complexity theory classifies problems according to the efficiency of the algorithms required for their solving. The classification criteria are the minimum time and space (memory, DNA molecules regarding DNA computing) required to solve the hardest instance of the problem. Figure 1 presents some of the complexity classes and their presumed relationships. Not much of the presented classification has been mathematically proven. Nevertheless, the classification gives a basic idea of computational complexity. The P class consists of all problems solvable in polynomial time. A larger class, called NP, contains problems which till now do not have solutions in polynomial time but could be verified that an attempted solution is a solution in polynomial time. The next class in the presented classification known as BPP refers to randomised computation on decisions. BPP problems are regarded as being 'solvable in practice' and not BPP problems are 'unsolvable in practice'. PSPACE problems can be solved using only polynomial memory space, but not necessary polynomial time. Finally, EXPTIME is solvable in exponential time.

It has been suggested that DNA computing is suitable for solving NP problems in polynomial time paying off with an exponentially increased memory space (different DNA molecules). The key advantages of nucleic acid-based computation seem to be the vast parallelism, high information density (10^6 Gbits per cm^2 in comparison to an electronic computer which has 1 Gbits per cm^2) and extremely high-energy efficiency (10^{19} operation per Joule in comparison to an electronic computer with 10^9 per Joule). It has been proven that general-purpose algorithms can be executed on DNA-based computers solving a large class of path-searching problems using nucleic acid hybridisation. Nucleic acid hybridisation has been using *in vitro* as a specific molecular recognition in many methods of molecular biology. Following

Adleman's experiment, it has been proposed that nucleic acid hybridisation is akin to massively parallel computation. Given a large enough quantity of different DNA sequences, a molecular computer using nucleic acid hybridisation logic could solve NP-complete problems in polynomial time in a contrast to conventional digital computers, which are accepted to need exponential time to solve problems of that class^{vi, vii}. That so-called 'brute force' approach to molecular computing has been recently demonstrated by Adleman's group by solving a 20-variable 3-SAT problem on a gel-based DNA computer^{viii}. An initial pool of 2^{20} (over 1 million) different DNA molecules were generated. Twenty subsequent selection steps were performed on the initial DNA pool as at each selection step three selection conditions had to be fulfilled. Eventually, from this huge pool of over one million different DNA molecules, one particular DNA sequence, representing the right solution, was obtained. This is the biggest computational problem solved on a non-electronic computer up to now. Nevertheless, that approach to molecular computation has provoked certain criticisms concerning its scalability^{ix}. The trade-off in such experiments is between the number of steps and the number of parallel processes. In that case, the number of steps is increased linearly as the number of processes (different DNA sequences) increases exponentially. A 40-variable problem tackled in the same fashion will require an initial DNA pool of over 1 trillion (2^{40}) different DNA sequences. The selection of one particular sort of DNA sequence out of 1 trillion different sequences does not seem trivial but nevertheless, it may be a solvable problem. In order to challenge the digital computers, a DNA computer should be able to solve at least a 200-variable NP problem, meaning an initial pool of 2^{200} different DNA molecules. Nowadays, it is not longer believed that DNA computers will solve a practically important NP-complete (a 200-variable problem or more) problem without a fundamental breakthrough in the algorithms used and in their implementation. The implementation of some kind of probabilistic or evolutionary algorithms, if possible, could reduce the number of different DNA sequences (the memory space) needed and it could present an opportunity for solving of bigger problems than that of using deterministic ones. Nevertheless, NP-complete problems, tackled in a conventional way should be considered as benchmark problems for evaluating the practical implementation of a given DNA computing architecture. Nowadays, a clear trend for the development of DNA computing from basic research towards integrated applications in the field of biotechnology exists. The presented PhD thesis could be considered as an example in that direction.

Let me try briefly to mention the major modules for molecular computation proposed up to now. The already described Adleman's approach comes under the category of the so-called 'brute force', generate and search approaches. Numerous architectures for DNA and RNA computing, based on this approach have been implemented. Some of them include an RNA solution to the nine-bit satisfiability problem^x,

chemistry^{xi, xii} for DNA computing on the surface, a DNA solution to a 6-bit maximal clique problem^{xiii}. Tom Head has proposed splicing systems in 1987^{xiv}, Hagiya et al.^{xv} have introduced autonomous string system based on hairpin PCR amplification. Erick Winfree proposed the use of self-assembly of two-dimensional DNA crystals as a universal computation machine at nano-scale^{xvi}. DNA has been used as a software in an autonomous computing machine as well^{xvii}.

The approach for generating a pool of different DNA sequences, representing all possible solutions of one NP-complete search problem, is very similar to the *in vitro* selection techniques (SELEX and others) used in evolutionary biotechnology to create DNA and RNA molecules with desired properties^{xviii}. The principles of evolution have had a direct impact not only on evolutionary biotechnology and DNA computing but also on the emergence field of genetic programming as a part of contemporary information theory. Biological systems have inspired computer science with new concepts, including genetic algorithms, artificial neural networks, computer viruses, and synthetic immune systems, DNA computing, artificial life, and hybrid VLSI (Very Large Scale Integration) DNA gene chips. An interesting development in nucleic acid computing is the idea of using nucleic acid molecular switches, created by *in vitro* selection procedures, for building molecular circuits. Breaker et al have proposed the usage of oligonucleotide sensitive hammerhead ribozymes as logic gates^{xix}. The *in vitro* selection techniques may have the potential to play an important role in DNA computing for the building of molecular circlets and for generating large pools of nucleic acids for computation by means of programmed mutagenesis^{xx} and others.

1.2 MOLECULAR BASED DIAGNOSTICS

The big things could have easily been overcome while they were still small.

Confucius.

Genetic analysis is generally comprised of multi-step processes, its primary goal being to discover genetic markers that predict phenotypic outcomes with high confidence. Consensus sequence data, genetic polymorphism databases^{xxi, xxii} and associated phenotype data are making genetic analysis increasingly powerful. The Human Genome Project (HGP) has generated a huge amount of information about human genetic diversity^{xxiii} with over a thousand disease phenotypes being described nowadays as single genetic variants with Mendelian inheritance. Nevertheless, these are more exceptions rather than the rule among the widespread diseases of the human population. The cardiovascular diseases, diabetes, cancer, and psychiatric disease seem to be polygenic disorders. More than 1400 diseases have been described today at the molecular level as polygenic disorders^{xxiv}. Even for diseases due to a single genetic defect, the disease phenotypes can be very broad. As the understanding of genetics is evolving, the phenotypic variability of some monogenic disorders seem to depend not only on the state of the defective gene (a genetic polymorphism, a dominant-recessive relationship, a homozygous-heterozygous state) but also on the genetic polymorphism of many other genes involved in the function of the mutant gene directly or indirectly. All these factors complicate the understanding of phenotype-genotype relationships at the molecular level. Genotyping, however, may provide some value for individual phenotype profiles, because more than 1100 disease susceptibility genes have already been identified. It is obvious that useful genetic profiling requires the existence of tools for analysing large numbers of genetic polymorphisms in parallel. Many technical approaches for parallel polymorphism analysis have been developed such as CAE; CE for microsatellite marker analysis; CMC; SSCP; DGGE; PCR with RFLP analysis; ASO PCR. However, none of those techniques is a fully automated and integrated process, with high throughput to accomplish economically efficient genetic profiling.

An extensive area of DNA-based diagnostics is gene expression analysis, with DNA-chip arrays allowing the study of genome-wide patterns of expression in any available cell type, under a variety of conditions and at any given time. In these arrays, total RNA is reverse-transcribed into

fluorescently labelled cDNA. The pool of different cDNAs generated is analysed on DNA-chip arrays, where different DNA oligomers are attached at certain positions on the chip surface. A huge amount of experimental data has been generated analysing simultaneously the RNA expression of hundreds of different genes^{xxv}.

Micro-fluidic devices could offer some important advantages for nucleic acid-based diagnostics, such as a high level of integration of multi-step processing on a single wafer, small reaction volumes needed, fast reaction rate under flow conditions, high level of automation, reusability, and programmability. All these features are very suitable for performing SNP genotyping, mRNA and protein expression profiling, DNA sequencing, RFTL genetic analysis by means of automated and integrated isolation, purification, detection, and characterisation of nucleic acids and polypeptides. This is applicable not only to economically efficient molecular diagnostics but also for performing a fully automated and programmable DNA computing. All that will be discussed in the next chapters.

1.3 MICROFLUIDICS AS A COMMON GROUND BETWEEN DNA BASED COMPUTATION AND DIAGNOSTICS

...It is important to recognize that progress in cell biology depends heavily on the availability of experimental tools that allow scientists (not the tools) to make new observations or conduct novel kinds of experiments.*

Cooper, Cell

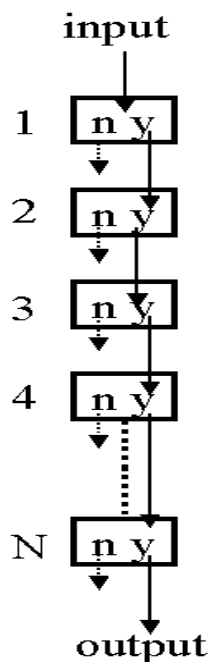
*How the small could also be beautiful.**

Contemporary advances in DNA-chip technology play an important role in modern biology and medicine. In recent years, microfluidic technology is improving rapidly using the huge expertise accumulated in the etching of tiny patterns in mass-producing of electronic chips. Miniaturisation and integration have played a key role in the development of current microelectronics technology. It seems that contemporary biotechnology is going to set off in the same way. What may be going to happen with the laboratory equipment in the near future is the same thing that happened with mainframe computers, i.e. it is going to become smaller, faster, cheaper and more functional.

Micro-fluidics circuits do not look very different from the integrated circuits on computer chips. It is easy to identify analogies between microelectronics and microfluidics because there are obvious similarities between microfluidic and microelectronic architectures. In fact, they are made in a similar fashion by etching tiny structures in silicon, glass or plastic. The current, voltage, and charge in the microelectronic systems are equivalent to the flow rate, pressure, and volume in microfluidic devices. A melding of high-tech (i.e. electronics, microfluidics, MEMS) and biotech is taking place in an effort to produce systems that can purify, amplify and detect nucleic acids. These so-called micro total analysis systems (μ TAS) or Sample-to-Answer devices could be utilized in health-care, agriculture, forensic medicine, military applications, environmental monitoring and animal husbandry. Ideally, these devices may be able to start with almost any sample input, utilize portable instrumentation, require no user intervention, and may be inexpensive to manufacture as well.

A large number of methods, availing themselves of micro-fluidics, have been already developed in numerous laboratories for various applications including enzyme assay, chemical processing, on-chip PCR^{xxvi}, peptides, and DNA analysis^{xxvii, xxviii, xxix, xxx, xxxi}, cell analysis^{xxxii}, biosensors^{xxxiii}.

Apart from the high throughput features, the micro-flow reactors offer some other important advantages such as nano-liter reagent volumes, parallel processing, on-board mixing of reagents, high reaction rates. A new venture has declared its aim to sequence the entire human genome in three years applying micro-flow reactors^{xxxiv}. The efforts to make labs-on-a-chip are based on the idea of the integration of different chemical processes, all requiring different reaction conditions,



on a single wafer. In practice, owing to the limitations imposed by the enzymatic amplification procedures, and the DNA detection platform, it is difficult to develop devices meeting these criteria^{xxxv}.

Figure 2 Multi-step bio-molecular processing in cascaded connected selection modules. *The input presents an initial pool of bio-molecules, which undergoes N number selection processing. Certain molecules from the initial pool bind reversibly to a certain selection module if a certain selection condition is fulfilled. If not the molecule is taken out of the system.*

However, applying micro-fluidics for multi-step sequence-specific DNA transfer could be very useful (see Figure 2). This is an advantageous method because of the fast DNA hybridisation kinetics on beads under flow conditions comparable to the reaction rate in the electric field-assistant DNA hybridisation and for the small sample values needed. The method is

applicable for gene expression analysis, SNP analysis and multi-step DNA selection from a complex initial pool of DNA in the field of molecular computing. The microfluidic technology provides a convenient platform for a high degree of automation and integration in both DNA computing and diagnostics.

In the field of DNA, computing micro-fluidics allow implementation of a dataflow-like architecture^{xxxvi} for multiple processing of DNA^{xxxvii}. It now seems quite difficult to try to predict the future of nucleic acid-based computation and to estimate its real computation power. However, the key features in the hardware implementation of DNA computing seem to be clearly defined. The first important feature concerns the programmability of the DNA computer. In the case of cascaded processing, as shown in Figure 2, the programmability could be considered in terms of programmable immobilisation of synthetic DNA to the beads placed in cascaded connected micro-chambers or to their surfaces. That process obviously has something to do with the DNA

microarray technology used in contemporary molecular biology and medicine. The next important aspect of any DNA computer concern the automation and integration of all the DNA computation processes including not only the programmability but also the computation process itself (multi-step DNA selection), and the readout (the detection). The DNA computer `hardware` (everything except the DNA itself, which could be regarded as the software of the DNA computer) should be a problem independent. The main task of the current Ph.D. thesis is to address all those essential questions relevant not only to DNA computing but also to DNA diagnostics employing a microfluidic technology.

The applications of contemporary microfluidic technology in the field of bio-molecular processing have been growing enormously in the last years. I would be very glad to be able to make a small contribution of my own to that field with the current Ph.D. thesis.

Let's go!

1.4 RESEARCH GOALS

*The journey is neither the only nor the main goal.
There are some others.**

The major goal of my research is to investigate the opportunities for creating a highly integrated, fully automated and programmable bead-based microfluidic platform for multi-step sequence-specific DNA selection taking into account different micro-fluidic architectures. The approach is targeted at applications in the fields of DNA-based computing and diagnostics. The research goals are defined as follows:

1. To establish a chemical procedure for multi-step DNA hybridisation transfers between bead-based micro-reactor selection modules under isothermal conditions and to investigate its efficiency.
2. To suggest a micro-fluidic architecture allowing programmed DNA immobilisation to beads placed in cascaded connected micro-reactors. The micro-flow architecture should provide a high degree of programmability and integration to the DNA selection procedure. The DNA immobilisation chemistry used, should be as cheap and simple as possible and should guarantee a high level of specific DNA attachment.
3. To investigate DNA/DNA hybridisation and denaturation kinetics on beads under flow conditions in terms of the chemical procedure for isothermal DNA hybridisation transfer.
4. To investigate the fidelity of DNA/DNA hybridisation on beads and in free solutions in relation to the chemical procedure for isothermal DNA hybridisation transfer.
5. To construct experimentally and to test a twelve-bit DNA library for molecular computation. The library should possess a high degree of specific DNA hybridisation for all library bits with at least a 50 % hybridisation yield and a low level of secondary structure formation under identical hybridisation conditions. The size of the library has been chosen to be bigger by two bits than the biggest library published at the moment (at the end of 2001).

2 MATERIALS AND METHODS

*You must remember this, a kiss is still a kiss,
A sigh is just a sigh;
The fundamental things apply,
As time goes by.*

*Herman Huupfeld
'As Time Goes By'*

2.1 MATERIALS

2.1.1 Chemicals, enzymes, and solutions

All chemicals used in this work, with the exception of DNA (see the next section), were purchased from the following companies:

Fluka, Buchs, Germany; **Merck**, Darmstadt, Germany; **Roth**, Karlsruhe, Germany; **Serva**, Heidelberg, Germany; **Sigma**, Deisenhofen, Germany; **Biozym Diagnostik**, Hess. Oldendorf, Germany; **Molecular Probes**, Eugene, OR; **Qiagen**, Hilden, Germany; **Roche**, Mannheim, Germany; **PerkinElmer**, Rodgau-Jügesheim, Germany; **Invitrogen**, Karlsruhe, Germany, **IBA-NAPS**, Göttingen, Germany, **Pierce**, Rockford, IL.

Taq DNA polymerase	Qiagen
Tsc thermostable DNA ligase	Roche
acrylamid:bisacrylamid (29:1) stock solution	Roth
1x SYBR Green One or Two	Molecular Probes
Biozym Small DNA Agarose	Biozym
2xBinding buffer	20 mM Tris-HCl, pH 7.5, 1.0 M LiCl, 2 mM EDTA
5xTBE buffer	Dissolve 54 g Tris base and 27,5 g boric acid in 800 ml of ddH ₂ O. Add 20 ml 0.5 M EDTA (pH 8.0). Adjust the volume to one litre with ddH ₂ O.

50xTAE	Dissolve 242 g Tris base and 57.1 ml acetic acid in 700 ml of ddH ₂ O. Add 100 ml 0.5 M EDTA (pH 8.0). Adjust the volume to one litre with ddH ₂ O.
20xSSPE	Dissolve 175.3 g of NaCl and 27.6 g of Na ₂ H ₂ PO ₄ ·H ₂ O 7.4 g of EDTA in 800 ml of ddH ₂ O. Adjust the pH to 7.4 with a 10 N NaOH. Adjust the volume to 1 litre with ddH ₂ O.
1 M Tris- acetate	Dissolve 121 g of Tris base in 700 ml of ddH ₂ O. Adjust the pH to 8.3 by acetic acid.
1 M Tris-HCl	Dissolve 121 g of Tris base in 700 ml of ddH ₂ O. Adjust the pH to 8.3 by hydrochloric acid.
1 M Tris-borate	Dissolve 121 g of Tris base and 66 g boric acid in 800 ml Adjust the pH to 8.3. Adjust the volume to 1 litre with ddH ₂ O
1 M HEPES	Dissolve 65,08 g of HEPES sodium salt and 59,50 g of HEPES in 400 ml of ddH ₂ O. Adjust the pH to 7.5. Adjust the volume to 0.5 litre with ddH ₂ O
200 mM MES	Dissolve 21,32 g of MES in 400 ml of ddH ₂ O. Adjust the pH to 6.1. Adjust the volume to 0.5 litre with ddH ₂ O
Loading buffer for native gels	0.25 % bromophenol blue; 0.25 % xylene cyanol FF; 15 % Ficoll (Type 400) in ddH ₂ O
loading buffer for denaturing gels	Dissolve 10 mg, 10 mg bromophenol blue, and 200 µl of 0.5 M EDTA (pH 8.0) in 10 ml formamide
DNA elution buffer from PA gels	0.5 M ammonium acetate, 10 mM magnesium acetate, 1 mM EDTA (pH 8.0), 0.1 % SDS

2.1.2 Nucleic acids and paramagnetic beads

A DNA ladder, 10 bp, was purchased from Invitrogen. The synthetic DNA oligomers were obtained from IBA-NAPS, all of them purified to HPLC grade.

Table 1 The DNA library words (bits) and their complementary sequences (capture probes). *Each capture probe is 5' amino-modified by an amino C6 linker or 5' biotin-labelled and has a spacer of 12 dT. The word sequences are computer generated by an algorithm described in ^{xxviii}(see section 2.2.8). The complete library contains all possible 'one' and 'zero' combinations among the bits at twelve different positions (4096 different DNA sequences, each 192 nt long). The DNA library was split into four oligomers (each 96 nt long) synthesized by a mix and split procedure (see Figure 6), the whole library was assembled by four ligation reactions (see Figure 51).*

N	Bits	5'-3' Word sequences 16 nt	5'-3' Capture probe sequences 28 nt
1	1.1	CCATCACTACCTTCAT	TTTTTTTTTTTTATGAAGGTAGTGATGG
2	1.0	TCCTCTATCATCTCA	TTTTTTTTTTTTGAGGATGATAGAGGA
3	2.1	TCCCTATCACTCTCT	TTTTTTTTTTTTAGAGAGTGAATAGGGA
4	2.0	CACACCTCAACTTCTT	TTTTTTTTTTTTAAGAAGTTGAGGTGTG
5	3.1	ACTTCCCTTCTACACA	TTTTTTTTTTTTGTGTAGAAGGGAAGT
6	3.0	CACCATCCTTATCTCA	TTTTTTTTTTTTGAGATAAAGGATGGTG
7	4.1	TCTCTCAATCCACTTC	TTTTTTTTTTTTGAAGTGGATTGAGAGA
8	4.0	TACAATCCCACACTTT	TTTTTTTTTTTTAAAGTGTGGGATTGTA
9	5.1	TCTCTTCTCTTACCA	TTTTTTTTTTTTGGTAAGAGGAAGAGA
10	5.0	TCATACCTAACTCCCT	TTTTTTTTTTTTAGGGAGTTAGGTATGA
11	6.1	CTCATCTTAACCACCT	TTTTTTTTTTTTAGGTGGTTAAGATGAG
12	6.0	ACCATTACTTCAACCA	TTTTTTTTTTTTGGTTGAAGTAATGGT
13	7.1	TTCTACAACCTACCCT	TTTTTTTTTTTTAGGGTAGGTTGTAGAA
14	7.0	TCCAACCTAACACTCC	TTTTTTTTTTTTGGAGTGTTAAGTTGGA
15	8.1	ACCTTACCTATCCT	TTTTTTTTTTTTAGGATAGGGTAAAGGT
16	8.0	ACACCCTAACAAATCAA	TTTTTTTTTTTTGATTGTTAGGGTGT
17	9.1	CACCCATTCCCTAATAC	TTTTTTTTTTTTGTATTAGGAATGGGTG

18	9.0	TCCTACACAAACATCA	TTTTTTTTTTTTGATGTTTGTGTAGGA
19	10.1	ATTCTCACTCACAACC	TTTTTTTTTTTTGGTTGTGAGTGAGAAT
20	10.0	ACCACTCCAATAACTC	TTTTTTTTTTTTGAGTTATTGGAGTGGT
21	11.1	TCCTACTCTCCAATCA	TTTTTTTTTTTTGATTGGAGAGTAGGA
22	11.0	TCTTTCACACATCCAT	TTTTTTTTTTTTATGGATGTGTGAAAGA
23	12.1	ACACCATTTACCTAA	TTTTTTTTTTTTTAGGTGAAATGGTGT
24	12.0	ACACTAATCCTCCAAC	TTTTTTTTTTTTGTTGGAGGATTAGTGT

The DNA library capture probes (see Table 1) were 5' amino-labelled using a C6 linker or 5' biotin-labelled, having also an additional linker of 12 dT at the 5' end because of my intention to use them in DNA hybridisation analyses on beads. The synthesis of the DNA library was divided into four deoxyoligonucleotides each 96 nt long (see Figure 6) and was assembled by four ligation reactions (see section 2.2.4 and Figure 51).

Table 2 Four individual library sequences with 11111111111, 00000000000, 10101010101, and 010101010101 bit values, representing all ligation sites among the DNA words (bits). Each sequence is 192 nt long and was synthesized in one run using long-range DNA synthesis procedure.

11111111111	00000000000	10101010101	010101010101
-------------	-------------	-------------	--------------

5'	5'	5'	5'
CCATCACTACCTTCAT	TCCTCTATCATCCTCA	CCATCACTACCTTCAT	TCCTCTATCATCCTCA
TCCCTATTCACTCTCT	CACACCTCAACTTCTT	CACACCTCAACTTCTT	TCCCTATTCACTCTCT
ACTTCCCTTCTACACA	CACCATCCTTATCTCA	ACTTCCCTTCTACACA	CACCATCCTTATCTCA
TCTCTCAATCCACTTC	TACAATCCCACACTTT	TACAATCCCACACTTT	TCTCTCAATCCACTTC
TCTCTTCTCTTACCA	TCATACCTAACTCCCT	TCTCTTCTCTTACCA	TCATACCTAACTCCCT
CTCATCTTAACCACCT	ACCATTACTTCAACCA	ACCATTACTTCAACCA	CTCATCTTAACCACCT
TTCTACAACCTACCCT	TCCAACCTAACACTCC	TTCTACAACCTACCCT	TCCAACCTAACACTCC
ACCTTTACCCTATCCT	ACACCCTAACAAATCAA	ACACCCTAACAAATCAA	ACCTTTACCCTATCCT
CACCCATTCTAATAC	TCCTACACAAACATCA	CACCCATTCTAATAC	TCCTACACAAACATCA
ATTCTCACTCACAACC	ACCACTCCAATAACTC	ACCACTCCAATAACTC	ATTCTCACTCACAACC
TCCTACTCTCCAATCA	TCTTTCACACATCCAT	TCCTACTCTCCAATCA	TCTTTCACACATCCAT
ACACCATTTCACCTAA	ACACTAATCCTCCAAC	ACACTAATCCTCCAAC	ACACCATTTCACCTAA
3'	3'	3'	3'

In addition, four individual library sequences, representing all ligation sites among the words (see Table 2) were synthesized in one run using long-range DNA synthesis procedure. Each sequence is 192 nt long.

Table 3 DNA sequences used in different hybridisation experiments.

N	Type of modification	Sequences 5'-3'	Length nt
1	5' QSY-7 or 5' R6G or non-labelled	GATGGTAACAGCTTGTCTGTA	21
2	5' QSY-7 or 5' R6G or non-labelled	GATAGTCACAGCATGGCTATA	21
3	5' QSY-7 or 5' R6G	GATAGTCACAGCATGTCTGTA	21
4	5' Amino C6 or 5' SH C6 or 5' Amino C6 3' and TAMRA	TTTTTTTTTTTTTTTACAGACAAGCTGTTACCATC	35
5	5' QSY-7 or 5' R6G or nonlabelled	GATGGTCACAGCATGTCTGTA	21
6	5' Amino C6	TTTTTTTTTTTTTTTACAGACAAGCTGTGACCGTC	35
7	5' R6G labelled or non-labelled	GACGGTCACAGCTTGTCTGTA	21
8	5' Amino C6 and 3' Fluorescein	TTTTTTTTTACAGACAAGCTGTGTCCGTCTCCCGGA	35
9	non-labelled	TACTGTGTCGAGCTTGTCTGTATTTTT	26
10	5' R6G labelled	TACTGTGTCGAGCTTGTCTGTA	21

Additional DNA sequences, presented in Table 3, were used for DNA immobilisation experiments to super-paramagnetic beads and for DNA/DNA hybridisation analyses on beads and in free solution.

Polystyrene super-paramagnetic beads were purchased from Micromod (Rostock, Germany), Chemagen (Baesweiler, Germany) and Dynal (Oslo, Norway). All beads are essentially monodisperse. Their properties are presented in Table 4 as specified by the manufacturer.

Table 4 The properties of the paramagnetic beads used as specified by the manufacturer.

Bead type	Size [μm]	Content of magnetite [%]	Functional groups on the surface	Particle Charge Density [nmol/mg]	Manufacturer
Amino polystyrene-co-maleic	15 \pm 2	15-20	(CH ₂) ₄ NH ₂	3.1	Micromod
Carboxyl polystyrene-co-maleic	15 \pm 2	20	Citric acid	3	Micromod
PVA	9 \pm 4	50	Carboxyl	-----	Chemagen
polystyrene	2,8 \pm 0,2	12	streptavidin	-----	Dynal

2.1.3 Micro-flow reactors

All the micro-flow reactors used were photolithographically etched on 4'' (100 mm) silicon wafers using TMAH and KOH at high temperature (80°C). The etched micro-reactors were sealed with anodically bonded 500µ thick pyrex (borosilicate) glass wafers. Ultrasonically drilled holes in the pyrex wafers (distance between the holes 3.5 mm) allowed the connection of capillary tubing (0.8 mm diameter) using UV-hardening glues to connect the micro-reactor channels with external fluids.

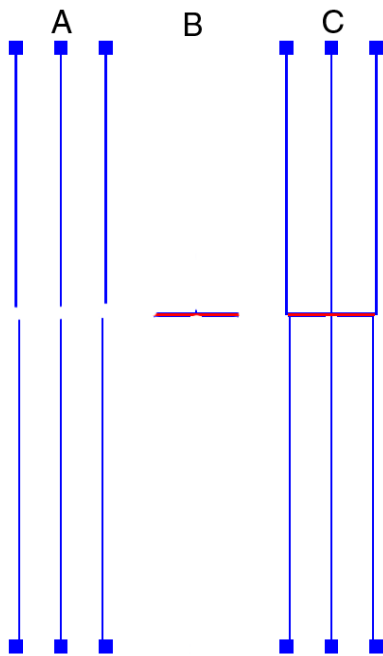


Figure 3 Scheme of the micro-flow reactor presenting one strand transfer module (STM) used for a single strand DNA transfer by moving beads under steady flow conditions. A: First mask: three inlet channels (at the top) and three outlet channels (at the bottom). Channels' width 180 µm and channels' depth 75 µm; B: Second mask a chamber with 10 µm depth; C: The complete micro-flow reactor.

The micro-flow reactor presented in Figure 3_C is produced by a two-step etching process applying two masks (see Figure 3_A and 3_B) etched to different depths^{xxxix}. The first mask, representing the inlet and outlet channels, is etched to a depth of 75 µm and to a width of 180 µm. The second mask, representing the bead chamber, is etched on a depth of 10 µm only. The etched bead barrier restricted 12 µm super-paramagnetic beads (Chemagen, see Table 4) with a 50 % magnetic content, delivered through the inlet (top) channels, into the bead chamber. The beads were moved from the left-hand part of the chamber to the right-hand part and backward applying a magnetic stand (IBS Magnet, Berlin, Germany) put on the micro-reactor bottom. A NdFeB block magnet, 30x18x10 mm, produced of DIN type material, code 360/95, possessing a magnetic strength as shown in Table 5 below was used.

Table 5 The properties of the magnetic stand used as specified by the manufacturer.

(BH) max	360-385	KJ/m ³
Br	1380-1410	mT
JHc	950-1030	KA/m
bHc	9±4	KA/m

The micro-flow reactor presented in Figure 4_C is produced by a three-step etching process applying three different masks (see Figures 4_A, 4_B, and 4_D) etched to different depths. The first mask, representing the inlet and outlet channels; the second mask, forming the bead chamber and the third mask, making the bead barrier were shown. 15 μm magnetic beads (Micromod, see

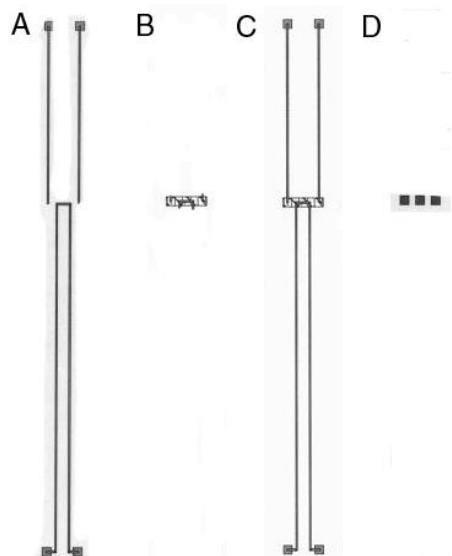


Table 4) were delivered through the inlet channels (at the bottom). The beads were restricted into the bead chamber by the etched bead barrier.

Figure 4 Scheme of the micro-flow reactor used in photo-dependent DNA immobilisation experiments. A: First mask: two inlet channels (at the bottom) and two outlet channels (at the top); B: Second mask: bead chamber; C: The complete micro-flow reactor; D: Third mask: etched bead barrier.

The micro-flow reactor presented in Figure 5 is produced by a two-step etching process employing two different masks. The first mask, forming the microfluidic chambers and channels, is etched to a depth of 220 μm , while the second mask, making the connection between the first and second chamber and between the second chamber and the outlet channel is etched to a depth of 10 μm only. 15 μm magnetic beads (Micromod, see Table 4) could be delivered to the second chamber through the first inlet channel and to the first chamber through the second and third inlet channels.

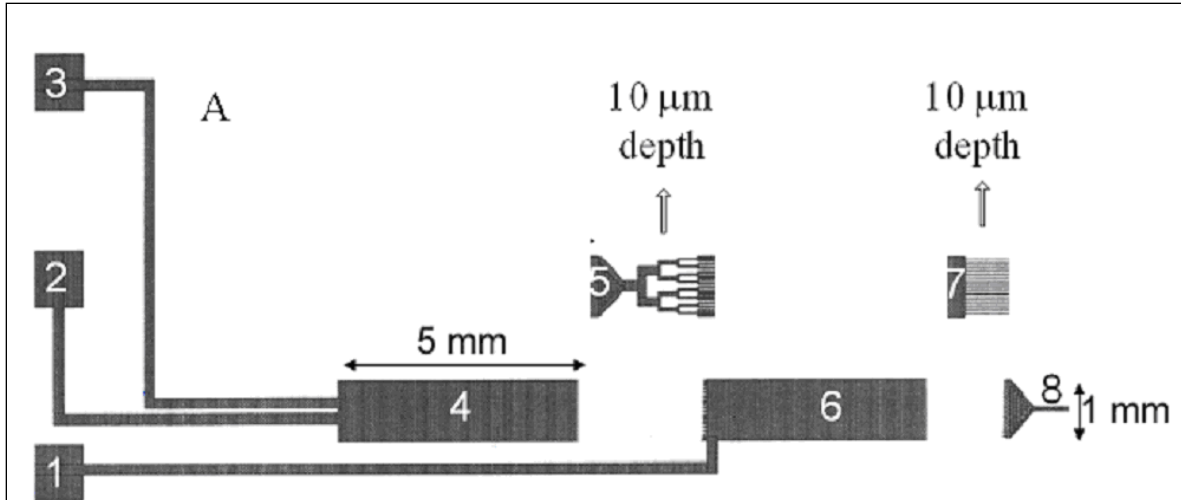


Figure 5 Scheme of the micro-flow reactor used in the DNA hybridisation transfer and DNA immobilisation experiments. *Two masks were used. The first mask, representing the channels and the chambers was etched to 220 μm depth while the second mask, representing one bifurcation structure (number 5) connecting the first and the second chamber, and one multi-channel structure (number 7) at the end of the second chamber, were etched to 10 μm depth. Magnetic beads delivered through the channels number two and three are restricted into the first chamber (number 4) while the beads delivered through the channel number one are restricted into the second chamber only.*

2.2 METHODS

2.2.1 Synthesis of DNA library

The quality of the synthesized DNA oligomers plays a critical role in the accuracy of the DNA computation. The synthesis of deoxyoligonucleotides up to 140 nt long is a standard procedure. In my case, the library sequences have a length of 192 nt. DNA with that length is not very stable in a 28% ammonium hydroxide solution (mainly as a result of depurination), which is used for cleavage of the synthesized DNA oligomers from the solid support.

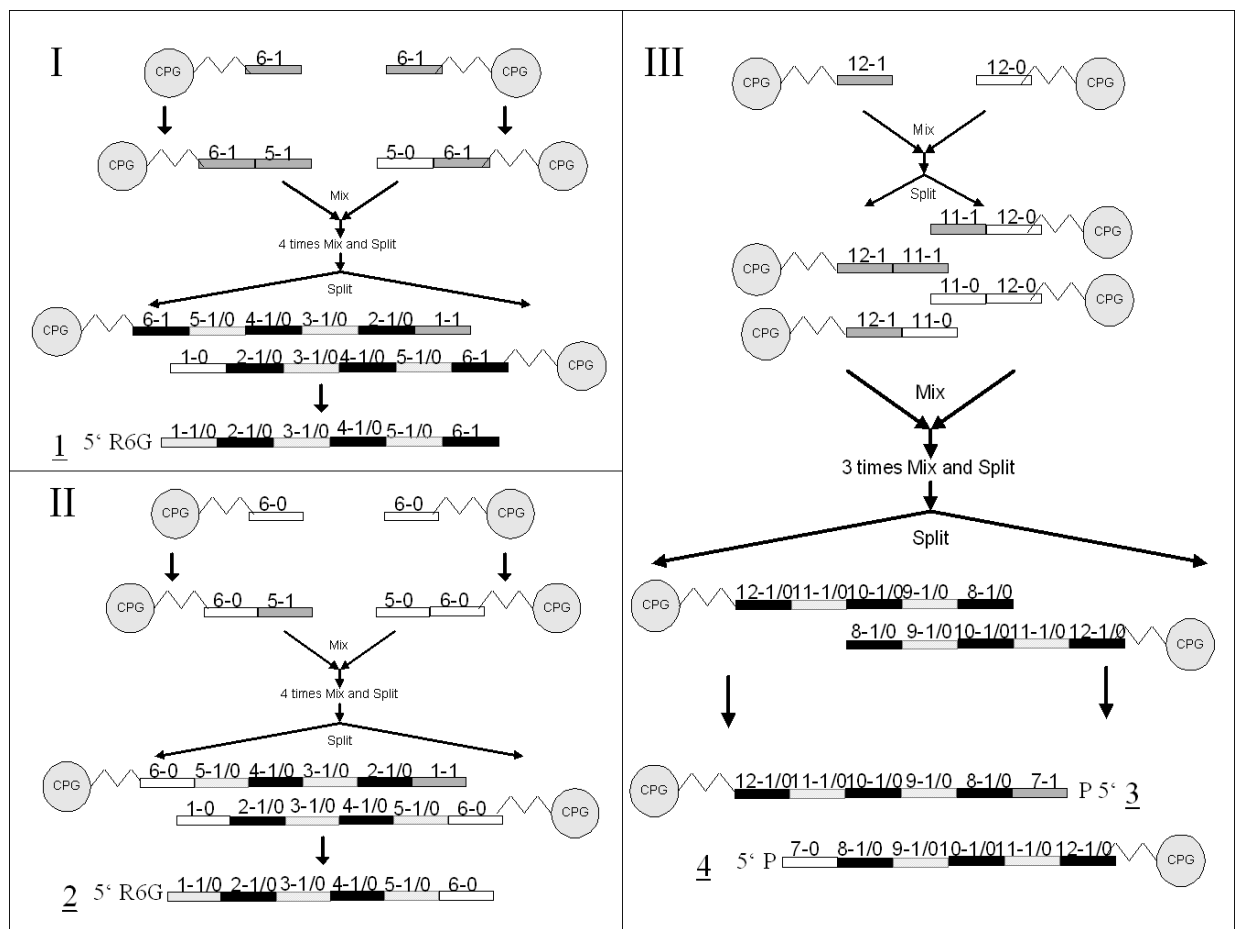


Figure 6 Synthesis of the DNA library. The library was synthesised by four oligodeoxynucleotides each 96 nt long by a mix and split procedure employed by Faulhammer et al. ¹⁰. **Oligomer number 1** (see I) contains all combinations among the first five bits (1-5) and has value 'one' in the sixth bit only. **Oligomer number 2** (see II) is identical in the first five bits to number 1 but has value 'zero' in the sixth bit only. **Oligomer number 3** (see III) contains all combinations among the last five bits (8-12 bits) and has the

value 'one' in the seventh bits and the **fourth oligomer** (see **III**) is identical in the last five bits to the third one but has value 'zero' in the seventh bit only. For the DNA word (bit) sequences see Table 1.

In order to reduce this effect the whole library was divided into four oligodeoxynucleotides each 96 nt long (see Figure 6 and for DNA word (bit) sequences see Table 1). All DNA oligomers were synthesized by the mix and split procedure applied by Faulhammer et al¹⁰. The first half of the library (from the first to the sixth bit) is represented by the oligomers numbers one and two (see Figure 6: I and II). They are identical in the first five bits. The oligomer with a number one has only a value 'one' at the sixth bit like that with a number two has only a value 'zero' at the same position. The second half of the library is represented by oligomers three and four (see Figure 6: III). They contain all possible combinations from the eighth to the eleventh bit. The oligomer number three possesses only value 'one' at the seventh as that with number four has only 'zero' at the seventh position. The first two deoxyoligonucleotides are 5' rhodamine 6G labelled as the second two are 5' phosphate modified. The whole library was assembled by four ligation reactions (see section 2.2.4)³⁸.

2.2.2 DNA immobilization procedures

2.2.2.1 Immobilization of amino-modified synthetic DNA to carboxyl-coated beads and inhibition of the immobilisation reaction by a pH-change

I: 5' amino-modified deoxyoligonucleotides at a concentration of 10 μM were immobilised to 5 mg 15 μm polystyrene carboxyl-coated polystyrene beads (Micromod, see Table 4) in the presence of 50 mM EDAC, 100 mM MES buffer, pH 6.1, and 100 mM NaCl in a final volume of 200 μl . The immobilisation reaction, shown in Figure 7, results in the formation of a peptide bond between the 5' amino-group of the modified DNA oligomer and the carboxyl-group on the bead surface.

II: To create a negative control for non-specific DNA attachment, the same reaction was performed in the absence of EDAC and to 30 mg beads instead of 5 mg beads.

Two additional sorts of immobilisation experiments were performed to prove the possibility for reversible pH-dependent inhibition of the DNA immobilisation reaction.

III: 10 μM 5' amino-labelled DNA and 5 mg polystyrene carboxyl-coated beads (Micromod, see Table 4) were incubated in a 200 μl buffer solution, containing 25 mM NaOH, 125 mM MES, pH 4.7, and 50 mM EDAC. The buffer solution was obtained by mixing equal volumes of a 50 mM

NaOH solution and a buffer containing 250 mM MES, pH 4.7, and 100 mM EDAC. The pH of the obtained upon mixing buffer was found to be 6.1.

IV: 10 μM 5' amino-labelled DNA and 30 mg polystyrene carboxyl-coated beads (Micromod, see Table 4), were incubated in a 200 μl buffer solution, containing 150 mM NaOH, 62.5 mM MES, pH 6.1, and 50 mM EDAC. The buffer was obtained by mixing equal volumes of a 250 mM NaOH solution and the buffer solution used in the first immobilisation reaction (25 mM NaOH, 125 mM MES, pH 6.1, and 50 mM EDAC) and it possesses a pH value of twelve units.

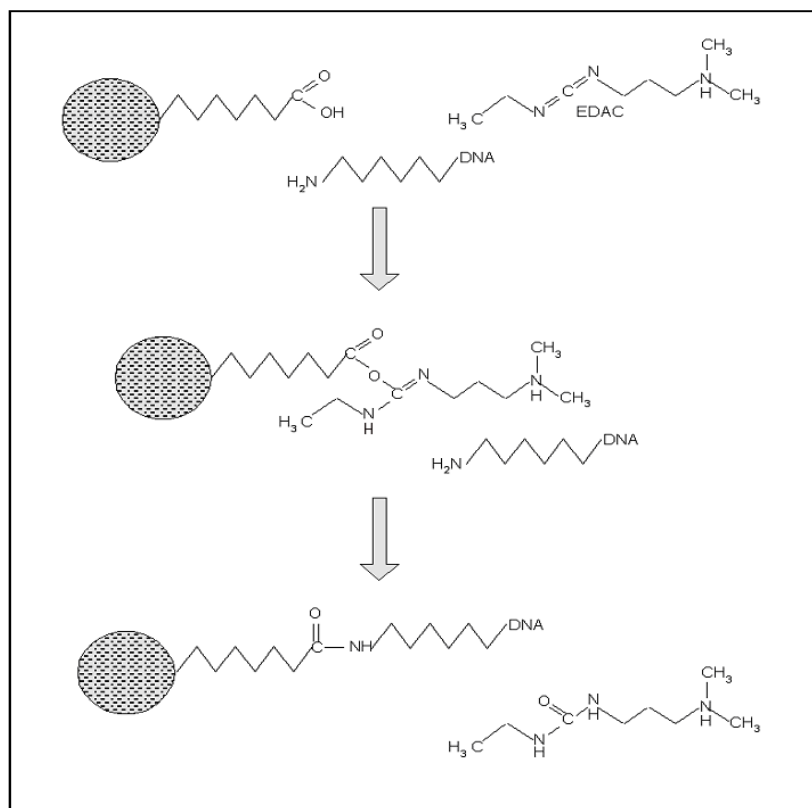


Figure 7 Scheme of immobilisation of amino-modified DNA to carboxyl-coated beads. As a first step, EDAC reacts with the carboxyl acid groups on the bead surface to form active-ester intermediate (*o*-Acylisourea). In the presence of an amino-modified DNA, a peptide bond is formed, releasing an isourea by-product.

All immobilisation reactions were incubated at 25°C under continuous shaking. After the immobilisation reactions, the beads were washed for three times in 500 mM Tris solution, pH 8.3, for 5 min under continuous shaking.

2.2.2.2 Cascadable DNA immobilisation to carboxyl beads placed in micro-chambers

Fifteen μm carboxyl-coated polystyrene beads (Micromod, see Table 4) were incorporated in chambers 1 and 2 of the micro-reactor shown in Figure 5. The fluids were delivered through the micro-reactor by a syringe pump (see section 5.1).

I: An immobilisation solution of 50 mM MES, pH 6.1, in the presence of 10 μM 5' end amino-modified synthetic DNA, 50 mM EDAC and 100 mM NaCl was pumped through inlets 2 and 3 with a flow rate of 0.005 $\mu\text{l}/\text{min}$ to immobilize DNA oligomers to the beads placed in the first chamber. A 250 mM NaOH solution was pumped simultaneously through inlet 1 one with a flow rate of 0.01 $\mu\text{l}/\text{min}$. As a result of the mixing between those two different buffers, the pH value in the second chamber was over twelve, resulting in no DNA immobilisation to the beads in the second chamber. The reaction was carried out for three hours at room temperature. Next, the flow was changed, while the 500 mM Tris-acetate solution was being pumped through all inlets with a flow rate of 0.1 $\mu\text{l}/\text{min}$.

In order to immobilise DNA oligomers to the beads placed in the second chamber by a separated delivery of the DNA molecules and the cross-linking reagents, two different immobilisation experiments were performed.

II: An immobilization solution of 50 mM MES, pH 6.1, in the presence of 10 μM 5' end amino-modified synthetic DNA and 100 mM NaCl was pumped with a flow rate of 0.005 $\mu\text{l}/\text{min}$ through inlets 2 and 3. A 50 mM MES solution in the presence of 50 mM EDAC was pumped simultaneously through inlet number 1 with a flow rate of 0.01 $\mu\text{l}/\text{min}$. The immobilisation reaction took place to the beads in the second chamber, but not in the first one.

III: A solution of 50 mM NaOH in the presence of 10 μM 5' end amino-modified synthetic DNA was pumped with a flow rate of 0.005 $\mu\text{l}/\text{min}$ through inlets number two and three. A 250 mM MES solution, pH 4.7, in the presence of 50 mM EDAC was pumped simultaneously through inlet number one with a flow rate of 0.01 $\mu\text{l}/\text{min}$. The immobilisation reaction took place to the beads placed in the second chamber because the cross-linking reagent was presented only there. In addition, any non-specific DNA immobilisation to the beads placed into the first chamber was avoided due to the alkali pH in that chamber.

2.2.2.3 Immobilisation of thiol-modified DNA to carboxyl-coated beads

5 mg carboxyl-coated beads (Micromod, see Table 4) were incubated in a 500 μ l buffering solution, containing 200 mM MES, pH 6.1, 10 mM PDPH and 50 mM EDAC at room temperature for three hours under continuous shaking. Next, the beads were washed twice in a 50 mM sodium phosphate buffer solution, pH 8.0, and incubated in 300 μ l of 100 mM sodium phosphate buffer solution in the presence of 10 μ M 5' thiol-modified DNA at room temperature for three hours under continuous shaking. Finally, the beads were washed twice with a 500 mM Tris-acetate buffer, pH 8.3. The immobilisation reactions are presented in Figure 8.

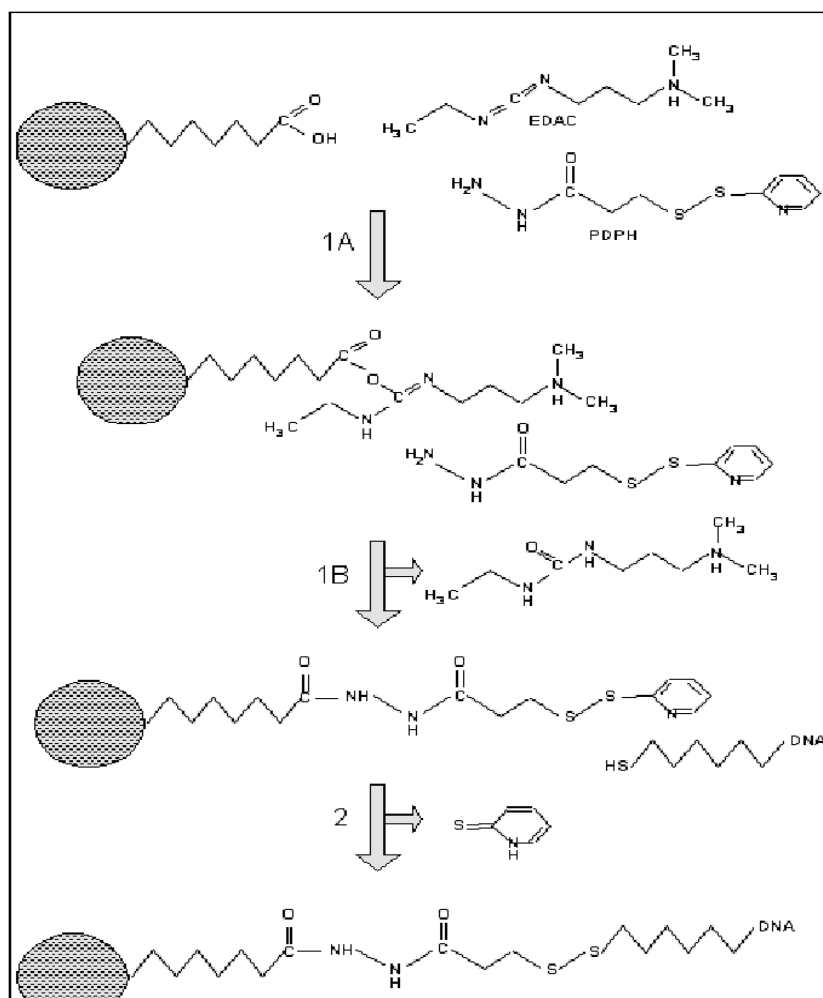


Figure 8 Immobilisation scheme of thiol-modified synthetic DNA to carboxyl – coated beads by using a heterobifunctional cross-linking reagent PDPH. Firstly, the hydrazide group of PDPH reacts with the carboxyl group on the bead's surface forming a peptide bond, see 1A and 1B. Secondly, the thiol group at the 5' end of the DNA oligomer reacts with the pyridyldithio group introduced on the bead's surface forming a disulfide bond.

2.2.2.4 Photo-dependent immobilisation of amino-modified DNA to amino-coated beads

Modification of amino-coated beads with a photoreactive bifunctional cross-linker 4-nitrophenyl 3-diazopyruvate

4-nitrophenyl 3-diazopyruvate was obtained from Molecular Probes, Inc. (Eugene, OR, USA). The cross-linker was dissolved to produce a 200 mM solution in dry DMSO. 100 µl of this solution was added to 5 mg amino-coated beads resuspended in 400 µl dry DMSO. The reaction was performed for 2 hours at room temperature with continuous shaking in the dark (see Figure.9, reaction 1)^{xl}. The beads were washed several times in the dark to remove any traces of nitrophenol with deionized H₂O until there was no longer any measurable absorbance at 412 nm in the rinsing solution. The beads were introduced into the inlet channels of the micro-flow reactor shown in Figure 4 in the dark. A part of the micro-flow reactor was covered by non-transparent foil ⁴⁰.

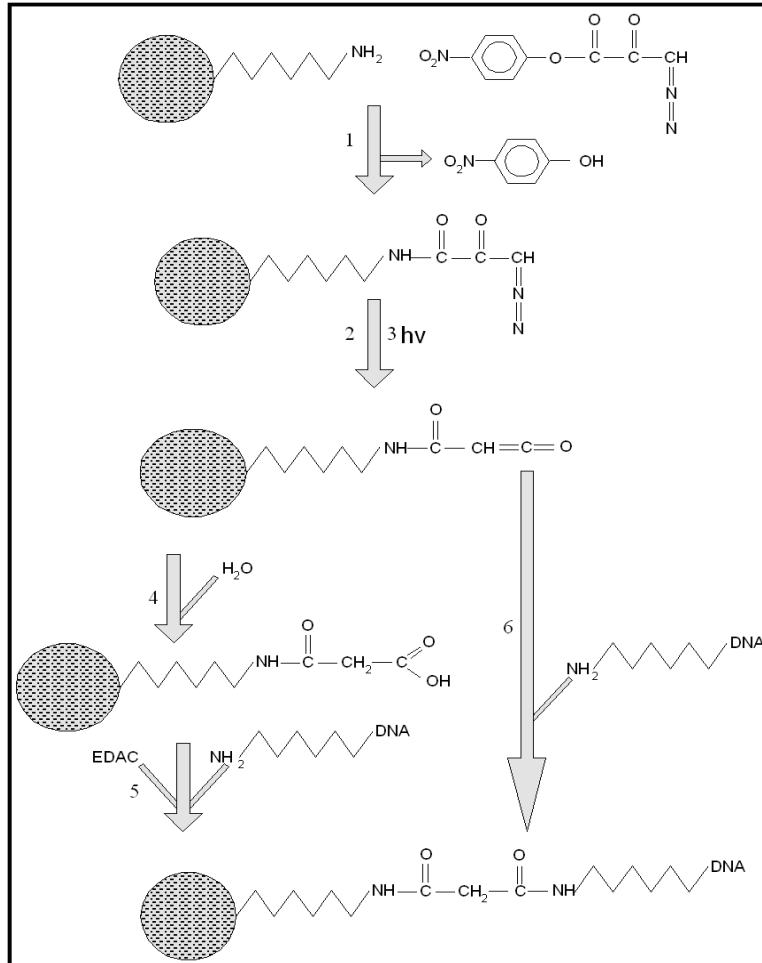


Figure 9 Overall scheme of photo-dependent DNA immobilisation. Left-hand route: the main photo-immobilisation scheme using the zero-crosslinker EDAC to attach 5' amino-modified DNA oligomers to beads. **1)** The 4-nitrophenyl ester group of DAPpNP reacts with amines on the beads producing diazopyruvic **2)** Photolysis of the diazo group attached to the beads by **3)** UV-illumination with **4)** conversion of the aldehyde group to carboxyl in water. **5)** Covalent immobilisation of 5' amino-modified oligomer to the photo-induced carboxyl group (attached to the beads) in the presence of EDAC via a peptide-bond formation.

Right-hand route: 6) Direct utilisation of the amino-ketene group for immobilisation of 5' amino-modified DNA oligomers.

The diazo group attached to beads was photolyzed by exposure twice to UV radiation for 30 seconds applying a mercury lamp with a power of 15 W from 280 to 315 nm and 75 W from 315 to 400 nm (UV-F400, Panacol-Elosol GmbH, Oberursel, Germany). 2.5 nmol of the 35 nt 5' amino-modified and 3' FITC-

labelled oligomers (see Table 3, line 8) was delivered through the inlet channels of the micro-reactor (see Figure 4) dissolved in H₂O in the presence of 10 mM EDAC. The reaction was performed for 3 hours at room temperature in the dark. Fluorescent images were obtained by the setup described in section 2.2.6.2.II. The overall scheme of the photo-dependent immobilisation procedure is shown in Figure 9.

In order to remove non-covalently bound DNA, the beads were flushed with SPSC buffer (50 mM sodium phosphate, 1 M NaCl, pH 6.5) for 1.5 hours at 42°C, and then with 100 mM Tris-acetate, pH 8.0, for half hour in the dark.

2.2.2.5 Immobilisation of biotin-labelled DNA to streptavidin-coated beads

Streptavidin-coated beads (Dynal, see Table 4) were washed twice in 2x B&W buffer. 10 µM 5' biotin-labelled synthetic DNA was incubated in 250 µl of 1xB&W buffer (see section 2.1.1) in the presence of 5 mg streptavidin-coated beads for one hour at room temperature, under continuous shaking. Finally, the beads were washed twice with 2x B&W buffer.

2.2.3 DNA hybridisation, denaturation, and sequence-specific transfer

2.2.3.1 DNA hybridisation analyses in solutions by using a quenching system

In order to investigate the fidelity of DNA/DNA hybridisation in different buffer solutions, a quenching system was used. One of the complementary strands was TAMRA labelled at the 3' end, while the other, was 5' end QSY-7 labelled. In both modifications, a C6 linker was used (see Table 3). Both DNA strands were used at a concentration of 1 µM in different buffers with a final volume of 100µl. The hybridisation reactions were carried out for 20 min at different temperatures. The quenching of the fluorescent signal was measured by a FluorMax-2 spectrofluorimeter (Instruments S.A., Inc, Edison, New Jersey) with excitation at 546 nm and an emission maximum at 579 nm and slit at 1.0. As a positive control, the fluorescent signal of TAMRA labelled DNA in the absence of complementary DNA was measured.

2.2.3.2 DNA hybridisation and denaturation on beads in Eppendorf tubes

The DNA hybridisation reactions were performed on 2 or 1 mg beads in the presence of 5 μ M oligomers in a 500 mM Tris-borate or Tris-acetate buffer, pH 8.3, (at 25°C) and 50 mM NaOH in a volume of 200 μ l at different temperatures. The hybridisation solutions were made by mixing equal volumes of a 1 M Tris-borate or Tris-acetate buffer, pH 8.3, and a 100 mM NaOH solution. The pH value of the solutions obtained did not vary more than 0.15 units at 25°C. The hybridisation reactions were incubated for one hour under continuous shaking. After each hybridisation, the beads were washed twice with a hybridisation buffer at a hybridisation temperature for 5 min under continuous shaking. The hybridised DNA on the beads was denatured by heating at 95 °C for 3 min or by applying 50 mM or 100 mM NaOH. The concentration of the denatured DNA was estimated by UV spectroscopy with a Cary 3E photometer (Varian Inc., Walnut Creek, CA) at 260 nm as described in section 2.2.6.1. When the DNA was fluorescently labelled, its concentration was additionally estimated by a spectrofluorimeter FluorMax-2 (Instruments S.A., Inc, Edison, New Jersey) by using of a standard titration curve as described in section 2.2.6.1.

2.2.3.3 DNA hybridisation and denaturation on beads under flow conditions

Carboxyl-coated beads, 15 μ m in diameter (Micromod, see Table 4) with immobilised DNA (as described above) were incorporated in a micro-reactor using a precision syringe pump (Model 260, World Precision Instruments Inc., Sarasota, FL). The hybridisation was carried out in a 500 mM Tris-acetate buffer, pH 8.3, and 50 mM NaOH in the presence of 1 μ M 5' rhodamine 6G labelled DNA oligomers (see Table 3) at 45°C under flow conditions with different flow rates. After each hybridisation step, the beads were washed with the hybridisation solution or with 150 mM Tris-acetate buffer, pH 8.3, at the same temperature. The hybridised DNA on the beads was denatured using 100 mM or 50 mM NaOH. Fluorescent images were obtained as described in section 2.2.6.2.1.

2.2.3.4 Sequence-specific DNA transfer between micro-reactor selection modules under isothermal conditions

In this experiment, the ability to select, restrain, transfer and pick up DNA between two modules was examined. The experimental procedure was performed at 40°C except that both chambers of the micro-flow reactors presented in Figure 5, were filled with carboxyl-coated beads (Micromod, see Table 4) with immobilised synthetic DNA (see Table 3, line 6) and separate buffer solutions were used at the inlets to the two chambers at various stages. Whereas in the integrated STM (see Figure 3), operating under steady

flow, switching buffers was achieved by a magnetic bead transfer, where the flows are switched in larger chambers to facilitate quantification of the transfer yields with constant bead locations.

The series of events for a complete transfer round from one module to the next was^{xli}:

- 1 The hybridisation of 1 μ M 5' R6G-labelled, perfectly matching DNA (see Table 3, line 7) to beads in both chambers. The hybridising buffer (500 mM Tris, pH 8.3, and 50 mM NaOH) containing the DNA was pumped in parallel (4 μ l/min) into all the three inlets of the microreactor shown in Figure 5.
- 2 Washing of the beads in both chambers (500 mM Tris, pH 8.3, and 50 mM NaOH without DNA), using inlets 1, 2 and 3 with a flow rate of 4 μ l/min.
- 3 Releasing the DNA from the beads in the second downstream chamber and washing of the beads in the first chamber. NaOH solution at 100 mM was pumped through inlet 1 with a flow rate of 4 μ l/min or 0.01 μ l/min and 150 mM Tris, pH 8.3, through inlets 2 and 3 with a flow rate of 2 μ l/min or 0.005 μ l/min.
- 4 Simultaneous release of the DNA from the beads in the first chamber and the pickup of the same DNA in the second chamber. 1 M Tris, pH 8.3, was pumped into the second chamber (inlet 1) with flow rates of 4 μ l/min or 0.01 μ l/min and 100 mM NaOH into the first chamber (inlets 2 and 3) with flow rates of 2 μ l/min or 0.005 μ l/min. The outflow from the first chamber was neutralised by the Tris buffer entering the second chamber from the side and then the DNA hybridises to the beads in the second chamber.

The denaturation solution was reversed to a hybridising solution by adding an equal volume of 1 M Tris-acetate buffer, pH 8.3. The capacity of the buffer is not exhausted by the NaOH solution so that no change bigger than 0.15 in the pH of the Tris-acetate buffer upon mixing was observed. Fluorescent images were obtained by the setup described in section 2.2.6.2.I.

2.2.4 DNA ligation, amplification, and melting temperature estimation

The ligation reactions were carried out at a concentration of ligated oligomers of 20 μ M each. The antisense oligomers were used at a concentration of 35 μ M (see Figure 51). Tsc thermostable DNA ligase (Roche, Mannheim, Germany) was used at a concentration of 0,2 U/ μ l. The oligonucleotides were

denatured at 93°C for 3 min and cooled to 25°C over 10 min. The ligation reactions were carried out for 2 hours at 30 °C in a gradient thermoblock (Biometra, Göttingen, Germany) in the presence of 100 mM Tris-HCl, pH 7.5, (at 25 °C), 10 mM NaCl, 20 mM KCl, 10 mM MgCl₂, 0,1% Nonidet P40 (v/v), 0,5 mM NAD and 1 mM DTT in a volume of 50 µl. The ligation products were separated from the unligated oligonucleotides on a 12% denaturing polyacrylamide gel electrophoresis in the presence of 63% urea and a 1x TBE buffer and stained in a 1x SYBR Green Two dye (Molecular Probes, Eugene, OR).

The PCR experiments were performed by a gradient thermoblock from Biometra. The amplification programme started with an initial denaturation at 93 °C for 3 min followed by 28 cycles of denaturation at 93 °C for 30 sec., annealing at 53 °C for 40 sec. and elongation at 72 °C for 30 sec. The Taq polymerase was purchased from Qiagen (Hilden, Germany) and used in a concentration of 0,1 U/µl. The amplification reactions were carried out in a 1x incubation buffer in the presence of 1 µM sense primer, 0,5 µM antisense primer (capture probes – see Table 1), 1 pM single-stranded DNA template and 250 µM dNTP's mixture. In a case of internal fluorescent labelling 500 µM R6G-dCTP was used instead of 250 µM dCTP. The PCR products were analysed on 8% non-denaturing gels in the presence of a 1x TBE buffer or on 4% agarose gel. The gels were stained in a 1x SYBRGreen One dye (Molecular Probes, Eugene, OR). The gel pictures were obtained by a gel documentation system from Biozym (Hess. Oldendorf, Germany). All gel pictures were inverted for better readability.

In order to determine the melting temperature of the words, a real-time PCR detection system iCycler iQ from BioRad (Hercules, CA) was used. Melting curves were obtained in a 10 mM sodium phosphate buffer, pH 7.2 in the presence of 50 mM or 100 NaCl, a 1x SybrGreen One dye, and 2 µM DNA strands in a final volume of 50 µl. The melting curve programme started with an initial denaturation at 95°C for 3 min followed by 160 repeats, each for 1 min, with a temperature decrease of 0.5°C per repeat.

2.2.5 DNA isolation, purification, and concentration

The peptide bond formed between the amino-modified DNA and the carboxyl groups on the surface of the bead was destroyed with 28 % NH₄OH (Sigma). The reaction was performed at 48°C for 3 hours under continuous shaking. NH₄OH was removed by evaporation with a SpeedVac Concentrator (Savant Instrument, Inc., Holbrook, NY, USA). The cleaved DNA was purified on a NAP-10 column (Pharmacia Biotech, Upsala, Sweden) as described by the manufacturer.

The ligated products were eluted from the gel by the 'Crush and Soak' method described by Sambrook et al.^{xliii}

2.2.6 DNA detection, quantification, and fluorescence imaging set-up

2.2.6.1 DNA quantification

DNA quantification by UV absorbance

Two different methods for DNA quantification were used. The first method was UV absorbance at 260 nm. Quartz cuvettes with a 1 cm path length were used. An absorbance of 1 optical unit was calculated to 2 nmol for short oligodeoxynucleotides, 50 nt in length, (see Table 6). In order to estimate the DNA purity, the UV absorbance was measured at 280 nm and 320 nm. The value of UV absorbance at 260nm/280nm should be 1,8 for pure oligodeoxynucleotides and there should be no absorbance at 320 nm.

Table 6 Quantification of DNA oligomers by UV absorbance

DNA oligomer - nt	DNA amount for 1 OD _{260 nm} - nmol
10	10
20	5
35	3
40	2,7
50	2

Quantification of prime end fluorescently labelled DNA by a standard titration curve

In addition, the amounts of 5' or 3' end fluorescently labelled oligodeoxynucleotides were estimated by measuring the fluorescence intensity and using a titration curve.

For every fluorescently labelled deoxyoligonucleotide an individual titration curve was made, for example, see Figure 10. For each concentration of the 5'R6G-labelled DNA (see Table 3, line 1) three different examples were measured by a FluorMax-2 spectrofluorimeter (Instruments S.A.,

Inc, Edison, New Jersey) with excitation at 524 nm and emission maximum at 557 nm and slits at 1.0 (see Tables 21 and 22).

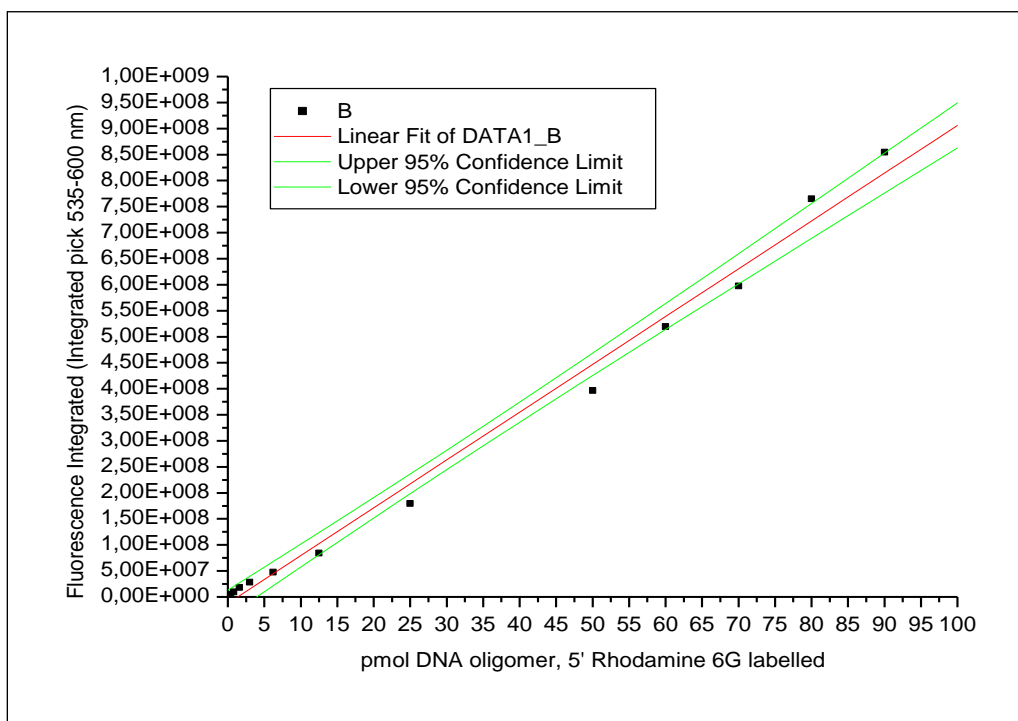


Figure 10 A standard titration curve for quantification of 5' Rhodamine 6G labelled DNA. The average fluorescent signal (integrated pick from 535 to 600 nm) of 5' R6G labelled DNA (see Table 3, line 1) in thirteen different concentrations (0,2 pmol; 0,4 pmol; 0,8 pmol; 1,6 pmol; 3 pmol; 6 pmol; 12,5 pmol; 25 pmol; 50 pmol; 60 pmol; 70 pmol; 80 pmol; 90 pmol) was measured. Each concentration was made in three independent repeats as the average values are plotted in the dark squares. The complete experimental data are presented in Tables 21 and 22. A linear fit was made based on the measured data – the red line. The two green lines enclosing a region of $\pm 5\%$ error rate defined by Origin software.

2.2.6.2 Fluorescence imaging set-up for DNA detection in micro-flow reactors

I: Fluorescence detection of DNA/DNA hybridisation on beads placed in micro-reactors

Fluorescence imaging of DNA/DNA hybridisation on beads placed in micro-reactor chambers was performed using an inverted microscope model Axiovert 100 TV (Carl Zeiss, Jena, Germany). The microscope was connected to an argon-ion laser (model 2080-15S, Spectra-Physics Lasers, Inc., CA) by an optical fiber. A homogeneous pool of light was created by the acoustic vibration of the

optical fiber at 80 Hz with an arbitrary wave by generator model 3312A from Hewlett-Packard (Palo Alto, CA). The images were detected by 12-bit CCD cameras (CH250 or Quantrix, see section 5.3) connected to the microscope by a C-Mount adapter. An emission filter opening at 540 nm and closing at 580 nm (Oriel Instruments, Stanford, CT) were employed (see Figure 11). The images were obtained and analysed by a PMIS image processing software (GKR Computer Consulting, Boulder, CO). The intensity of the exposure light coming out of the objective (10 x times magnification) had a value of 18 ± 1 mV.

II: Spatially resolved detection of DNA immobilisation to beads placed in micro-reactors and micro-flow stability

A CCD camera model LN/1024 TKB/1 (Princeton Instrument Inc., see section 5.3) was employed to capture images from the micro-flow reactors. The illumination was performed either by white light or by the laser beam at 514.5 nm from an argon-ion laser model 2080-15S manufactured from Spectra-Physics Lasers, Inc. (Mountain View, CA, USA). A homogenous pool of light of diameter *ca* 10 cm was created by the acoustic vibration of a multi-mode optical fiber at 80 Hz. An interference filter was placed between the camera and the sample, custom designed from AHF-Analysentechnik (Tübingen, Germany) with an optical density of O.D. 6 at 514 nm and transmission of 85-90 % at 523-600 nm (see Figure 11).

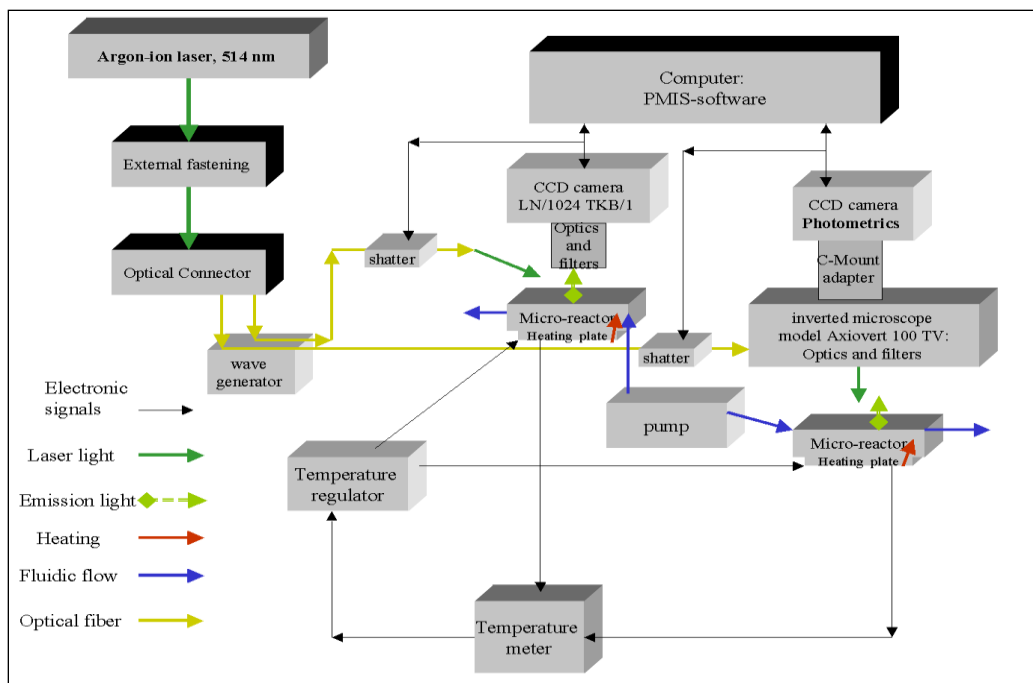


Figure 11 Scheme of two different set-ups for a fluorescence image acquisition in micro-flow reactors. Both set-ups apply common laser (argon-ion laser, external fastening, optical connector, wave generator, optical fibers, shatters, and fluorescent filters) temperature control (temperature regulator, temperature meter, and heating plates) fluidic control (syringe pumps), and software (PMIS programme) interfaces. The difference between the two set-ups is due to the special CCD cameras (CCD LN camera or CCD photometrics cameras, see section 5.3) and optics (tandem optics or inverted microscope) used.

2.2.7 Flow stability and bead movement in micro-flow reactors

In order to estimate the mixing efficiency in the second chamber of the micro-reactor presented in Figure 5, 100 mM NaOH solution was delivered at the flow rate of 0.005 $\mu\text{l}/\text{min}$ through inlets 2 and 3. A 500 mM Tris-acetate buffering solution, containing 50 mM NaOH and 1 μM Rhodamine 6G was delivered simultaneously through inlet number 1 at a flow rate of 0.01 $\mu\text{l}/\text{min}$. Fluorescence images were taken from the different parts of the second chamber by the setup described in section 2.2.6.2.I.

In order to test the flow stability in the micro-flow reactor presented in Figure 3, three solutions were delivered through the three different inlet channels at a flow rate of 0.5 $\mu\text{l}/\text{min}$. In the first case, a 500 mM Tris-acetate buffering solution, containing 50 mM NaOH and 1 μM Rhodamine

6G was delivered through all inlets. In the second case, a 500 mM Tris-acetate buffering solution, containing 50 mM NaOH was pumped through the left-hand channel, a 1 M Tris-acetate buffering solution was delivered through the middle channel and 100 mM NaOH and 1 μ M Rhodamine 6G solution was pumped through the right-hand inlet channel. In the first case, the fluorescence images were taken from the whole micro-reactor by the setup described in section 2.2.6.2.II while, in the second case, the images were obtained using the fluorescence imaging setup described in section 2.2.6.2.I.

Super-paramagnetic beads (Chemagen, see Table 4) 12 μ m in diameter were incorporated into the bead chamber applying a magnetic stand (see Table 5) put below the micro-reactor. The magnetic stand was moved slowly from the left-hand channel position to the right-hand channel and backwards. Three different solutions were pumped simultaneously through the inlet channels. Images were obtained as described in section 2.2.6.2.I.

2.2.8 Algorithm used for DNA library design

The library sequences were obtained in two separate steps applying a procedure implemented by Jörg Ackermann³⁸. In the first step, the hybridisation properties of a set of 24 words were optimised by a random search algorithm. In the second step, the set obtained was utilized to construct a twelve-bit DNA library.

The random search algorithm, applied in the first step, can be described as follows:

1_1: Generate a set of 24 random words, each 16 nt long, over the alphabet of A, T, and C. The sequences should not have four or more consecutive identical nucleotides as well as runs of three consecutive C's at either the 5'- or the 3'-ends.

1_2: Calculate the free energies by using a partition function for the hybridisation reactions of all words to their complements. For each word, compute the free energies for all hybridisation reactions to other words in the set and to their complements. Compute the melting temperatures T_m thermodynamically for all words in the set.

1_3: Select a word randomly from the set.

1_4: Generate a new random word, 16 nt long, over the alphabet of A, T and C.

1_5: Check the new sequence for the occurrence of four or more consecutive identical nucleotides as well as for runs of three consecutive C's at either the 5' or the 3' ends. Reject the sequence if one of these conditions is not fulfilled and go back to step 1_4.

1_6: Compute the melting temperature T_m thermodynamically for the new word. If the melting temperature is outside of the range of melting temperatures of the previous words go back to step 1_4.

1_7: Compute the free energy E_b for the hybridisation reaction of the word to its complement. If the formed hybrid is thermodynamically weaker than the weakest specific hybridisation for the previous words, go back to step 1_4.

1_8: Compute all free energies for the hybridisation reaction of the generated new word to the word set of 24 words and the corresponding complements. If one of these non-specific bindings is stronger than the strongest non-specific binding for the previous words, go back to step 1_4.

1_9: Replace the randomly chosen word in step 1_3 by the new generated word in step 1_4 and go back to step 1_2.

The words were ordered in the library by the following algorithm:

2_1: Generate all possible concatenations of two words for the set of 24 words optimised in the first step.

2_2: For each such concatenation calculate the free energies for all (non-specific) hybridisation reactions to words from the set and their complements. Save for each concatenation the free energy for the strongest non-specific hybridisation.

2_3: Determine the concatenation with the weakest such non-specific hybridisation.

2_4: Find the concatenation with the weakest non-specific hybridisation.

2_5: Search for a word that gives the weakest hybridisation for the two concatenations.

2_6: The search process for the position of the remaining words can proceed iteratively.

Finally, four sequences (111111111111, 000000000000, 101010101010, 010101010101) of the library, representing all ligation subsequences, were tested for slide mismatches with all words by using of an ADNA programme. In addition, no word should have a run of more than 7 consecutive nucleotides identical to any combination of the other 23 words in the library verified by using of

an ADNA programme. A few such sequences (14 for the complete library) were found and fixed by a single nucleotide transversion or transition.

3 RESULTS AND DISCUSSIONS

I am not bound to please thee with my answer.

Shakespeare,

The Merchant of Venice

3.1 DNA IMMOBILISATION TO BEADS

DNA immobilisation procedures play an important role in the implementation of a variety of molecular biological methods. In the present chapter, I focus my attention on different DNA immobilisation protocols based on EDAC (or EDC; 1-ethyl-3-(3-dimethylammonopropyl) carbodiimide hydrochloride). EDAC tends to be the most popular carbodiimide used in bio-conjugational chemistry. It belongs to the class of the so-called zero-length cross-linkers, mediating the conjugation of two molecules by forming a chemical bond, which contains no additional atoms from the cross-linker.

Because of its water solubility, EDAC could be directly added to the reaction without prior dissolving in organic solvents. The excess reagent and the by-product formed in the course of the reaction (isourea) are water-soluble and may be removed by gel filtration or dialysis. The conjugation procedure could be carried out in the water. However, under stationary conditions, the accumulation of isourea could cause the pH change, resulting in decreasing the reaction yield or even complete stopping of the reaction. In order to avoid that, buffering solutions could be applied so long as they do not contain any chemical groups reactive to EDAC. The MES solution (pH 4 - 6.1) is the most popular buffer used in EDAC coupling reactions. EDAC is employed to immobilise 5' or 3' amino-modified DNA to carboxyl-coated surfaces and 5' phosphate-modified DNA to amino-coated surfaces.

3.1.1 Immobilisation of amino-modified synthetic DNA to carboxyl-coated beads and inhibition of the immobilisation reaction by a pH-change. Non-specific DNA attachment

The immobilisation of 5' amino-modified DNA to carboxyl-coated surfaces in the presence of EDAC is a well-established and widespread procedure in bio-conjugate chemistry. The immobilisation chemistry

results in the formation of a peptide bond between the carboxyl group on the surface and the 5' amino-group of the DNA (see Figure 7). The reaction is quite efficient with the usual incubation time of two hours. However, the DNA immobilisation yield depends a lot on the surface used and on its carboxylation. It was important to investigate the reproducibility of the DNA immobilisation reaction to super-paramagnetic polystyrene carboxyl-coated beads in relation to their use in bead-based DNA selection experiments in micro-flow reactors as described in the following sections. The polystyrene carboxyl-coated beads were chosen for these experiments because they possess the lower capacity for non-specific DNA attachment than amino-coated polystyrene beads or silica beads.

Table 7 Quantification of 5' amino-modified DNA immobilisation to carboxyl-coated beads for two hours.

Number	OD 260 nm	OD 280 nm	OD 260 nm/ OD 280 nm	OD 320 nm	total DNA amount from 5 mg beads - pmol	pmol DNA / mg beads
1	0,117	0,065	1,800	0,009	351,000	70,200
2	0,100	0,055	1,810	0,008	300,000	60,000
3	0,110	0,058	1,890	0,010	330,000	66,000
4	0,092	0,050	1,840	0,007	276,000	55,200
5	0,090	0,049	1,830	0,008	270,000	54,000
6	0,095	0,051	1,860	0,009	285,000	57,000
stdev	0,011	0,006	0,033	0,001	32,181	6,436
average	0,101	0,055	1,838	0,009	302,000	60,400
(St/Av)%	10,656%	11,137%	1,801%	12,339%	10,656%	10,656%

In the first set of immobilisation experiments 5' amino-modified DNA (see Table 3, line 4) was immobilised to 5 mg super-paramagnetic polystyrene carboxyl-coated beads (see Table 4, line 2) in a 100 mM MES buffering solution, pH 6.1, 100 mM NaCl and in the presence of 50 mM EDAC as described in section 2.2.2.1.I. The DNA immobilisation reaction was incubated for two hours. Being immobilised with DNA the beads were washed to remove the non-specifically attached DNA (see section 2.2.2.1). The covalently attached to the beads DNA was cleaved and purified as described in section 2.2.5. The DNA concentration was estimated by UV absorbance as described in section 2.2.6.1.

Table 8 Quantification of 5' amino-modified DNA immobilisation to carboxyl-coated beads for twelve hours.

Number	OD 260 nm	OD 280 nm	OD 260 nm/ OD 280 nm	OD 320 nm	total DNA amount from 5 mg beads - pmol	pmol DNA / mg beads
1	0,129	0,070	1,843	0,011	387,000	77,400
2	0,115	0,067	1,716	0,009	345,000	69,000
3	0,120	0,068	1,765	0,012	360,000	72,000
4	0,113	0,062	1,823	0,008	339,000	67,800
5	0,130	0,075	1,733	0,009	390,000	78,000
6	0,125	0,069	1,812	0,010	375,000	75,000
stdev	0,007	0,004	0,051	0,001	21,466	4,293
average	0,122	0,069	1,782	0,010	366,000	73,200
(St/Av)%	5,865%	6,176%	2,883%	14,969%	5,865%	5,865%

The results, from six independent immobilisation experiments, are presented in Table 7. The average DNA immobilisation yield per mg beads was found to be 60,4 pmol with a standard deviation of 6,4 pmol (10%).

In order to obtain more uniform immobilisation yield, the reaction time, in the second type of DNA immobilisation experiments, was extended to twelve hours under the same reaction conditions as described above. The results obtained are presented in Table 8. The average DNA immobilisation yield per mg beads was established to be 73,2 pmol with a standard deviation of 4,3 pmol (5,9%). The standard deviation was 41 % less than that for two hours' reaction time while the immobilisation increased by 17,5%.

Table 9 Quantification of non-specific DNA attachment to carboxyl-coated beads for two hours.

Number	OD 260 nm	OD 280 nm	OD 260 nm/ OD 280 nm	OD 320 nm	total DNA amount from 30 mg beads - pmol	pmol DNA / mg beads
1	0,089	0,049	1,816	0,010	267,000	8,900
2	0,095	0,051	1,863	0,015	285,000	9,500
3	0,085	0,046	1,848	0,017	255,000	8,500
stdev	0,005	0,003	0,024	0,004	15,100	0,503
average	0,090	0,049	1,842	0,014	269,000	8,967
(St/Av)%	5,613%	5,171%	1,286%	25,754%	5,613%	5,613%

The key point in every DNA immobilisation procedure is the amount of non-specifically attached DNA. In order to estimate that, the two sorts of DNA immobilisation experiments described above were repeated in the absence of the cross-linking reagent (EDAC) to 30 mg beads instead of 5 mg ones. Each type of

experiment was repeated three times. The results obtained for reaction time of two hours are presented in Table 9. The average non-specific DNA attachment per mg beads was established to be 9 pmol with a standard deviation of 0,5 pmol (5,9%). That means a 10 % non-specific DNA immobilisation yield.

Table 10 Quantification of non-specific DNA attachment to carboxyl-coated beads for twelve hours.

Number	OD 260 nm	OD 280 nm	OD 260 nm/ OD 280 nm	OD 320 nm	total DNA amount from 30 mg beads - pmol	pmol DNA / mg beads
1	0,114	0,062	1,839	0,010	342,000	11,400
2	0,115	0,061	1,885	0,015	345,000	11,500
3	0,119	0,064	1,859	0,017	357,000	11,900
stdev	0,003	0,002	0,023	0,004	7,937	0,265
average	0,099	0,057	1,488	0,063	262,611	11,600
(St/Av)%	2,679%	2,658%	1,567%	5,750%	3,022%	2,281%

The results obtained for reaction times of twelve hours are presented in Table 10. The average non-specific DNA attachment per mg beads was found to be 11,6 pmol with a standard deviation of 0,27 pmol (2,3%). That means a 16 % non-specific DNA immobilisation yield.

3.1.2 pH-dependent immobilisation of amino-labelled DNA to carboxyl-coated beads placed in cascably connected micro-fluidic chambers

The results described in the pervious section suggest that it could be difficult to reduce the non-specific DNA attachment to satisfactory minimum and to achieve a complete saturation of the immobilisation reaction to the beads by the means of the above described procedures. In order to increase the specificity of the immobilisation reaction of 5' amino-modified DNA to polystyrene carboxyl-coated beads placed in cascably connected micro-chambers, a novel reversible inhibition of the DNA immobilisation reaction was investigated. The procedure is based on a reversible pH change with a combination of segregated delivery of the amino-modified DNA and the cross-linking reagent (EDAC) used.

Most references to the use of EDAC describe an optimal reaction pH-range between 4,7 and 6, with the reaction, taking place efficiently up to at least pH 7.5 with a significant immobilisation yield. However, that reaction, like many other chemical reactions, is pH sensitive. The formation of the active intermediate o-Acylisourea (see Figure 7) is not possible in a highly alkali pH and

EDAC may be instable under that pH, thus affording an opportunity to apply the EDAC coupling procedure for a pH-directed, patterned DNA immobilisation using micro-fluidic networks.

Table 11 Quantification of 5' amino-modified DNA immobilisation to carboxyl-coated beads for two hours under pH reversible conditions.

Number	OD 260 nm	OD 280 nm	OD 260 nm/ OD 280 nm	OD 320 nm	total DNA amount from 5 mg beads - pmol	pmol DNA / mg beads
1	0,113	0,060	1,883	0,010	339,000	67,800
2	0,115	0,062	1,855	0,009	345,000	69,000
3	0,119	0,064	1,859	0,013	357,000	71,400
4	0,090	0,049	1,837	0,008	270,000	54,000
5	0,100	0,055	1,818	0,012	300,000	60,000
6	0,110	0,059	1,864	0,010	330,000	66,000
stdev	0,011	0,005	0,023	0,002	32,501	6,500
average	0,108	0,058	1,853	0,010	323,500	64,700
(St/Av)%	10,047%	9,317%	1,224%	18,018%	10,047%	10,047%

The results of the pH-dependent immobilisation of 5' amino-labelled synthetic DNA to carboxyl-coated beads, placed in eppendorf tubes and in micro-reactor chambers are presented here. An alkali pH shift of the immobilisation solution was employed to inhibit the DNA immobilisation reaction. Two sorts of experiments were performed in order to demonstrate experimentally a pH-dependent immobilisation of amino-labelled synthetic DNA to carboxyl-coated beads. The first type of DNA immobilisation experiments was performed in eppendorf tubes in order to check whether the immobilisation chemistry was working according to expectations. As far as the second type of experiments, is concerned, the established pH-dependent immobilisation procedure was utilised for spatially defined DNA attachment to carboxyl-coated beads placed in cascably connected micro-reactors.

As a positive control for DNA immobilisation, 5 mg carboxyl-coated beads (see Table 4, line 2) were incubated in a 125 mM MES buffer solution, pH 4.7, 25 mM NaOH in the presence of 10 μ M of 5' amino-labelled DNA (see Table 3, line 4) and 50 mM EDAC as described in section 2.2.2.1.III. The DNA immobilisation results obtained are presented in Table 11. They are very similar to those obtained under standard buffer conditions presented in Table 7.

Table 12 Inhibition of 5' amino-modified DNA immobilisation to carboxyl-coated beads by a pH change

Number	OD 260 nm	OD 280 nm	OD 260 nm/ OD 280 nm	OD 320 nm	total DNA amount from 30 mg beads - pmol	pmol DNA / mg beads
1	0,013	0,011	1,182	0,001	0,000	0,000
2	0,016	0,012	1,333	0,009	0,000	0,000
3	0,001	-0,001	-1,000	0,013	0,000	0,000
4	0,001	-0,007	-0,143	0,007	0,000	0,000
5	0,002	-0,002	-1,000	0,013	0,000	0,000
6	0,009	0,007	1,286	0,010	0,000	0,000
stdev	0,113	0,008	1,130	0,004	0,000	0,000
average	0,007	0,003	0,276	0,009	0,000	0,000

As a control for pH-dependent inhibition of the DNA immobilisation reaction, 30 mg carboxyl-coated beads (see Table 4, line 2) were incubated in a 62.5 mM MES buffer, pH 6.1, in the presence of 10 μ M 5' amino-labelled DNA (see Table 3, line 4), 50 mM EDAC and 150 mM NaOH. The pH value of the solutions was found to be above 12. The immobilisation reaction was performed in six repeats as described in section 2.2.2.1.IV. The DNA immobilisation results obtained are presented in Table 12. As one can see no DNA immobilisation yields could be detected by UV absorbance in those experiments. In order to test the accessibility of the immobilised 5' amino-modified DNA to hybridisation the carboxyl-coated beads five different types of hybridisation experiments were carried out. In all hybridisation experiments 1 mg carboxyl-coated beads immobilised with the same DNA oligomers (see Table 3, line 4) used before, were employed. The hybridisation experiments were performed in a 500 mM Tris-acetate buffer, pH 8.3, and 50 mM NaOH in the presence of perfectly complementary 5' R6G labelled DNA (see Table 3, line 1) as described in section 2.2.3.2. Next to the hybridisation, the beads were washed and DNA hybridised to the beads was denatured by heating as described in the same section.

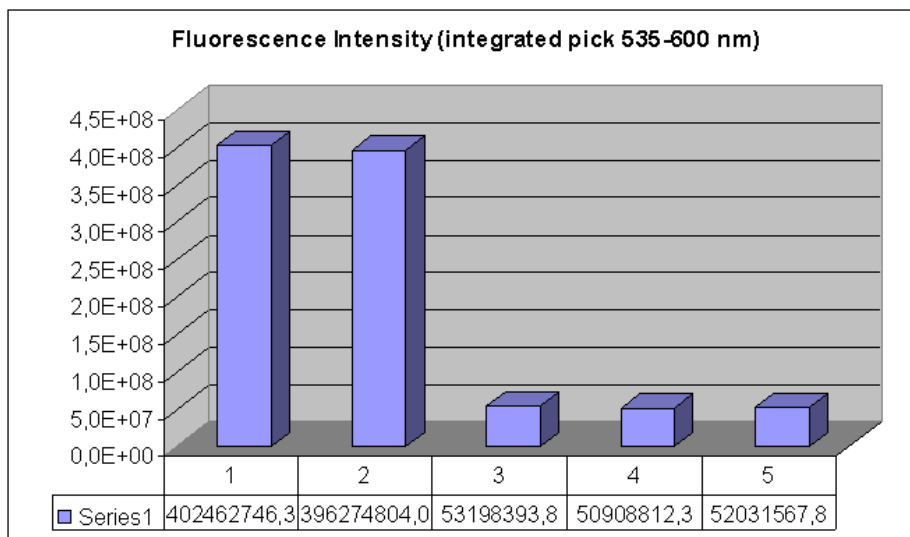


Figure 12 Hybridisation analyses of 5' amino-labelled DNA immobilisation to carboxyl-coated beads.

1: a positive immobilisation; 2: a positive immobilisation; 3: without any immobilisation reaction; 4: an immobilisation reaction in alkali pH (NaOH); 5: a negative immobilization control in the absence of EDAC. Each experiment was performed in four repeats and the average values are plotted. The complete experimental data are presented in Table 23.

Each hybridisation experiment was repeated four times. The average results are presented in Figure 12, while the complete experimental data are presented in Table 23. The amount of denatured DNA was established using the titration curve presented in Figure 10. In the first design of hybridisation experiments, beads with an immobilisation yield of 66 pmol/mg (Table 11, line 6) were used. The hybridisation yield was found to be 46 pmol/mg beads. In the second design of hybridisation experiments, beads with an immobilisation yield of 60 pmol/mg (Table 7, line 2) were used. The hybridisation yield was 44 pmol/mg beads. In order to find the amount of non-specifically attached DNA, beads without immobilised DNA were used. The non-specific DNA attachment was found to be 8 pmol/mg beads (see Figure 12_3). Beads from the pH-dependent inhibition of the immobilisation reaction were used in subsequent hybridisation experiments (see Table 12, line 5). The DNA amount was established to 7.0 pmol/mg beads, which means that no immobilisation took place on those beads. Almost the same result (7.5 pmol/mg) was obtained in the last hybridisation experiments using beads immobilised with DNA in the absence of EDAC (see Table 9, line 3).

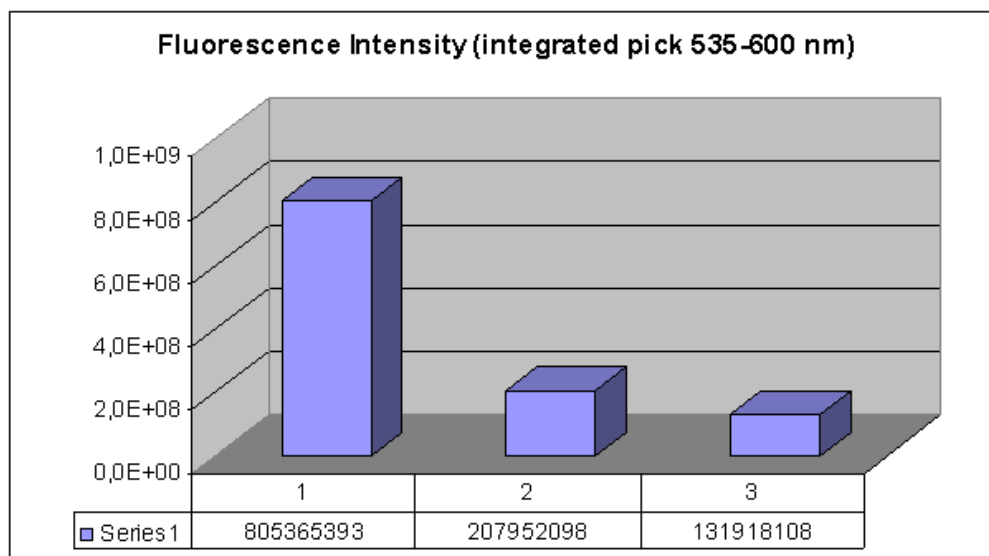


Figure 13 Hybridisation analyses of 5' amino-labelled DNA immobilisation to carboxyl-coated beads by sodium hydroxide and temperature denaturing. 1: a DNA hybridisation 2: a DNA attachment to non-immobilised with DNA beads: 100 NaOH denaturing: 3: As 2 but a temperature denaturing applied. Each experiment was made in three repeats as the average values are plotted. The complete experimental data are presented in Table 24.

In the next hybridisation experiments 2 mg beads with immobilised DNA (54 pmol/mg, see Table 11, line 4) were used for the same hybridisation experiments as described above, with the difference that sodium hydroxide denaturing was employed instead of temperature. Every experiment was made in three repeats complete experimental data are presented in Table 24. The DNA amount per mg beads was 43 pmol. Beads without immobilised DNA were used in the next experiments. In one case DNA non-specifically attached was denatured by 100 mM NaOH (at 25 °C, for 1 min) while in the other case, temperature denaturing (at 93 °C for 2 min), was employed. As one can see from Figure 13, the sodium hydroxide denaturing (second column) yielded 11 pmol DNA/mg beads, while the temperature denaturing resulted in 8 pmol DNA/mg beads. It is obvious that sodium hydroxide denaturing of DNA on a surface is stronger than denaturing by using temperature it is therefore important to use beads with the lowest possible level of non-specific DNA attachment when sodium hydroxide denaturing is applied. Carboxyl-coated beads possess lower level of non-specific DNA attachment than the amino-coated ones.

All DNA immobilisation experiments performed up to now suggested that it is possible to inhibit the immobilisation of amino-modified DNA to carboxyl-coated beads by a pH-change. It is next demonstrated how that immobilisation procedure could be employed for programmable immobilisation of specific DNA to beads incorporated in cascadably connected micro-chambers.

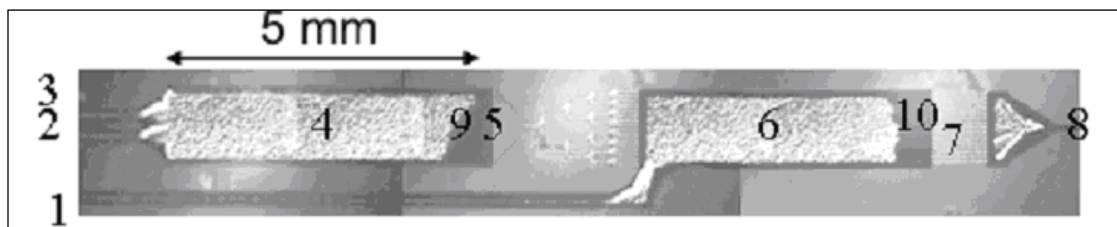


Figure 14 A picture of two cascadably connected micro-chambers: *The three inlet channels (1, 2, 3), the outlet channel (8) and the two chambers (4, 6) each with its own bead barrier (5, 7) are shown. Beads are introduced into the first (9) and second (10) chamber and restrained there by the bead barrier. The depth of the channels and the two chambers is 140 μm . The depth of the intervening bead barriers is 10 μm .*

The use is presented here of the chemical procedures already described in the current chapter for spatially defined DNA immobilisation to carboxyl-coated beads (see Table 4, line 2) incorporated in cascadably connected micro-chambers. The micro-reactor used is presented in the Figures 14 and 5.

The pH-dependent inhibition of the immobilisation reaction upon mixing in cascadably connected micro-chambers was tested as described in section 2.2.2.2.I. A 50 mM MES buffering solution, pH 6.1, containing 50 mM EDAC and 10 μM 5' end-amino-modified DNA and 100 mM NaCl (see Table 3, line 4) was delivered through inlets number 2 and 3 (see Figure 14). 250 mM NaOH was delivered simultaneously through inlet number 1. The applied flow rates (see Figure 41) allowed complete mixing between the flow coming from the first chamber and the solution delivered through the first inlet. The immobilisation was carried out for three hours. After a washing step (see section 2.2.2.2.I) 1 μM , 5' R6G- labelled, perfectly matching DNA (see Table 3, line 1), dissolved in 500 mM Tris-acetate, pH 8.3, and 50 mM NaOH, was delivered through all inlets at a flow rate of 0.5 $\mu\text{l}/\text{min}$ for an hour at 40 $^{\circ}\text{C}$. Next, the beads were washed with the hybridisation buffer in the absence of DNA for half an hour under the same conditions. Fluorescence images were taken from the beads placed in the two chambers using a CCD Photometrix, CH250, camera as described in section 2.2.6.2.I (see Figure 11). The results obtained are presented in Figure 15. As one

can see, there is a fluorescence signal on the beads placed in the first chamber (see Figure 15_A) while there is no fluorescence signal on the beads in the second chamber (see Figure 15_B). The intensity profiles of both images across the indicated transects are plotted in Figure 15_C. As can be seeing from the plot, the signal of the second images had values of 500 cps, which was equal to the camera's bias. The results prove the feasibility of using of inhibition of the immobilisation reaction by mixing in cascably connected micro-chambers.

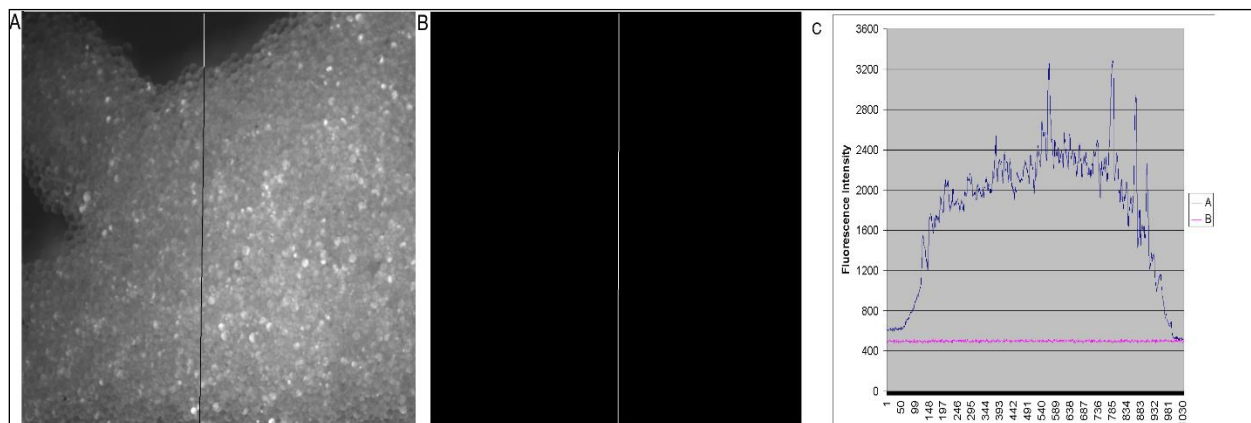


Figure 15 Inhibition of the DNA immobilisation upon mixing in cascably connected micro-chambers. Hybridisation analyses. Carboxyl-coated beads were incorporated in two cascably connected micro-reactor chambers as shown in Figure 14. $10 \mu\text{M}$ 5' amino-labelled DNA, solved in 50 mM MES, pH 6.1, 50 mM EDAC was pumped through inlets number 2 and 3 (see the previous Figure 14). A 250 mM NaOH solution was pumped simultaneously through inlet number 1. The reaction was performed for 3 hours at 25 °C. After washing, $1 \mu\text{M}$ 5' rhodamine-labelled DNA, perfectly complementary to the immobilised DNA, dissolved in a 500 mM Tris-acetate buffer, pH 8.3, 50 mM NaOH was pumped through all inlets for one hour at 40 °C. The beads were washed by pumping of a 500 mM Tris-acetate buffer, pH 8.3, 50 mM NaOH. **A:** A laser light image from the beads placed in the first chamber. There is hybridisation. **B:** A laser light image from the beads placed in the second chamber. There is no hybridisation. The bias of the camera (CH250) was found to be 500 cps. The exposure time was one second. **C:** Fluorescence intensity profiles from images A and B are plotted.

A spatially defined DNA immobilisation to beads placed in cascably connected micro-chamber was achieved in the next experiment by a segregate delivery of the DNA and the cross-linking reagent used (EDAC), see section 2.2.2.2.II. The same amino-modified DNA and the same flow rates as in the previous experiment were applied. The DNA dissolved in 50 mM MES solution, pH 6.1, was delivered through inlets number two and three (see Figure 14). 50 mM EDAC dissolved

in 50 mM MES, pH 6.1, was pumped simultaneously through inlet 1. After to the immobilisation the same DNA hybridisation and washing procedures were performed as described above. Fluorescence images were taken from the beads placed in the two micro-chambers. The results are presented in Figure 16. As one can see there is a fluorescence signal only on the beads incorporated into the second chamber (Figure 16_B). As expected DNA immobilisation took place to the beads situated in the second chamber because EDAC was presented only there but not in the first chamber.

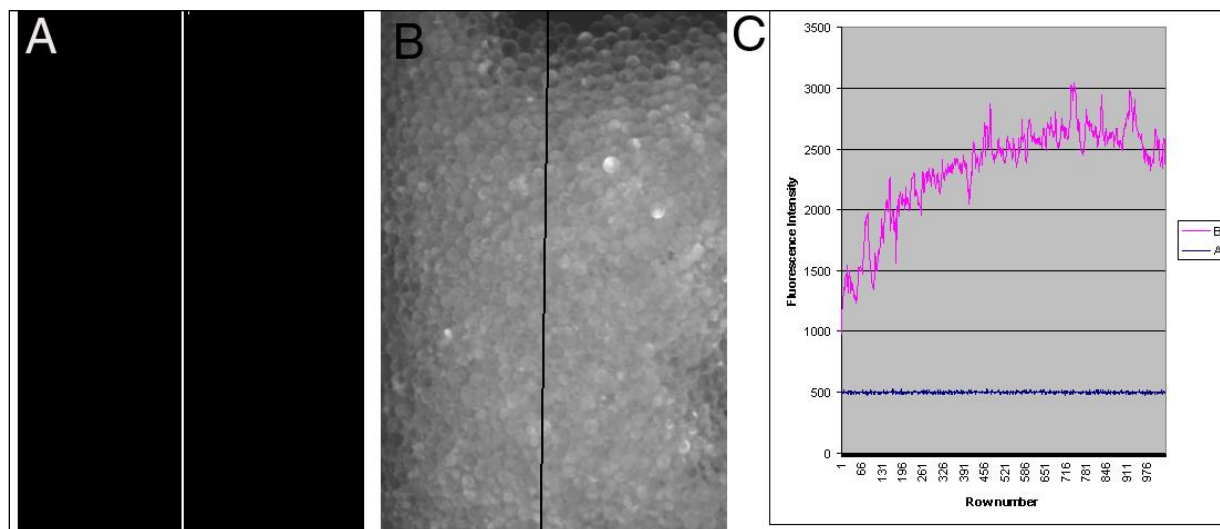


Figure 16 Specific immobilisation by a separate delivery of the DNA oligomer and the cross-linking reagent in cascably connected micro-reactor chambers. Hybridisation analyses. *10 μ M 5' amino-labelled DNA dissolved in 50 mM MES, pH 6.1 was pumped through the second and third inlet (see Figure 14). 50 mM EDAC solved in 50 mM MES was pumped simultaneously through the first inlet. The process was carried out for two hours at 25 °C. The DNA immobilisation took place to the beads in the second chamber just because EDAC was supplied only in that chamber. After the immobilisation, the beads were washed with a 100 mM Tris, buffer, pH 8.3 for twenty minutes and were hybridised with 5' R6G-labelled perfectly matching DNA. The unbound DNA was removed. A: Laser light image from the beads placed in the first chamber. There is no any hybridisation. B: Laser light image from the beads placed in the second chamber. There is a hybridisation. The bias of the camera (CH250) was found to be 500 cps. The exposure time was one second. C: Fluorescence intensity profiles from images A and B are plotted.*

Finally, a pH reversible chemistry for DNA immobilisation in the same micro-flow reactor using the same beads and DNA was demonstrated (see section 2.2.2.2_III). 10 μ M 5' amino-labelled DNA dissolved in 50 mM NaOH was delivered through inlets number two and three (see Figure

14). 50 mM EDAC dissolved in 250 mM MES, pH 4.7, was pumped simultaneously through inlet number one. After the immobilisation the same DNA hybridisation and washing procedures were performed as described above. The fluorescence images are shown in Figure 17. As is obvious, there is a fluorescence signal only from the beads incorporated into the second chamber (Figure 17_B). As expected, DNA immobilisation took place on the beads situated in the second chamber while any kind of non-specific attachment of DNA on the beads placed in the first chamber was avoided. In sections 3.1.5 and 3.4.4 is presented how all DNA immobilisation procedures, established here, could be used for spatially defined immobilisation of DNA in parallel for the producing of microfluidic DNA chips.

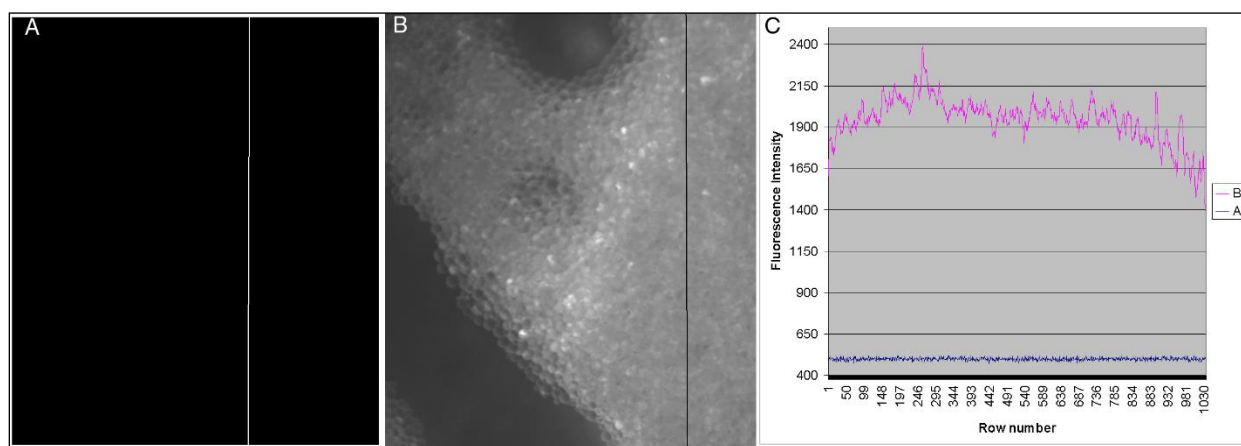


Figure 17 Specific DNA immobilisation by a reversible pH change in cascadedly connected micro-reactor chambers. Hybridisation analyses. *10 μ M 5' amino-labelled DNA dissolved in 50 NaOH was pumped through the second and third inlet. 50 mM EDAC solved in 250 mM MES was pumped simultaneously through the first inlet. The process was carried out for two hours at 25 °C. DNA immobilisation took place just to the beads in the second chamber. After the immobilisation, the beads were washed in a 100 mM Tris, buffer, pH 8.3, for twenty minutes. A DNA hybridisation and washing were performed under the same conditions as described in the two previous Figures. **A:** Laser light image from the beads placed in the first chamber. There is no hybridisation. **B:** Laser light image from the beads placed in the second chamber. There is hybridisation. The bias of the camera (CH250) was found to be 500 cps. The exposure time was one second. **C:** Fluorescence intensity profiles from images A and B are plotted.*

3.1.3 Immobilisation of thiol-modified DNA to carboxyl-coated beads

The results of immobilisation of 5' end thiol modified DNA (see Table 3, line 4) to carboxyl-coated beads (see Table 4, line 2) by the use of bifunctional cross-linking reagent PDPH are presented here. The immobilisation procedure is described in section 2.2.2.3. It consists of two main reactions (see Figure 8). Firstly, the hydrazide group of PDPH reacts with the carboxyl group on the beads surface forming a peptide bond (see Figure 8_1A and 1B) using EDAC. Next, the thiol group of the DNA reacts with the pyridyldithio group on the bead surface forming a disulfide bond (see Figure 8_2).

Table 13 Quantification of 5' end thiol-modified DNA immobilisation to carboxyl-coated beads

Number	OD 260 nm	OD 280 nm	OD 260 nm/ OD 280 nm	OD 320 nm	total DNA amount from 10 mg beads- pmol	pmol DNA / mg beads
1	0,163	0,090	1,811	0,008	489,000	48,900
2	0,145	0,081	1,790	0,012	435,000	43,500
3	0,149	0,084	1,774	0,010	447,000	44,700
4	0,161	0,093	1,731	0,009	483,000	48,300
5	0,143	0,079	1,810	0,011	429,000	42,900
6	0,139	0,075	1,853	0,007	417,000	41,700
stdev	0,010	0,007	0,041	0,002	29,577	2,958
average	0,150	0,084	1,795	0,008	450,000	45,000
(St/Av)%	6,573%	8,130%	2,288%	18,893%	6,573%	6,573%

After washing, the immobilised DNA was cleaved from the beads and purified as described in section 2.2.5. The DNA amount was established by UV absorbance as described in section 2.2.6.1. The obtained results are presented in Table 13. As one can see the average DNA immobilisation yield per mg beads was established to be 45 pmol.

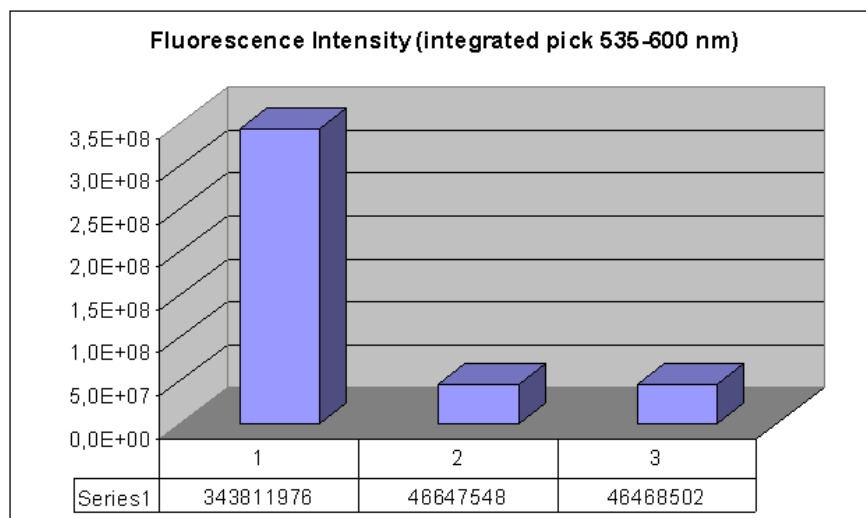


Figure 18 DNA/DNA hybridisation analysis on 5' thiol immobilised DNA to carboxyl-coated beads.
1: Positive immobilisation reaction. **2:** Negative immobilisation reaction in the absence of PDPH. **3:** Negative immobilisation reaction on non-treated beads. Each experiment was made in three repeats as the average values are plotted. The complete experimental data are presented in Table 25.

The immobilised thiol-modified DNA on 1 mg beads was used in hybridisation analyses with perfectly complementary, 5' R6G-labelled DNA (see Table 3, line 1) at 35°C as described in section 2.2.3.2. The amount of hybridised DNA was established by quantification of the fluorescent signal of R6G using the standard titration curve (see Figure 10) as described in section 2.2.6. The obtained results are presented in Figure 18. The first column shows a DNA hybridisation yield of 36.5 pmol per mg beads carrying DNA immobilised through 5' end thiol as described above. The second column demonstrates the non-specific attachment yield (6.7 pmol/mg) on 1 mg beads treated as described above but in the absence of PDPH. The same amount of DNA was detected in the last case in which untreated beads were used (see Figure 18, column 3). The complete experimental results of those experiments are presented in Table 25.

3.1.4 Photo-dependent immobilisation of synthetic DNA to amino-coated beads

In recent years, DNA chip-based assays have become a familiar approach suitable for a broad range of applications such as expression analysis, polymorphism analysis and genotyping, and the detection of pathogens. The expansion of DNA chip technology has encouraged the rapid development of light-directed oligonucleotide synthesis. Light-directed oligonucleotide synthesis has proven to be an efficient method for fabricating probe arrays with densities as high as 10^6 unique sequences/cm²^{xliii}. Nevertheless,

there are some common errors in optical oligonucleotide synthesis, such as premature truncations of the growing strand and base deletions, which seem difficult to avoid^{xliv}. Potentially, replacing the light-directed oligonucleotide synthesis with light-directed oligonucleotide immobilisation could reduce the error rate in DNA chips due to these factors. Despite the existence of a great number of different chemical methods for specific 5' and 3' end covalent DNA attachment, there are only few approaches for the photo-immobilisation of DNA.

Here is proposed a novel method⁴⁰ for light-dependent covalent immobilisation of 5' end amino-modified synthetic DNA, based on the hetero-bifunctional, photoreactive cross-linking agent 4-nitrophenyl 3-diazopyruvate (DAPpNP)^{xlv}. As a solid support for the photo-immobilisation of DNA polystyrene amino-coated super-paramagnetic beads are applied (see Table 4, line 1).

In contrast to chemical cross-linking reagents such as PDPH, which have been successfully applied for DNA immobilisation, photo-reactive cross-linking reagents have been primarily employed as tools for defining interactions among proteins, nucleic acids, ligands and their receptors. The major disadvantage in using photoreactive cross-linking reagents for DNA immobilisation is that such agents form extremely reactive groups after photo-activation, usually causing many non-specific side reactions.

In this work, for the attachment of DNA I avoid directly utilising the amino-ketene group, formed after photolysis of a diazo group of diazopyruvic acid^{xlvi}, because of its high reactivity and its instability in aqueous solutions. Instead, I facilitate the transformation of the ketene group into a carboxyl group, which is then utilised for reaction with 5' amino-modified deoxynucleotide oligomers (see Table 3, line 8) in the presence of EDAC (see Figure 9).

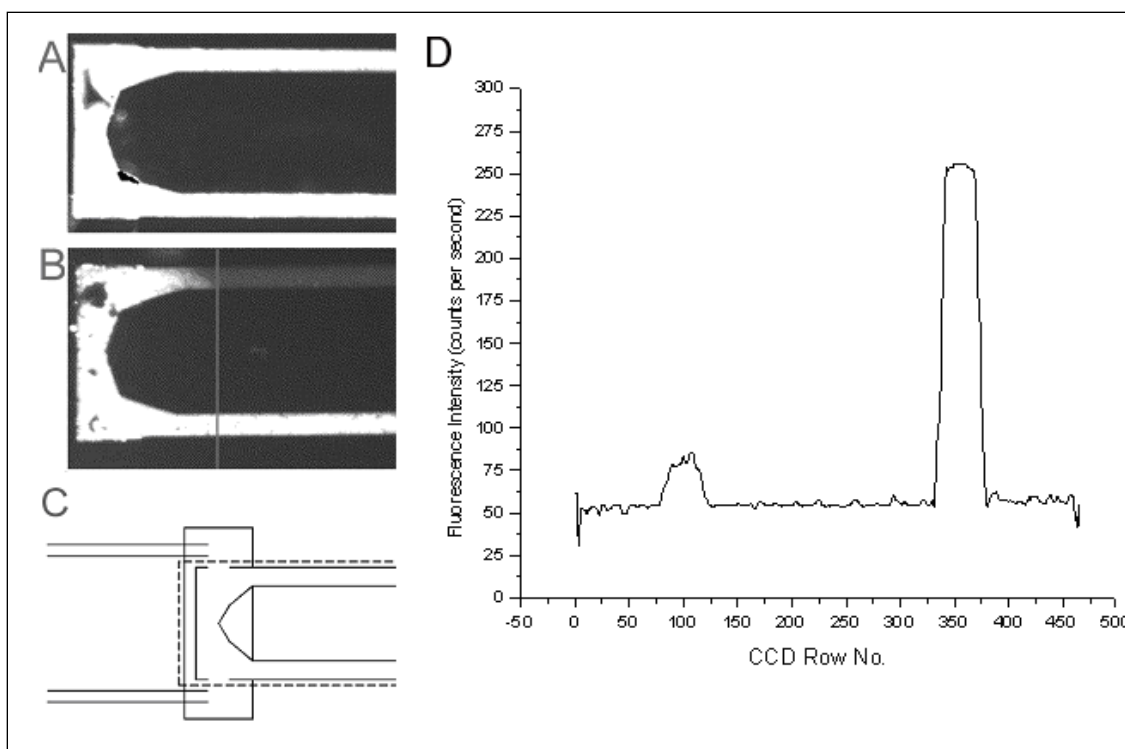


Figure 19 Light-dependent DNA immobilisation to beads in micro-flow reactor channels. **A:** *White light image. Both inlet channels of a micro-reactor are filled with beads.* **B:** *Fluorescence image. Fluorescent signal from the beads incorporated in a micro-flow reactor obtained by a CCD LN camera. The greyed column indicates the area profiled in D and shows the line of segregation between the irradiated part (on left hand) and non-irradiated part (on right hand) of the inlet channel on the top of the picture.* **C:** *Micro-flow reactor scheme. The two inlet channels (on the right hand side of the scheme), two outlet channels (on the left-hand side of the scheme) and the bead barrier are shown. The dashed square shows the part of the micro-flow reactor presented on images A and B.* **D:** *Quantification of the fluorescent signal of spatially defined light-directed DNA immobilisation to beads in a micro-flow reactor. An intensity section of Image 3B is shown. Between rows 75 and 125 – the signal from the beads in the channel not exposed to light with an intensity of 80 cps (counts per second). Between row 325 and 375 – the signal from beads in the channel exposed to light with intensity above 250 cps. The background signal is around 50 cps.*

Here it is demonstrated a spatially defined light-directed DNA immobilisation to magnetic beads incorporated in a micro-flow reactor (see Figure 4)⁴⁰. The light-directed DNA immobilisation reaction was carried out as described in section 2.2.2.4. As one can see from the fluorescent image in Figure 19_B, the beads in the channel not exposed to light show a very low fluorescent signal in comparison with the fluorescent signal from the beads exposed to light. Both inlet channels of

the micro-flow reactor are indeed filled with beads as shown in the white light image of Figure 19_A. The quantification of the fluorescent signal is shown in Figure 19_D.

3.1.5 Discussion

A light-directed DNA immobilisation has only one photo-reactive step in contrast to the light-directed DNA synthesis, which has many photo-reactive steps. The photo-activation efficiency is in any case lower than the reactive efficiency of a non-photodependent chemical reaction. To this effect, the use of light-directed DNA immobilisation instead of light-directed DNA synthesis could potentially increase the density of the different DNA oligomers attached to the chip surface. The approach, for photo-directed immobilisation of DNA, proposed by me⁴⁰, depends to a great extent on the quality of the used photo-reactive chemical. In the presence of water, DAPpNP undergoes hydrolysis, forming nitro-phenol and diazopyruvate, which has a carboxyl group. That carboxyl group in free solution could react with the diazo group introduced on the bead surface reducing the photo-activation yield. The carboxyl group on the bead surface formed as a result of the photo-activation cannot react with the non-photo-activated diazogroup that is attached to the chip surface. The photo-activation on beads seems to be more difficult than that on a plane surface. It could be an additional problem for the photochemical activation if the beads are in several layers.

It is well known that amino-coated beads demonstrate much more non-specific DNA attachment than the carboxyl-coated ones, due to the positive charge of the amino-group^{40, 50, 51}. It has been proven that the DNA non-specifically attached to the beads is not available for hybridisation⁴⁰. Nevertheless, the non-specifically attached DNA is almost completely washed by a 50 mM NaOH solution. That does not make the amino-coated beads the best choice when using a sodium hydroxide denaturation of DNA.

Actually, there is no need for spatially defined DNA immobilisation with a high resolution, when one wants to immobilise specific DNA to beads placed in cascably connected micro-reactors. When applying novel micro-fluidic architecture which I here propose (see Figures 20 and 46) one can use any cross-linking coupling procedure for programmable bio-molecular immobilisation of unique molecules to beads placed in cascably connected micro-chambers or to their surfaces in parallel.

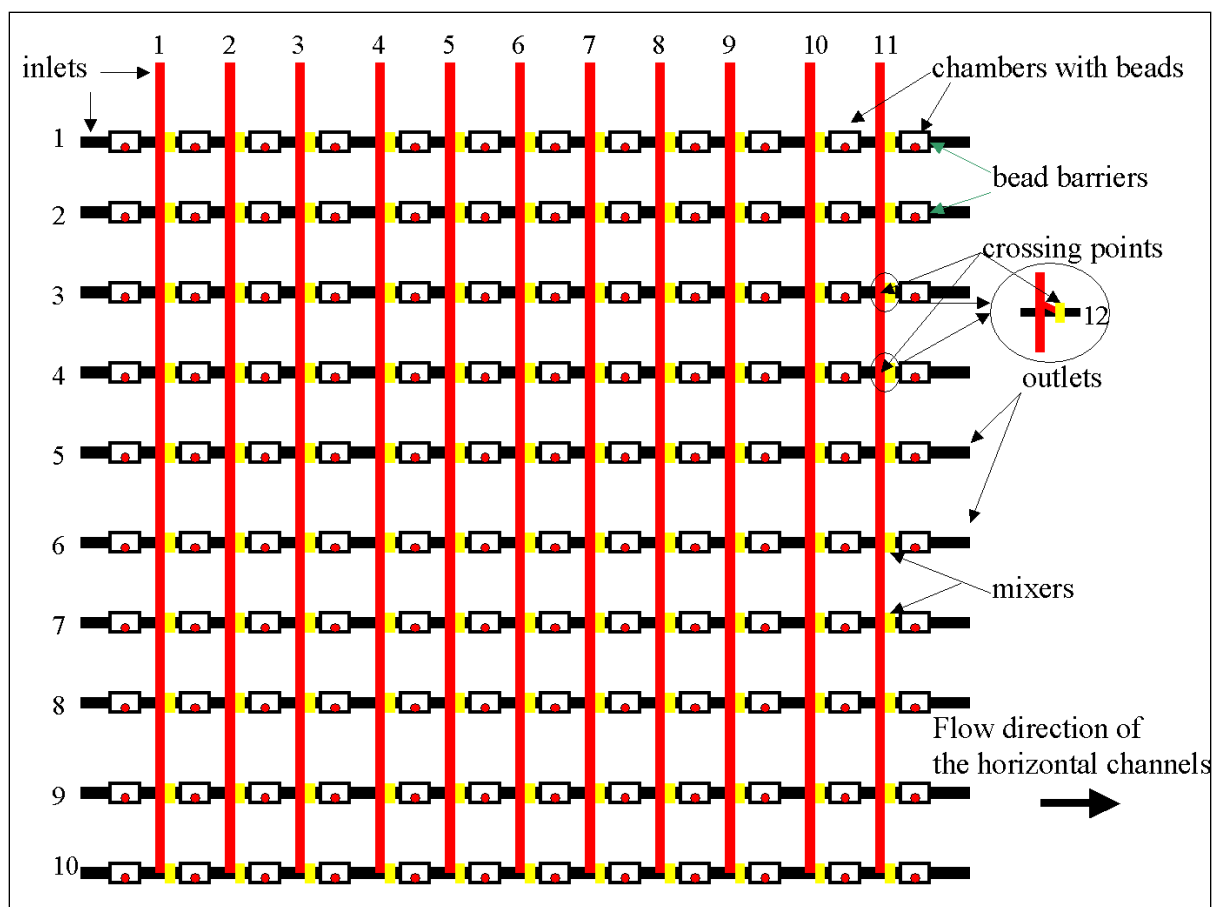


Figure 20 Micro-fluidic architecture for spatially defined parallel bio-molecular immobilisation to beads incorporated in cascadably connected micro-reactor chambers or to their surfaces. *There are ten horizontal channels crossed by eleven vertical channels (110 crossing points secured by small connecting channels). After each crossing point there is a mixing structure. There are 120 chambers with an etched bead barrier at the bottom of each one. Carboxyl-coated magnetic beads are incorporated in all 120 chambers. The horizontal chambers are used to pump different sequences of 5' or 3' end amino-modified DNA in 50 mM MES, pH 6.1. The vertical channels are used to deliver 100 mM NaOH or EDAC. The presented micro-fluidic architecture allows parallel immobilisation of specific bio-molecules (DNA, RNA, polypeptides) to the bead incorporated in different chambers applying almost any type of cross-linking bio-conjugate chemistry.*

The scheme of the micro-flow reactor's architecture presented in Figure 20 contains 10 horizontal channels crossed by eleven vertical channels via small connecting channels (see Figure 20, point 12) in 110 crossing points. There is a mixing structure, after each crossing point, followed by a chamber, representing a part of the horizontal channels. The number of chambers is 120. Each chamber has a bead

barrier at the bottom. Paramagnetic beads could be delivered to each chamber via the vertical channels except for the chambers of the first row, the beads being delivered by the horizontal channels. The micro-flow reactor has 21 inlets and 10 outlets. The number of inlets from the vertical channels could be reduced to not more than two regardless of the number of vertical channels as shown in Figure 46. For more details on the concrete implementation of the microfluidic design see section 3.4.4, Figures 46 and 47.

I here present the use of the procedures established by me for programmable attachment of DNA to beads placed in cascably connected micro-chamber (see section 3.1.2) using the above described microfluidic architecture. Firstly, ten different 5' amino-labelled DNA sequences solved in 25 mM MES buffer, pH 6.1, are pumped through the horizontal channels. 50 mM EDAC dissolved in 25 mM MES, pH 6.1, is pumped simultaneously through a vertical channel number 11. All other inlets from the vertical channels are closed. The pressure in the small connecting channels of the eleventh vertical channel is similar to the pressure in the ten horizontal channels so that the flow direction is as shown in Figure 20 (for more details see Figure 47). Under those conditions, the EDAC is delivered only to the beads incorporated in the micro-chambers of the last row. Thus DNA immobilisation takes place only to the bead in the chambers of the last row.

In the next step, the other ten 5' amino-modified DNA oligomers are pumped through the horizontal channels. EDAC is delivered via the tenth vertical channel. In order to prevent any DNA immobilisation to the already addressed beads in the chambers of the last row, 250 mM NaOH is pumped simultaneously through the last vertical channel. That process could be used for immobilisation of 120 unique DNA sequences to beads placed in 120 different chambers or to carboxylate surfaces of the chambers in 12 steps. As already demonstrated experimentally the chemical procedure guarantees an absolute level of specific DNA immobilisation to the beads (see section 3.1.2).

The hybridisation accessibility of the immobilised DNA was about 80 % in the case of thiol-modified DNA oligomers and about 70% in the case of amino-modified DNA oligomers. That difference could be due to some additional immobilisation reaction to the amino-group of the bases in the immobilisation process of amino-modified DNA. The difference is compensated by the different DNA immobilisation yield between the two immobilisation procedures. However one should pay note that the thiol group is pretty unstable in water solutions due to oxidation, which could decrease additionally the DNA immobilisation yield.

The presented microfluidic design is universal, since any type of bio-molecule (DNA, RNA, polypeptides) could be selectively immobilised to the beads placed in different chambers or to their surface using almost any bio-conjugate chemistry. Thus, the microfluidic chip could be used to making DNA, RNA or polypeptide based arrays with applications in molecular diagnostics, bio-molecular *in vitro* selection techniques, drug discovery, DNA computing.

The main immobilisation scheme based on the proposed micro-fluidic architecture with a combination of micro-valves is presented in section 3.4.4 (see Figure 46). The use of any cross-linking reagent in this scheme can be described as follow: N in number different bio-molecules are delivered through N in number horizontal channels. The molecules could be either modified or not depending on the chemistry employed. The cross-linking reagent is simultaneously delivered through the last vertical channel. As a result, a bio-molecular attachment takes place in the chambers from the last column (vertical row). In the next step, other N in number different bio-molecules are delivered through the horizontal channels as the cross-linking reagent is delivered, this time, through the M-1 vertical channel. An inhibitor of the immobilisation reaction is simultaneously delivered through the last vertical channel. The immobilisation scheme could be repeated M+1 times (row chamber number), that guarantees specific immobilisation of unique bio-molecule to each micro-chamber ($M+1 \times N$ in number) in M number immobilisation steps. The use of already established micro-fluidic mixers^{xlvii} offers the opportunity for integrating large number of selection modules (chambers). Both processes – the immobilisation and the selection (see section 3.4) could be implemented using the microfluidic device described, with a high level of parallelism and could be fully automated by using of liquid handling systems. The number of vertical inlets could be reduced to one or maximum two, by the use of valves as shown in Figure 46, section 3.4.4. The microfluidic chip is fully reusable (re-programmable) due to the possibility of replacement of the used super-paramagnetic beads, using a magnetic stand (see Table 5).

3.2 FIDELITY OF DNA HYBRIDISATION

When using a pool of different oligonucleotides in hybridisation analysis, the goal is to find uniform conditions for all oligomers that are stringent enough to guarantee specificity, on one hand, and, relaxed enough to allow formation of stable DNA hybrids at an acceptable rate, on the other hand. In this chapter I am investigating the ways of finding the optimal conditions to achieve the compromise between the DNA hybridisation yield and the accuracy of the DNA hybrids formed.

3.2.1 Fidelity of DNA hybridisation in different solutions

The solutions used in nucleic acid hybridisation analysis influence the fidelity of the hybridisation reaction. Here, I am testing different buffer solutions in regard to their capacity to discriminate between perfectly matching DNA hybrids, on one hand, and those with some mismatches, on other hand. The tested buffer solutions are selected for their buffer capacity. All selected solutions should be able to buffer an equal volume of 100 mM NaOH while deviating from their pH within 0.15 units because my aim was to establish chemistry for multi-step DNA hybridisation transfer under isothermal conditions by reversible pH alterations as will be described in section 3.4. In order to estimate the stability of certain DNA hybrids the free energy of the hybridisation reaction was computed using thermodynamic parameters, defined by John SantaLucia.

In order to investigate the DNA hybridisation fidelity in different buffer solutions, a quenching system was used (see section 2.2.3.1). One of the DNA strands was 3' end TAMRA, 5-isomer, labelled. The complementary strand was 5' end QSY-7 labelled. TAMRA, 5-isomer, has an absorption maximum at 546 nm, an emission maximum at 579 nm and an extinction coefficient of $91\,000\text{ cm}^{-1}\text{ M}^{-1}$. The quencher QSY-7 has an absorption maximum at 560 nm and an extinction coefficient of $92\,000\text{ cm}^{-1}\text{ M}^{-1}$, making it a suitable quencher for TAMRA. The ability of QSY-7 to quench the emission signal of TAMRA was tested using two perfectly matching strands, one 3' TAMRA labelled and other 5' QSY-7 labelled, as shown in Figure 21. Three series of experiments were performed. During the first sort of experiments $1\text{ }\mu\text{M}$ 3' end TAMRA labelled DNA (see Figure 21_B.1) was incubated for 30 min at $25\text{ }^{\circ}\text{C}$ in a $100\text{ }\mu\text{l}$ solution of a 500 mM Tris-acetate buffer, pH 8.3, and 50 mM NaOH. The second type of experiments was performed under the same conditions but an additionally $0.5\text{ }\mu\text{M}$ 5' end QSY-7 labelled DNA oligomer complementary to the $1\text{ }\mu\text{M}$ 3' end TAMRA labelled DNA was added (see Figure 21_B.2). The last type of experiments was

performed under the same conditions but in the presence of 1 μM 5' end QSY-7 labelled DNA oligomer and complementary 1 μM 3' end TAMRA labelled DNA (see Figure 21_B.3). Each type of experiments was performed five times. The average results with a standard deviation of $\pm 3\%$ are plotted in Figure 21_A. As one can see, the quenching effect was 41 times, which implies 97.50 % quenching efficiency. The complete experimental data are presented in Table 26.

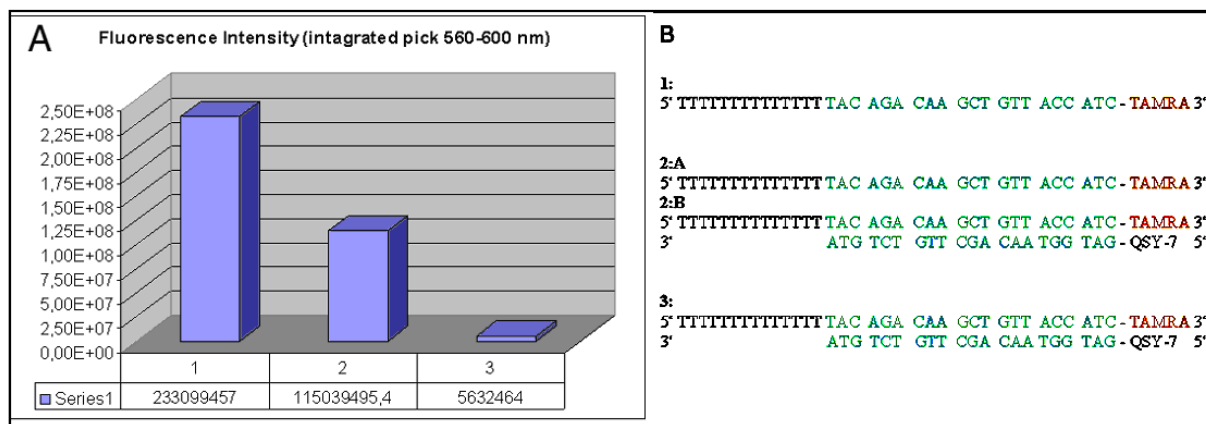


Figure 21 Quenching efficiency of QSY-7 towards TAMRA. 1: Fluorescence intensity signal (the integrated pick from 560 to 600 nm) of 3' TAMRA labelled DNA oligomer in a concentration of 1 μM ; 2: Fluorescence intensity signal of 1 μM 3' TAMRA labelled DNA in the presence of 0.5 μM , 5' QSY-7 labelled, perfectly-matching complementary oligomer. 3: Fluorescence intensity signal of 1 μM 3' TAMRA labelled DNA in the presence of 1 μM , 5' QSY-7 labelled, perfectly-matching complementary oligomers. Both reactions were carried out at 25 °C in a 100 μl solution of a 500 mM Tris – acetate buffer, pH 8.3, and 50 mM NaOH in five repeats as the average values are presented. The complete experimental data are presented in Table 26. The quenching efficiency was established to be about 97.5 %.

The free energy (ΔG_{37}°) gap between the perfect DNA hybrids shown in Figure 22_B_4 and those with five mismatches shown in Figure 22_B_3 was 17.0 kcal/mol over the length of 21 nt. That is a significant difference, which allows the DNA hybridisation reaction to reach an equilibrium (in 500 mM Tris-borate, pH 8.3, and 50 mM NaOH at 45 °C), in which no DNA hybrids with five (no quenching, see Table 14, line 2, column 3) mismatches (see Figure 22_A; 3_first column and 5_first column) were formed. In the case of perfectly matching strands, there was ca 89 % hybridisation yield (see Table 14: Tris-borate line: (column 3/column 4) *100). A similar result was obtained for a Tris-acetate buffer solution, where the hybridisation yield was higher than 94 % (see Table 14: Tris-acetate line: (column 3/column 4) *100). In order to convert the fluorescence signal into DNA amount, a standard titration curve of the 3' TAMRA labelled DNA was made (see Figure 24).

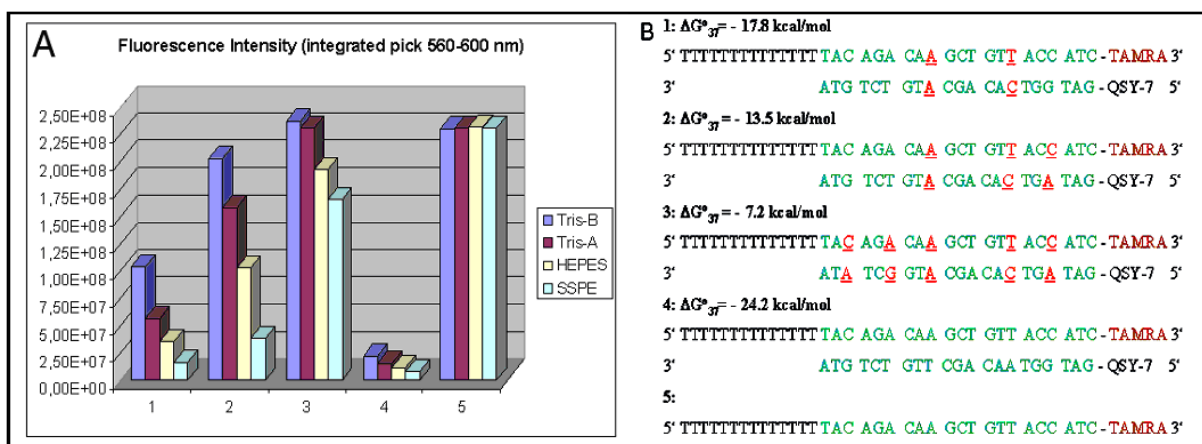


Figure 22 Estimation of DNA/DNA hybridisation yields in different buffer solutions by using of a quenching system (see Table 14). Five different types of experiments (B) were carried out in five repeats at 45 °C as the average intensity signal of each type of experiment is presented (A). Four different buffer solutions were used. In the blue, a 100 μ l buffer solution of 500 mM Tris-borate buffer, pH 8.3, and 50 mM NaOH; red, a 100 μ l buffer solution of 500 mM Tris – acetate buffer, pH 8.3, and 50 mM NaOH; yellow, a 100 μ l buffer solution of 500 mM HEPES buffer, pH 7.6, and 50 mM NaOH, the last, 6xSSPE. The minimal free energy (ΔG_{37}°) of DNA hybrids formed is calculated as described in section 3.5.1.

The free energy difference between the strongest non-specific hybridisation and weakest specific hybridisation among all DNA library sequences and their capture probes was found to be -6.8 kcal/mol, calculated by the partition function (see section 3.5), which is similar to the free energy difference between the perfectly matching DNA hybrid presented in Figure 22_B_4 and that with two mismatches shown in Figure 22_B_1.

Table 14 Average fluorescence intensity signal (integrated pick 560-600 nm) plotted in Figure 22. Each experiment was made in five repeats and the average values are presented. The complete experimental data are presented in Tables 27 (1), 28 (2), 29 (3), 30 (4), and 31 (5).

buffer solutions	1:(2 mismatches)	2:(3 mismatches)	3:(5 mismatches)	4:(0 mismatches)	5:(ss DNA)
TRIS-borate	104717057.20	201277434.60	237540194.20	21929319.4	231620116.6
TRIS-acetate	56055146.80	156345934.80	233722086.40	14887473.8	231071819.2
HEPES	35134089.20	104255259.20	194157640.8	11222617.4	232590096.6
6xSSPE	16037522.40	38921294.00	162023793.80	8271381.4	232822925.8

The results for all formed DNA hybrids (perfectly matching hybrids, or with two, three, and five, mismatches) and those from single-stranded 5' TAMRA-labelled DNA were very consistent and suggested that the 6xSSPE buffer solution possesses the highest DNA melting points, followed by HEPES, Tris-acetate and Tris-borate buffer solutions. It is well known that DNA has higher diffusion coefficient in a Tris-borate buffer than in Tris-acetate. It is interesting to observe the significant difference in the DNA melting points in Tris-acetate and Tris-borate buffer solutions. The DNA melting points in those buffer solutions were established in additional experiments presented in Table 15.

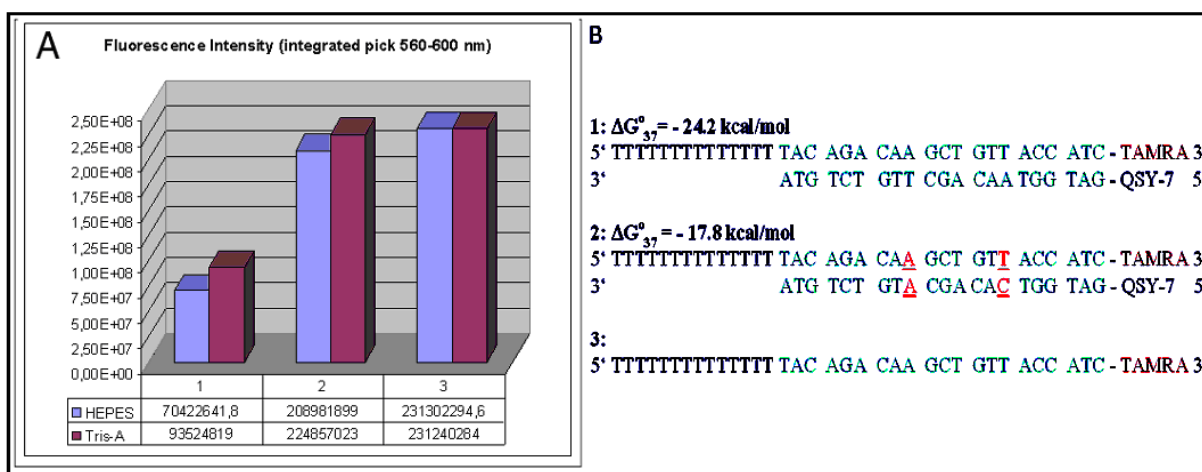


Figure 23 Estimation of hybridisation yield of DNA hybrid with two mismatches over length of 21 by using of a quenching system. The experiments were carried out in five repeats and the average intensity signal is presented. The complete experimental data are presented in Tables 32 and 33. Two different buffer solutions, both, at 45 °C were used. The blue one is a 100 µl buffer solution of 500 mM HEPES buffer, pH 7.6, 30 % formamide and 50 mM NaOH and the red one, a 100 µl buffer solution of 500 mM Tris – acetate buffer, pH 8.3, 30 % formamide and 50 mM NaOH.

There is a small difference between the free energy value for a DNA hybrid computed by the minimal free energy (the free energy of one structure only) and the free energy, based on the partition function, which considers the probable weight of the dominant structure in regard to all possible structures. A DNA hybrid, with two mismatches over a length of 21 nt, was designed, having a minimal free energy difference of – 6.4 kcal/mol to the perfectly matching hybrids (see Figure 23_B), thus being very close to the library free energy gap between specific and non-specific DNA hybridisation (see section 3.5.1). My goal was to establish hybridisation conditions

under which there will be non-hybridisation between the complementary strands with those two mismatches and to estimate the DNA hybridisation yield for perfectly matching strands under the same conditions. The quenching system, described above, was used in two different hybridisation solutions (a 500 mM HEPES buffer, pH 7.6, 50 mM NaOH, 30% formamide or 500 mM Tris-acetate buffer, pH 8.3, 50 mM NaOH, 30% formamide) under the same DNA concentrations (1 μ M) and temperature (45 °C). As one can see from Figure 23, there was no hybridisation (no quenching) between the complementary strands with two mismatches in a Tris buffer and there was a quenching of about 40 % in the case of perfectly matching strands under the same hybridisation conditions. In a HEPES buffer, there was ca 10 % quenching of the DNA hybrid with two mismatches and ca 30 % quenching in the case of perfectly matching strands under that hybridisation conditions.

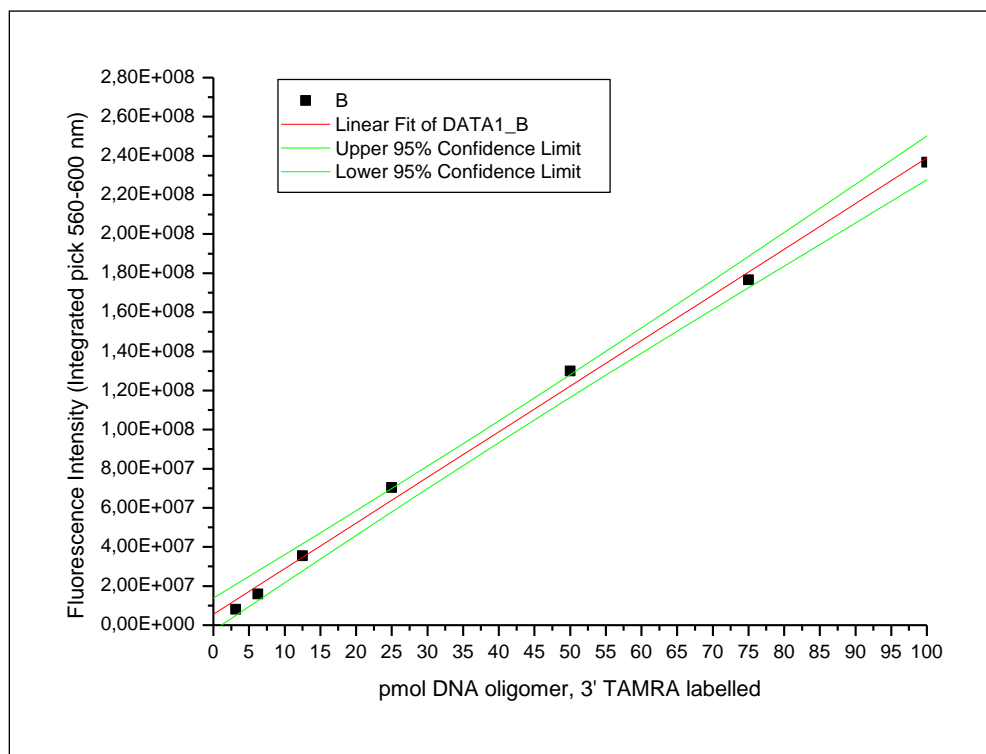


Figure 24 A standard titration curve for quantification of 3' TAMRA labelled DNA. The fluorescence signal (integrated pick from 560 to 600 nm) of 3' TAMRA labelled DNA (see Table 3, line 4) in seven different concentrations (3 pmol; 6 pmol; 12,5 pmol; 25 pmol; 50 pmol; 75 pmol; 100 pmol) was measured; the values being plotted in the dark squares. A linear fit was made, based on the measured data – the red line. The two green lines enclose a region of ± 5 % error rate (calculated by Origin Software). Each

concentration was made three times and the average intensity signal is presented. The complete experimental data are presented in Table 34.

The results obtained for the DNA melting points in different solutions (see Table 15) confirmed once again the already established stability order of DNA/DNA hybrids formed in the different solutions used. The highest DNA melting points were observed in 500 mM NaCl equivalent to 6xSSPE, followed by 500 mM HEPES (about - 0.6 lower than that of NaCl), 500 mM Tris-acetate (about - 1.7 lower than that of NaCl), and 500 mM Tris-borate (about - 6.4 lower than that of NaCl). The thermodynamically predicted DNA melting points for different concentrations of NaCl differed from the experimentally established ones by -1 °C.

It is important to mention that the absolute values of the experimentally established melting points depend on the concentration of the used SYBR Green One dye. In general, a higher dye concentration results in higher melting points. In all presented experiments, a constant concentration of 1xSYBR Green One was obtained from one stock solution in order to guarantee the same dye influence to the DNA/DNA hybridisation stability in all different buffer solutions.

Table 15 DNA melting points in different buffer solutions. *Two perfectly matching DNA strands over a length of 21 nt (see Table 3, lines one and four) were used to estimate the melting temperature in four different solutions as described in section 2.2.4. A DNA 4.1 computer programme was used to obtain the predicted melting temperatures.*

Concentration mM	Predicted T _m °C for NaCl	NaCl: T _m °C	TRIS-acetate pH 8.3: T _m °C	HEPES pH 7.6: T _m °C	TRIS-borate pH 8.3: T _m °C
200	60,5	61,5	62,0	63,1	53,5
300	62,6	63,5	63,5	64,3	55,8
400	64,1	65,0	64,2	65,1	58,2
500	65,3	66,4	64,7	65,8	59,5
500 and 50 mM NaOH	-----	-----	65,3	66,3	60,0

Let me discuss, which of the three tested buffer solutions (HEPES, Tris-acetate, and Tris-borate) is the best one as a neutralisation buffer in the reversible chemistry for an isothermal DNA hybridisation transfer by an alteration in the pH. There are at least three important criteria for a consideration: the buffering capacity, the ability to discriminate between perfectly matching DNA hybrids and those with some mismatches, and the chemical stability of DNA in a certain solution.

All tested buffer solutions could be successfully used for the isothermal DNA hybridisation transfer. A HEPES buffer possesses a little bit higher buffering capacity than that of Tris-acetate and Tris-borate buffers and probably long DNA is chemically more stable in HEPES buffer than in Tris buffers^{xlviii}. HEPES possesses the highest DNA melting points as well. I would prefer to use Tris-acetate buffer, because it is in the middle of all criteria and has a moderate DNA melting points for 16-mers DNA hybrids in a concentration of 500 mM. The choice of one of those buffers should mostly depend on the expected melting points of the DNA hybrids.

3.2.2 Fidelity of DNA hybridisation on beads. Non-specific DNA attachment to beads

In principle, there is no difference between DNA hybridisation accuracy in a free solution and on a surface. Nevertheless there are two specific points due to the influence of the surface to nucleic acid hybridisation. Firstly, the synthetic DNA attached to a surface should have a spacer in order to be accessible to hybridisation^{xlix}. The second point concerns non-specific DNA attachment to the surface. DNA/DNA hybridisation on 1 mg polystyrene beads was performed at 40 °C as described in section 2.2.3.2. The DNA attached to beads was denatured by heating at 93 °C for 3 min. Then, the beads were incubated in 100 mM NaOH for 3 min at room temperature. In all hybridisation experiments 5' amino-modified DNA (see Table 3 line 4) was immobilised to 15 µm beads (see Table 4, line 2) as described in section 2.2.2.1.I 5' R6G-labelled perfectly matching DNA (see Figure 25_1) was used in a concentration of 1 µM in the first type of hybridisation experiments.

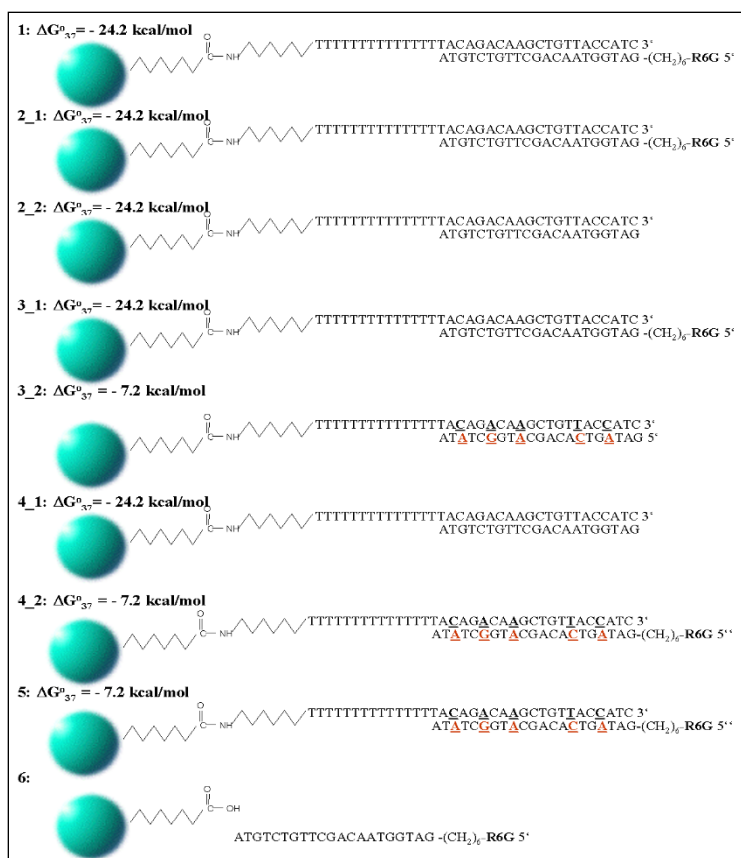


Figure 25 Scheme of DNA/DNA hybridisation fidelity analyses on beads. All DNA/DNA hybridisation analyses were done on 1 mg polystyrene beads. **1:** Hybridisation with 1 μ M perfectly matching 5'R6G-labelled DNA; **2:** Hybridisation with 1 μ M perfectly matching 5'R6G-labelled DNA half 5'R6G-labelled and half non-labelled; **3:** Hybridisation with 0.5 μ M perfectly matching 5'R6G-labelled DNA and 0.5 μ M non-labelled DNA with five mismatches; **4:** Hybridisation with 0.5 μ M perfectly matching non-labelled DNA and 0.5 μ M 5'R6G-labelled DNA with five mismatches; **5:** Hybridisation with 0.5 μ M 5'R6G-labelled DNA with five mismatches; **6:** Non-specifically 1 μ M 5'R6G-labelled DNA attachment to beads without immobilised DNA. The experimental results are presented in Figure 26. The free energy of the formed hybrids was computed (see section 3.5.1).

The same concentration of perfectly matching DNA was used in the second type of experiments, with half of the DNA being 5' R6G-labelled and the other half being non-labelled (see Figure 25_2_1 and 25_2_2). In the third type of hybridisation experiments half of the DNA was perfectly matching 5'R6G-labelled and the other half was non-labelled DNA with five mismatches. In the next experiments half of the DNA was perfectly matching non-labelled DNA and the other half was 5'R6G-labelled DNA with five mismatches. In the fifth type of hybridisations 5'R6G-labelled

DNA with five mismatches in a concentration of 1 μM was used. In the last experiments the non-specific attachment of 5'R6G-labelled DNA to beads without immobilised DNA was tested. The experimental results are presented in Figure 26. The free energy of the formed hybrids was computed as described in section 3.5.1.

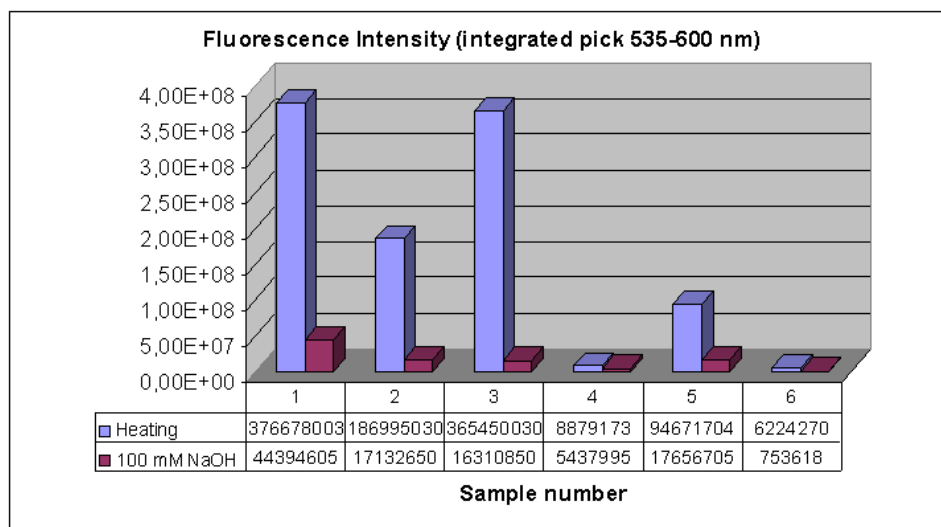


Figure 26 DNA/DNA hybridisation fidelity analyses on beads. For the DNA sequences see Figure 25. All DNA/DNA hybridisation analyses were done on 1 mg polystyrene beads (see Table 4, line 2). **1:** Hybridisation with matching 5'R6G-labelled DNA; **2:** Hybridisation with perfectly matching DNA - half 5'R6G-labelled and half non-labelled; **3:** Hybridisation with half perfectly matching 5'R6G-labelled DNA and half non-labelled DNA with five mismatches; **4:** Hybridisation with half perfectly matching non-labelled DNA and half 5'R6G-labelled DNA with five mismatches; **5:** Hybridisation with 5'R6G-labelled DNA with five mismatches; **6:** Non-specific 5'R6G-labelled DNA attachment to beads without immobilised DNA (see Table 35).

As one can see from Figure 26 there was a complete discrimination between the perfectly matching hybrids and those with five mismatches in the third and in the fourth cases, in which there was a competition between perfectly matching strand and one with 5 mismatches. In the case of a DNA hybridisation with 5 mismatches (see column 5) there was a 24% hybridisation yield in a comparison to the hybridisation yield of the perfectly matching hybrid under the same hybridisation conditions (see Figure 26, column 1). In all cases the denaturing by high temperature did not remove all the DNA from attracted the beads. The alkali pH DNA denaturation is stronger than temperature-mediated denaturation.

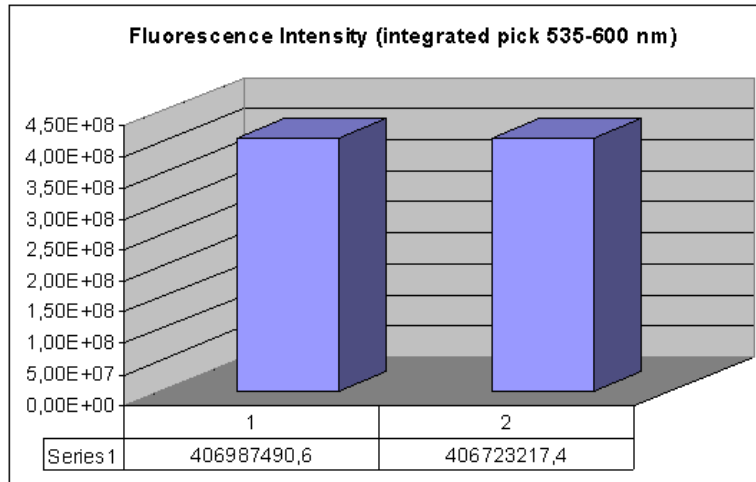


Figure 27 Testing stability of the fluorescence signal of rhodamine 6G in 100 mM NaOH. 50 pmol 5' rhodamine 6G-labelled DNA (Table 3, line 1) was incubated in two different solutions: **1**: 100 mM Tris-acetate buffer, pH 8.3; **2**: 100 mM NaOH for two hours at 45 °C. Every experiment was performed five times as the average values are plotted. The complete experimental data are presented in Table 36.

In the next sort of experiments the stability of the fluorescent signal of 5' rhodamine 6G-labelled DNA in 100 mM NaOH solution was tested. As clear from Figure 27 the alkali pH (over 13) had no any influence on the fluorescent signal.

Next hybridisation experiments were carried out on beads under flow conditions. One chamber of the micro-reactor shown in Figure 14 was filled with beads (see Table 4, line 2) immobilized with DNA (see Table 3, line 6) as described in section 2.2.2.1.I. The reactor was held at temperature of 45 °C while series of different buffer solutions were pumped through the chambers as described below (see Figure 28). The selective hybridisation in flow involved firstly exactly matching DNA (1 µM ssDNA, see Figure 29_1) fluorescently labelled with rhodamine 6G in the hybridising buffer solution (500 mM Tris-acetate, pH 8.3, and 50 mM NaOH). This buffer was chosen since it is the solution in which DNA released from a previous module will be immersed (see section 3.4.2). It arises in a previous module through a neutralization of the denaturing solution (100 mM NaOH) by mixing with an equal volume flow of buffer (1 M Tris-acetate, pH 8.3) as demonstrated in section 3.4.2. In a separate measurement, it was confirmed that the pH change of the buffer on mixing is negligible. The series of fluorescence measurements, monitoring the amount of hybridised DNA on the beads, is shown in Figure 28. After switching to the hybridising solution, a rapid increase in signal, compatible with the time scale induced by partial mixing lengthwise along the inlet

tubes (upon buffer change from water), was followed by a slower increase towards saturation as more DNA flowed past the beads.

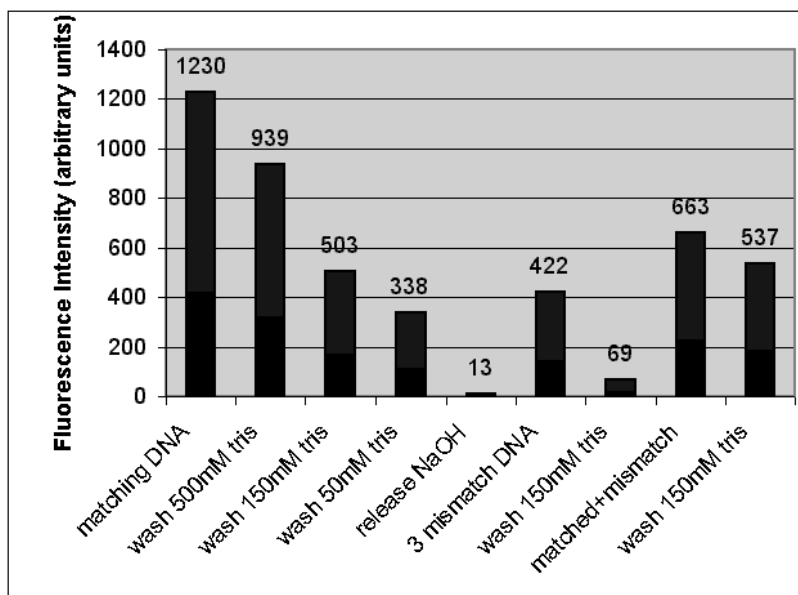


Figure 28 DNA hybridisation fidelity analyses on beads placed in a micro-flow reactor under flow conditions. The average fluorescence intensity (minus background signal) of the region of the micro-reactor containing beads is shown under various flow conditions. A single chamber of the micro-reactor shown in Figure 14 was employed in this experiment. The measurements are averages over several images, after allowing time for reaction. For details, see the text and Figure 29. The main features are successful hybridisation (column 1), release (column 5), the ability to separate matching and weakly mismatching DNA (cf columns 3 vs 7) with the appropriate buffer (Tris 150 mM), and the ability to obtain high yield selective hybridisation of matched DNA in the presence of mismatched DNA (columns 8 and 9). The exposure time was one second and CH250 camera was used.

The beads were then washed with an identical buffer solution, not containing DNA, to remove unbound DNA and the fluorescent signal from the free solution. The reduction in fluorescence signal (Figure 28) was consistent with just removing the signal from DNA in the surrounding free solution. Next, the buffer solution was changed to 150 mM Tris-acetate, which at lower ionic strength provides a more stringent test of DNA binding than the 500 mM solution.⁴¹ This buffer concentration was suggested as a wash solution by batch experiments in Eppendorf tubes and, as we shall see above, allows the discrimination of imperfectly matching DNA. The data reported in Figure 28 confirms that significant signal is retained, with the exactly matching DNA, after a

period of 30 min washing with this solution (Decreasing the buffer concentration further to 50 mM Tris caused a steady depletion of DNA, 50% over the next 30 min). Next the remaining DNA was dehybridised completely (see Figure 28) using a solution of 100 mM NaOH. The fluorescent signal returned to its starting value. Separate measurements with a fluorimeter (see Figure 27) confirmed that there is no significant change of fluorescent signal of rhodamine 6G labelled DNA through the NaOH solution, so that the removal of fluorescent implies that DNA is released from the beads.

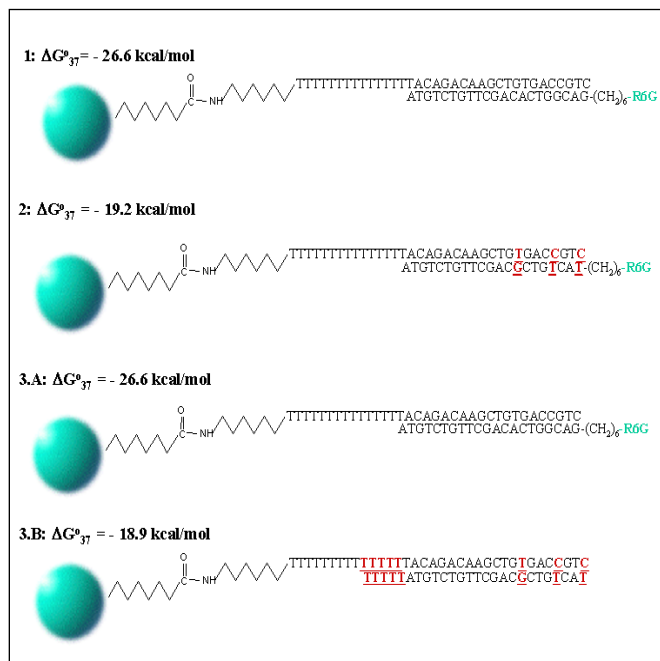


Figure 29 Scheme of DNA/DNA hybridisation fidelity analyses on beads under flow conditions. Polystyrene paramagnetic beads (see Table 4, line 2), immobilized with DNA, were incorporated into a micro-chamber (see Figure 14). Three different DNA hybridisation experiments were performed. In the first experiment, 5' R6G labelled perfectly matching DNA was hybridised and released (see Figure 28 columns form 1 to 5). In the second case 3 mismatches DNA was used (see Figure 28 columns 6 and 7). Finally, hybridisation experiments were done in the presence of 5' R6G-labelled exactly matching DNA and non-labelled DNA with some mismatches (see Figure 28 column 8 and 9).

After completion of this basic selection-wash-release cycle, a second round was initiated with an imperfectly matching DNA (1 μ M, see Figure 29) labelled with rhodamine 6G as above. This DNA contained three mismatches over a length of 21 nt, at separated locations in the sequence. A smaller amount of DNA bound to the beads (even after 10 min hybridisation at 45 $^{\circ}$ C) than in the case of perfectly matched DNA,

as shown in Figure 28. Washing with the discriminating buffer (150 mM Tris-acetate, see above) was sufficient to remove the imperfectly matched DNA from the beads (see Figure 28).

Finally, the ability of the wash buffer to discriminate in cases of simultaneous competitive hybridisation between matched and imperfectly matched DNA was tested. This was done by using a solution of a hybridising buffer as at the outset but with 0.5 μM of each of the two types of DNA (Figure 29_3), this time only the perfectly matching DNA was fluorescently labelled. The fluorescent signal on the beads rose to about 50 % of its value from the first phase of the experiment (with 1 μM of labelled matching DNA), which is consistent with a successful competitive hybridisation of the matched form. After washing with the discriminating buffer (150 mM Tris-acetate), the signal reduction was consistent with a removal of free labelled DNA as in the first phase of the experiment (see Figure 28). These results demonstrate that selective DNA hybridisation and release can be performed with appropriate buffer solutions and temperature, compatible with a steady flow implementation of DNA Computing as well (see section 3.4.3).

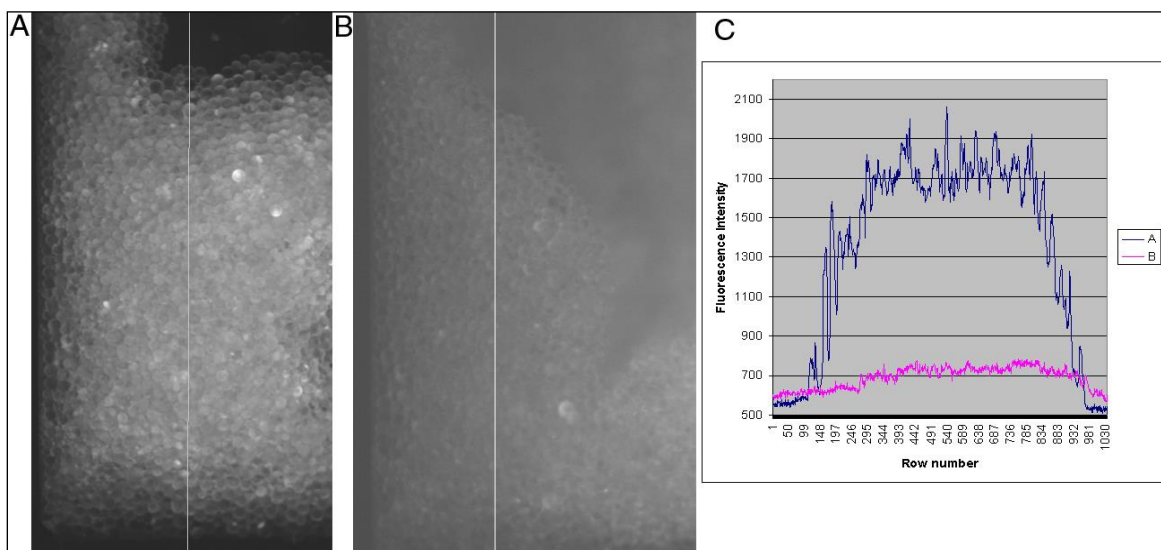


Figure 30 DNA/DNA hybridisation fidelity analyses on beads placed in micro-chambers under flow conditions without washing. 35 nt amino-labelled DNA was immobilised to 15 μm carboxyl coated beads (see Table 4, line 4). **A:** Perfectly matching, 5' R6G labelled, DNA (see Figure 31_1) was pumped through the beads while a fluorescence image was being taken. **B:** Five mismatching, 5' R6G labelled, DNA (see Figure 31_2) was pumped through the beads while a fluorescence image was taken. The camera's (CH250) bias was 500 cps. The exposure time was one second. **C:** Image Intensity profiles of image A and B.

Fluorescence images of DNA/DNA hybridisation experiments on beads under flow conditions are presented in Figures 30 and 32. Carboxyl-coated beads (see Table 4, line 2) immobilised with DNA (see Figure 31) as described in section 2.2.2.1_I were incorporated in micro-reactor chamber (see Figure 14).

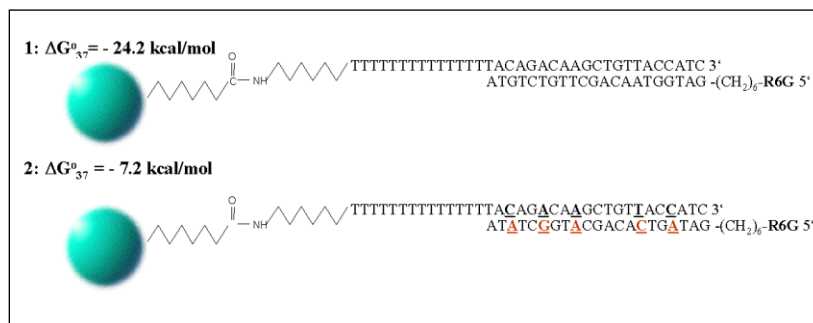


Figure 31 Scheme of DNA/DNA hybridisation analyses on beads placed in micro-chambers under flow conditions. 1:Hybridisation with perfectly matching DNA see Figures 30_A (during the hybridisation) and 32_A (after washing of unbound DNA) 2:Hybridisation with five mismatching DNA see Figures 30_B (during the hybridisation) and 32_B (after washing of unbound DNA).

Two different 5' R6G-labelled ssDNA strands dissolved in a 500 mM Tris-acetate buffer, pH 8.3, and 50 mM NaOH were pumped through the beads at 45 °C (see Figure 31). In the first case, 5' R6G perfectly matching DNA was used in the hybridisation experiments presented in Figures 30_A and 32_A (see Figure 31_1). In the second case (see Figures 30_B and 32_B), the hybridisation experiments were carried out with five mismatching 5' R6G DNA (see Figure 31_2).

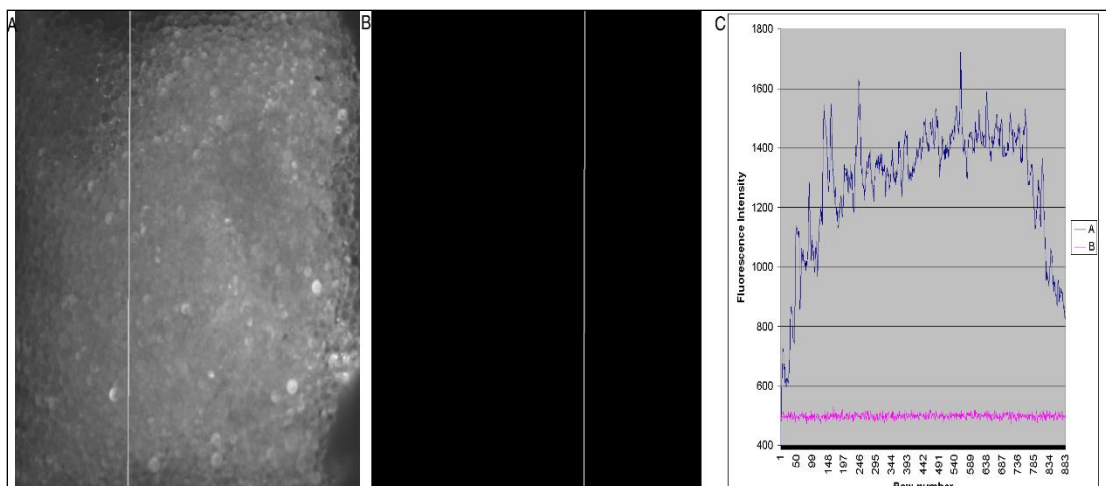


Figure 32 DNA/DNA hybridisation fidelity analyses on beads placed in micro-chambers after washing. *A: Perfectly matching, 5' R6G labelled, DNA (see Figure 31_1) was pumped through the beads. After washing a fluorescence image was being taken. B: Five mismatching, 5' R6G labelled, DNA (see Figure 31_2) was pumped through the beads. After washing a fluorescence image was being taken. C: Image Intensity profiles of image A and B. The camera's bias (CH250) was 500 cps. The exposure time was one second.*

The fluorescence profile of both images is plotted in Figure 30_C. The intensity of the fluorescent signal of the hybridisation experiment with the five mismatching DNA on the beads and in the free solution was almost equal (about 150 cps) as obvious from the plot, hybridisation on the beads did not take place in a contrast to the situation with a perfectly matching DNA (see Figure 30_A). In Figure 32 the same experiments are demonstrated after removing of unbound fluorescently labelled DNA from the free solution by pumping a 500 mM Tris-acetate buffer, pH 8.3, and 50 mM NaOH for 15 min at a flow rate of 1 $\mu\text{l}/\text{min}$ and 45 $^{\circ}\text{C}$. As can be seen no fluorescence was detected on the beads hybridised with the 5 mismatching DNA (see Figure 32_B).

3.2.3 Discussion

The specificity of DNA/DNA hybridisation reaction in different buffer solutions was experimentally demonstrated by using of a quenching system. The experiments allow very accurate quantification of the formed DNA hybrids. The hybridisation solutions were selected in terms of their capacities to buffer an equal volume of 100 mM NaOH, which allows them to be used for a reversible DNA hybridisation transfer under isothermal conditions as will be demonstrated in section 3.4. The three tested buffering solutions

were proven to be suitable for DNA/DNA hybridisation experiments and applicable for an isothermal hybridisation transfer. An absolute discrimination between perfectly matching DNA hybrid and the one with two mismatches over a length of 21 nt was demonstrated under conditions of a high Tris concentration, allowing successful buffering of an equal volume of 100 mM NaOH. It is important to mention the fact a complete discrimination between perfectly matching DNA hybrid and one with two mismatches was achieved under hybridisation conditions, in which the hybridisation yield in the case of perfectly matching hybrid was 60% and 0% in the case of the two mismatching hybrid. The free energy gap between those hybrids was designed to be 6.4 kcal/mol. The free energy gap between the weakest specific DNA/DNA hybridisation and the strongest non-specific hybridisation among the DNA library sequences was estimated to be 6.8 kcal/mol. It is interesting that a perfect discrimination between two words using the complete DNA library was achieved under hybridisation conditions with a 60 % hybridisation yield (see section 3.5.3). The specificity of DNA/DNA hybridisation was shown in hybridisation experiments on beads. The washing step was proven to be very important to increase fidelity of the hybridisation reaction under flow conditions. The use of the fluorescence-imaging set-up allowed the detection of DNA/DNA hybridisation on a single bead under flow conditions. The carboxyl-coated beads used had a relatively low level of non-specific DNA attachment^{l, li}.

3.3 DNA/DNA HYBRIDISATION AND DENATURATION KINETICS ON BEADS UNDER FLOW CONDITIONS

Nucleic acid hybridisation on surfaces has played an important role in the development of a variety of techniques in molecular biology such as Northern and Western blot analysis, screening of genome or copy DNA libraries. In recent years, DNA-chip technology has offered high-throughput methods for nucleic acid hybridisation analysis. Now it is believed that DNA-chip arrays are going to reshape molecular biology by producing a huge amount of data, something that was not possible ten years ago. There are two areas in the developing DNA-chip technology. On one hand there are technical aspects concerning the practical implementation of the DNA-chip arrays. On the other hand there are theoretical problems, connected with the question of how the huge amount of the obtained data could be analysed. An important progress has been made in improving various practical implementations of DNA arrays such as a DNA hybridisation detection, DNA synthesis and immobilisation, acceleration of nucleic acid hybridisation rate and accuracy.

DNA hybridisation on beads under flow conditions has proved to be an advantageous approach to nucleic acid hybridisation. It has been shown that the DNA/DNA hybridisation on beads under

flow conditions takes place in a few seconds^{lii, liii} in contrast to a few hours for the same process under stationary conditions^{liv}. Here I am going to investigate in details the DNA/DNA hybridisation and denaturation kinetics on beads under flow conditions.

3.3.1 DNA/DNA hybridisation kinetics on beads under flow conditions

It is well known that nucleic acid hybridisation on surface (when one of the complementary DNA strands is attached to a surface) is much slower than in a free solution^{lv} (when both complementary strands are dissolved into the hybridisation solution). This problem arose with the development of the Northern and Western blot analysis. One of the first approaches for increasing the hybridisation rate was to exclude much of the volume of the hybridisation solution with inert polymers such as dextran sulphate. In some DNA-chip arrays the hybridisation rate was accelerated by stirring the hybridisation solution. The electric field-assistant DNA hybridisation was proven to be an accelerated one^{lvi, lvii}. It was suggested that the DNA hybridisation rate on beads under flow conditions is comparable to the reaction rate in the electric field-assistant DNA hybridisation.

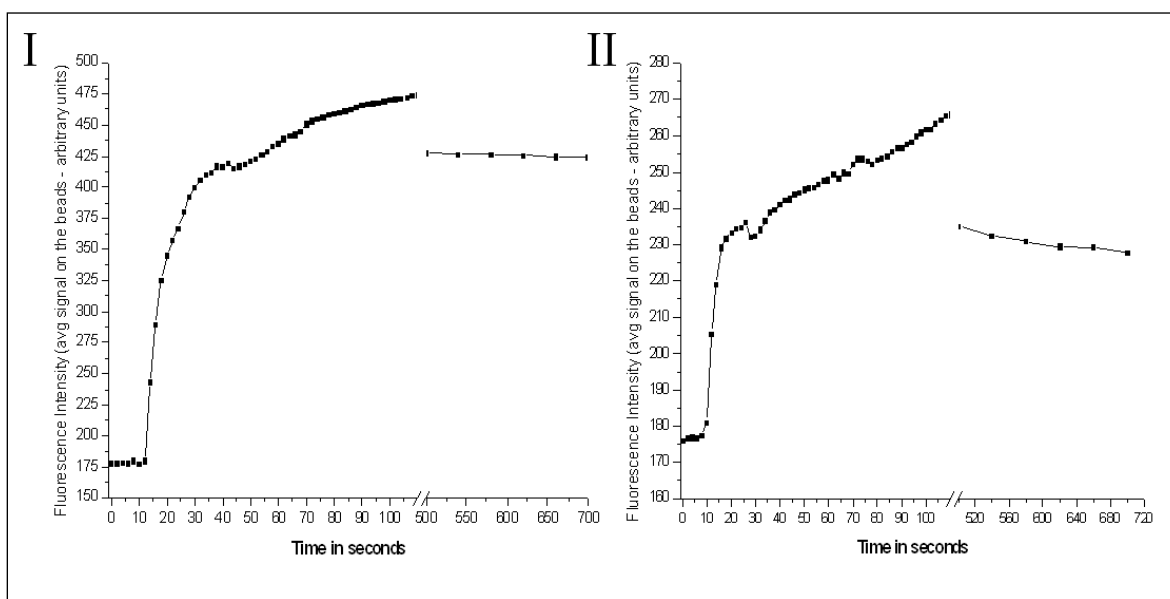


Figure 33 DNA/DNA hybridisation kinetics on beads under high flow rate conditions. The average fluorescence intensity signal on beads incorporated in a micro-flow reactor is plotted. 35 nt DNA was immobilized (see Table 3, line 4) to 15 μm beads (see Table 4, line 2) placed in a micro-flow reactor (see Figure 3). 5' Rhodamine 6G labelled DNA at a concentration of 1 μM was dissolved in a 500 mM Tris-acetate buffer solution, pH 8.0, and 50 mM NaOH. The solution was pumped through the beads at a flow

rate of 10 $\mu\text{l}/\text{min}$ at 40 °C. After the 110th second the beads were washed with the hybridisation solution in the absence of DNA. I: 21 nt perfectly matching DNA was used (see Table 3, line 1); II: 21 nt DNA with five mismatches was used (see Table 3, line 2). Fluorescence images were obtained by a qantrix camera (see Figure 11). The exposure time was one second.

In order to investigate DNA/DNA hybridisation kinetics under flow conditions carboxyl-coated beads (see Table 4, line 2) immobilised with 35 nt DNA (see Table 3, line 4) as described in section 2.2.2.1_I were incorporated in micro-flow reactor channels (see Figure 3). In the first type of kinetics experiments 21 nt, 5' Rhodamine 6G labelled, perfectly matching DNA (see Table 3, line 1) was delivered through all inlets at a flow rate of 10 $\mu\text{l}/\text{min}$ and 40 °C. Fluorescence images from the beads were obtained using the set-up described in section 2.2.6.2_I. The average bias signal of the used camera was found to be 132 cps. The results obtained are presented in Figure 33_I. As one can see the average fluorescent signal on the beads reached over 80 % saturation within 26 seconds (a little bit less than a half of min). The results of similar hybridisation experiments are shown in Figure 33_II. The only difference from the previous case was the different 5' Rhodamine 6G labelled DNA used, which had five mismatches (see Table 3, line 2). As one can see from Figure 33_II 70 % of the fluorescent signal on the beads was reached about a 80 % saturation within 20 seconds while that signal was approximately half of the hybridisation signal of perfectly matching DNA. The small increasing of the fluorescent signal on the beads after the 30th second (see Figure 33) may be more a result of a non-specific DNA attachment than a DNA/DNA hybridisation reaction. It is interesting to see that the equilibrium of the DNA/DNA hybridisation of about 70 % was achieved in both cases within 20 seconds (see Figure 33). In the last type of DNA/DNA hybridisation kinetics experiments a 100 times smaller flow rate compared to the experiments described above was used. The DNA/DNA hybridisation kinetics was found to be about half speed (see Figure 34) of that at a higher flow rate (see Figure 33).

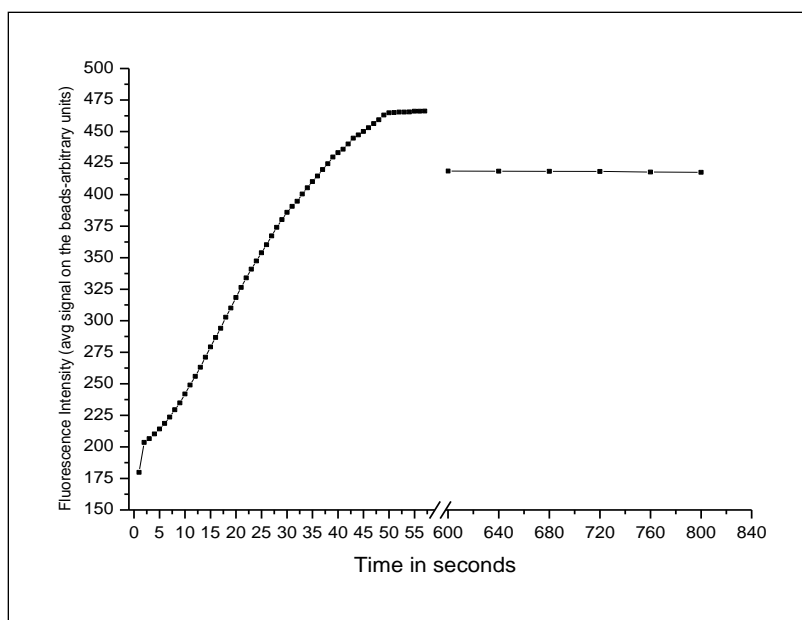


Figure 34 DNA/DNA hybridisation kinetics on beads under low flow rate conditions. *The average fluorescence intensity on beads incorporated in a micro-flow reactor (see Figure 3) is plotted. 35 nt DNA was immobilized (see Table 3, line 4) to 15 μm beads (see Table 4, line 2) placed in a micro-flow reactor (see Figure 3). 5' Rhodamine 6G labelled, 21 nt perfectly matching DNA was used (see Table 3, line 1) at a concentration of 1 μM dissolved in a 500 mM Tris-acetate buffer solution, pH 8.3, and 50 mM NaOH. The solution was pumped through the beads at a flow rate of 0,1 $\mu\text{l}/\text{min}$ at 40 $^{\circ}\text{C}$. After the 55th second the beads were washed with the hybridisation solution in the absence of DNA at a flow rate of 2 $\mu\text{l}/\text{min}$. Fluorescence images were obtained by a quantrix camera (see Figure 11). The exposure time was one second.*

3.3.2 Kinetics and efficiency of DNA/DNA denaturation on beads

Here I investigate the efficiency of DNA/DNA denaturation by sodium hydroxide and high temperature (93 $^{\circ}\text{C}$) and DNA/DNA denaturation kinetics on beads under flow conditions using sodium hydroxide in concentrations of 50 and 100 mM.

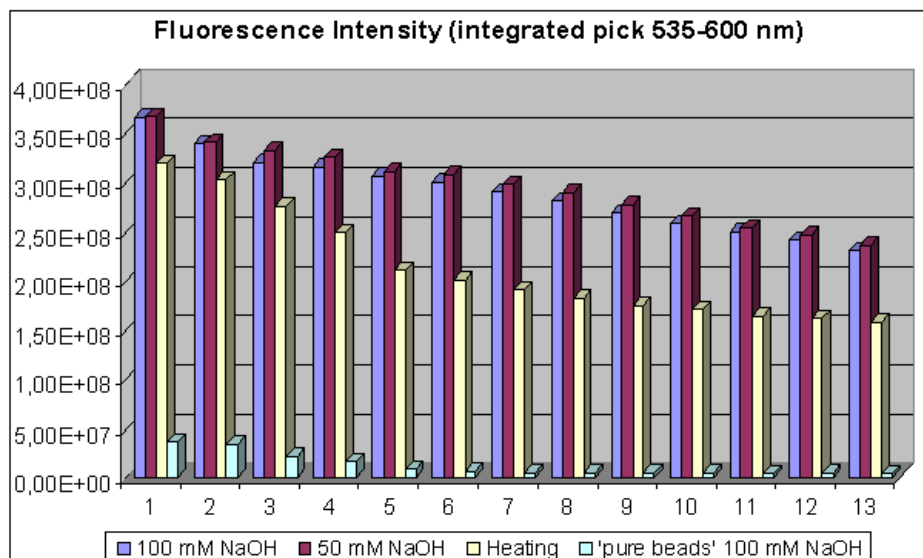


Figure 35 DNA/DNA hybridisation/denaturation cycles on beads. *The DNA hybridisation/ denaturation yield to three aliquots of 1.0 mg beads (see Table 4, line 2) from 13 consecutive DNA/DNA hybridisation/denaturation cycles and one aliquot of non-immobilised with DNA beads, using three different denaturation procedures, are shown. The fluorescent signal from the denatured of 5' Rhodamine 6G labelled DNA is plotted (for all values, see Table 37).*

5' amino-modified DNA (see Table 3, line 4) was immobilised on carboxyl-coated beads (see Table 4, line 2) as described in section 2.2.2.1_I. The beads were divided into three aliquots of 1 mg each and one additional aliquot of 1 mg beads non-immobilised with DNA. The aliquot of beads was used in 13 consecutive DNA/DNA hybridisation/denaturation cycles at 38 °C applying perfectly matching, 5' R6G-labeled DNA oligomers (see Table 3, line 1). The hybridisation analyses were performed in a 500 mM Tris-acetate buffer solution, pH 8.3, and 50 mM NaOH as described in section 2.2.3.2. Three different denaturation procedures, 100 mM NaOH or 50 mM NaOH for one min and heating at 93°C for 3 min, were used. As can be seen from Figure 35, the sodium hydroxide denaturing is stronger than temperature. There is no difference in the denaturing efficiency between 100 mM and 50 mM sodium hydroxide denaturation in terms of DNA denaturation yield. It should be mentioned that after the last hybridisation/denaturation cycle 15 % of the bead was lost. Taking into account that fact, DNA/DNA hybridisation/denaturation yield on beads decreased with 27 % in the cases of sodium hydroxide denaturing and 42 % in the case of temperature denaturing. That difference is likely to be a result of lower bead stability at 93°C than that in 100 or 50 mM NaOH. An additional factor could be the ability of 100 and 50 mM NaOH

to denature all DNA from the beads including the non-specifically attached one. The non-specific DNA attachment to the beads after NaOH treatment decreased 90 % (see Figure 35 and Table 37).

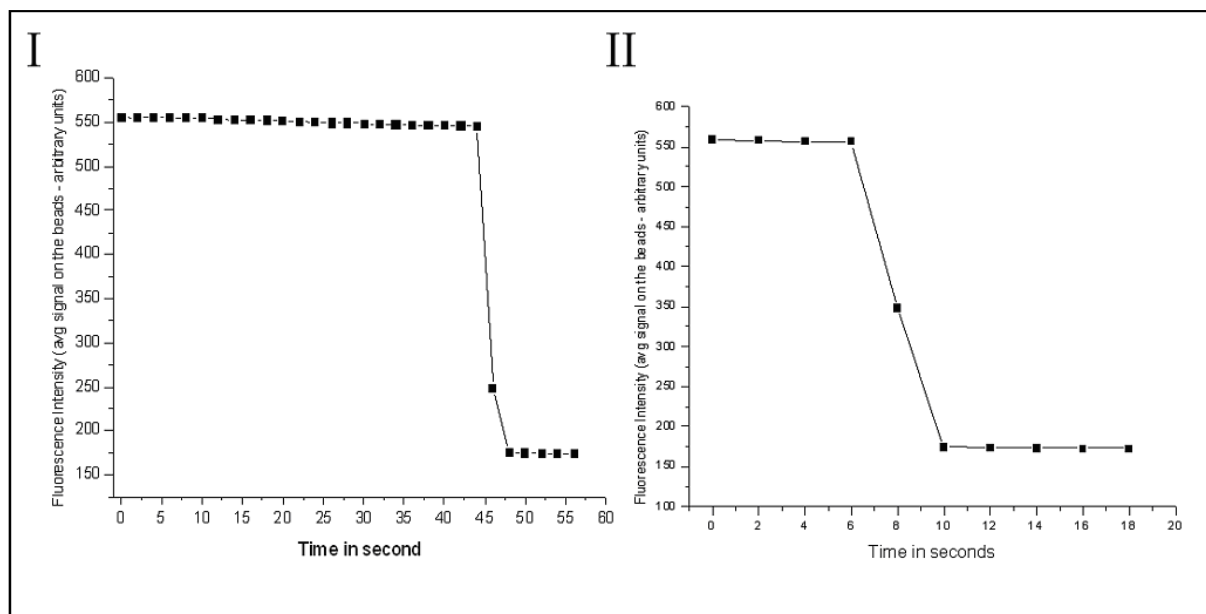


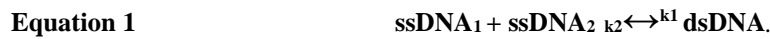
Figure 36 DNA/DNA denaturation kinetics on beads under flow conditions. *The average fluorescence intensity on beads (see Table 4, line 2) incorporated in a micro-flow reactor (see Figure 3) is shown. 21 nt 5' Rhodamine 6G labelled DNA (see Table 3, line 1) was being hybridised on 35 nt perfectly matching (see Table 3, line 4) one attached to the beads as not hybridised DNA from the solution was removed with a hybridisation solution without DNA. All solutions were pumped through the beads at a flow rate of 10 $\mu\text{l}/\text{min}$ and 42 $^{\circ}\text{C}$. **I:** The hybridised to the bead DNA was released with a 100 mM NaOH solution pumped through the beads. The sodium hydroxide solution started passing the beads from the 46th second. **II:** It was used a 50 mM NaOH solution. The sodium hydroxide solution started passing the beads from the 7th second. The average bias signal of the used camera was found to be 132 cps. A quantrix camera was used (see Figure 11). The exposure time was one second.*

In the last experiments of the section the DNA/DNA denaturing kinetics on beads under flow conditions was tested using two different concentrations of sodium hydroxide (100 mM and 50 mM). Carboxyl-coated beads (see Table 4, line 2), DNA immobilised (see Table 3, line 4) as described in section 2.2.2.1_I, were incorporated in the micro-flow reactor shown in Figure 3. Perfectly matching, 5' R6G labelled DNA (see Table 3, line 1), dissolved in a solution of 500 mM Tris-acetate, pH 8.3, and 50 mM NaOH, was pumped for 20 min through all inlet channels at a flow rate of 10 $\mu\text{l}/\text{min}$ and 42 $^{\circ}\text{C}$. Next, the unbound DNA was replaced by pumping for 10 min

through all inlet channels a 500 mM Tris-acetate solution, pH 8.3, in the absence of DNA, at a flow rate of 10 $\mu\text{l}/\text{min}$ and 42 $^{\circ}\text{C}$. Finally, two different solutions of NaOH (100 mM and 50 mM) were delivered through all inlet channels at a flow rate of 10 $\mu\text{l}/\text{min}$ and 42 $^{\circ}\text{C}$ while the fluorescence images of the beads were taken. The average fluorescence signal on the beads is presented in Figure 36. As one can see from the figure, the DNA/DNA denaturation kinetics on beads using those two different concentrations of sodium hydroxide is an almost instantaneous process taking place within 2-4 seconds. The denaturation kinetics with 100 mM NaOH seems to be a little bit faster (about a second) than the with 50 mM NaOH. It should be mentioned here that a solution of 100 mM NaOH does not influence the fluorescent signal of R6G (see Figure 27). It seems that the flow rate has less influence on DNA/DNA denaturation kinetics than on hybridisation kinetics.

3.3.3 Discussion

Let us assume that ssDNA_1 and ssDNA_2 be two complementary deoxyoligonucleotides and let dsDNA be the double stranded DNA formed as a result of their hybridisation. According to Wetmur⁷⁹ there are two possible scenarios for hybridisation reaction of polynucleotides in free solution depending on the concentrations of the complementary strands ssDNA_1 and ssDNA_2 .



The hybridisation reactions are second order if the concentrations of the complementary strands are equal ($\text{ssDNA}_1 = \text{ssDNA}_2$). If the concentration of one of the strands is in excess ($\text{ssDNA}_1 \gg \text{ssDNA}_2$ or $\text{ssDNA}_1 \ll \text{ssDNA}_2$) it is a pseudo-first order reaction. For oligonucleotides up to 1 kb in length the hybridisation reaction in a homogenous mixture should be no diffusion-limited.

The approximation for diffusion limited second order rate association between two complementary strands ssDNA_1 and ssDNA_2 of contact radius R and diffusion coefficients $D_{\text{ssDNA}_1} + D_{\text{ssDNA}_2}$ is

Equation 2
$$k_1 = 4 \pi (D_{\text{ssDNA}_1} + D_{\text{ssDNA}_2}) R.$$

It is assumed by this expression that the reaction is instantaneous when the complementary strands reach the radius R , which is expressed in $\text{M}^{-1} \text{s}^{-1}$ with the factor $10^{-3} N_0$, where N_0 is Avogadro's number. For 20 mer oligonucleotides, diffusion constants above $10^{-7} \text{ cm}^2/\text{s}$ give rise to diffusion-

limited values of $k_1 > 10^8 \text{ M}^{-1} \text{ s}^{-1}$ whereas measured hybridisation rates $k < 10^8 \text{ M}^{-1} \text{ s}^{-1}$ (typically $k=10^7$). That means the hybridisation for DNA with lengths up to 1 kB in free homogenous solution is not diffusion limited. What will be the situation if one of the complementary strands is attached to a surface, for instance to bead? According to McCaskill³⁷ that is a first order rate constant for association to a beads from volume V as

Equation 3
$$k_1 = 4 \pi D_{ssDNA} R/V = 4 \pi \underline{R} \underline{D} / \underline{V} [\text{s}^{-1}],$$

where the dimensionless parameters \underline{R} , \underline{D} and \underline{V} express R, D and V in units of 10μ , $10^{-6} \text{ cm}^2/\text{s} = (10\mu)^2/\text{s}$ and $(10\mu)^3$ respectively. For close packed beads and values of $\underline{R}=0.5$ and $\underline{D}= 0.2$ $k_1=2\pi/5$ should be 1.2 s^{-1} . After a short initial period, k_1 became a diffusion-limited reaction^{lviii}. The reaction rate increases inversely with the square of the bead's radius until the homogeneous rate is attained. Those theoretical considerations made by McCaskill³⁷ do not take into account the difference between DNA hybridisation on beads under flow and under stationary conditions, or the hybridisation conditions, and the fact that DNA hybridisation is not an instantaneous reaction. It is important to emphasis that DNA hybridisation on beads under flow conditions is not a diffusion-limited reaction in contrast to the same reaction under stationary conditions.

The DNA/DNA hybridisation on beads under flow conditions has proven to be a very fast reaction which obviously depends on the flow rate. It can reach saturation in half a min under high flow rate⁴¹. At a low flow rate, the same hybridisation reaction required double the time to reach saturation. Nevertheless the DNA hybridisation kinetics under flow conditions is much faster than in stationary conditions. DNA/DNA denaturation kinetics by sodium hydroxide has proven to be a matter of 2-4 seconds. The denaturation kinetics depends much less on the flow rate than does hybridisation. There is a small difference between the DNA denaturising kinetics with 50 mM and 100 mM NaOH.

3.4 MULTI-STEP DNA HYBRIDISATION TRANSFER BETWEEN MICRO-REACTOR SELECTION MODULES UNDER ISOTHERMAL CONDITIONS. AN INTEGRATED AND AUTOMATED MICRO-FLUIDIC CHIP FOR BIO-MOLECULAR ANALYSES.

3.4.1 Reversible chemistry for multi-step DNA hybridisation transfer under isothermal conditions by a pH change

A general scheme for applying solutions with a reversible pH change to perform DNA hybridisation transfer under isothermal conditions is presented here. Let me use the micro-flow reactor presented in Figure 37 to describe that basic idea.⁴¹

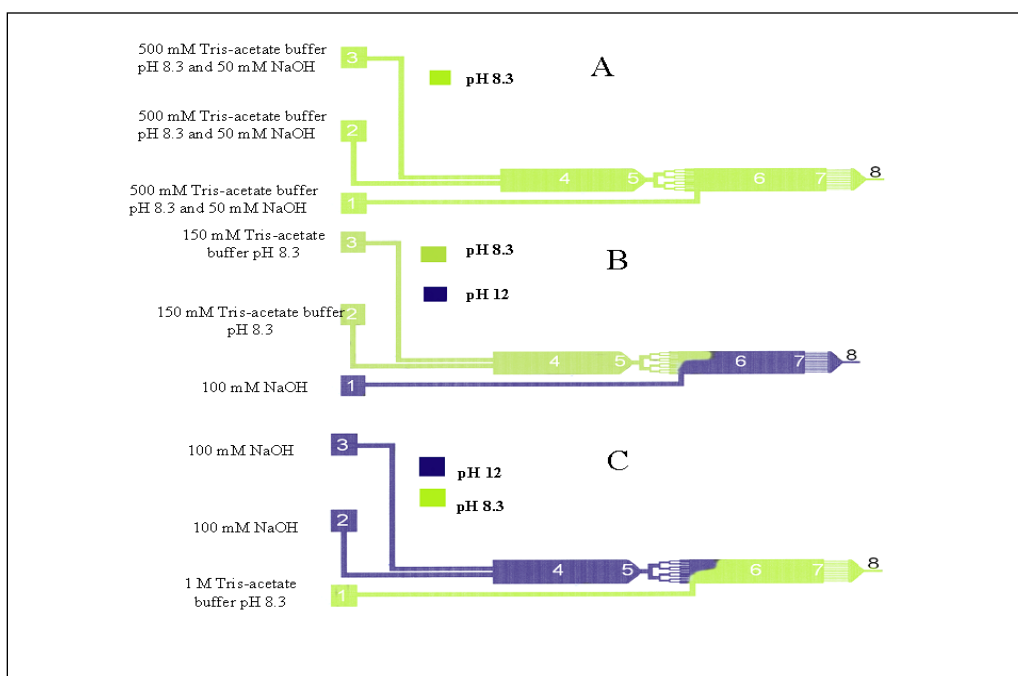


Figure 37 Reversible chemistry for a multi-step DNA hybridisation transfer under isothermal conditions by a pH change. **A:** DNA hybridisation: a 500 mM Tris- acetate buffer, containing ssDNA was pumped through all inlets. As a result the pH in both chambers was 8.3. Hybridisation could take place on beads carrying immobilised DNA placed in both chambers under those conditions. **B:** Washing: a 150 mM Tris- acetate buffer solution was pumped through inlets number 2 and 3 while a 100 mM NaOH solution was delivered through inlet number 1. As a result the pH in the first chamber had a value of 8.3 while the pH in the second chamber had a value of above 12. Under those conditions the beads in the first chamber were washed with a low ionic strength buffer, while the DNA hybridised on the beads from the second chamber was released. **C:** a 100 mM NaOH solution was pumped through inlets number 2 and 3 while a 1 mM Tris-acetate buffer, pH 8.15, being delivered through inlet number 1. As a result the pH in the first chamber had a value of over 12 while the pH in the second chamber had a value of about 8.4. Under those

conditions DNA on the beads in the first chamber was released and specifically picked up on the beads in the second bead chamber (see Figures 39, 40, 42 and 43).

The same chemistry could be employed in the micro-flow reactor schemes presented in Figure 38. The difference between the two micro-fluidic architectures is not in the chemistry applied but in the flow conditions³⁹. In the micro-flow reactor architecture presented in Figure 38, the DNA hybridisation transfer takes place by moving magnetic beads immobilised with ssDNA between spatially separated solutions under steady flow conditions.

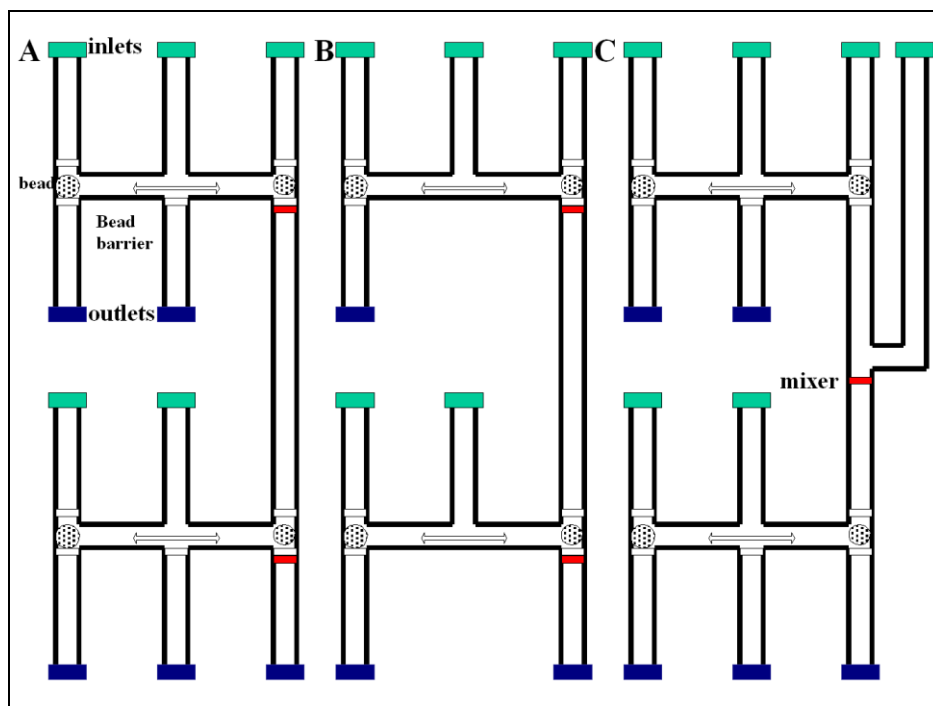


Figure 38 Schemes of two coupled modules for an automated, multi-step DNA selection under isothermal conditions based on moving magnetic beads in spatially separated laminar flows. The coupled selection modules are clocked to allow a synchronised bead movement. The green squares indicate inlets, the blue squares indicate outlets, the red ones are mixers and the white ones are bead barriers. **A:** There are five inlets and five outlets. In the first module, the left-hand inlet delivers the DNA pool, the middle channel is used for pumping of a neutralisation buffer (1 M Tris-acetate, pH 8.3) and the right-hand inlet delivers the denaturing buffer (100 mM NaOH). In the second module, the left-hand inlet delivers the denaturing buffer and the middle channel, as in the first module, is used for pumping of a neutralisation buffer. **B:** The scheme is similar to the previous one. The difference is in the absence of the middle outlet channels⁶⁰. **C:** In this case the middle channels are used for pumping of washing buffer (150 mM Tris-

acetate) solutions instead of neutralisation ones. The neutralization buffer is delivered through an additional inlet channel^{lix}. The pressure values in the third right-hand channel and in the neutralisation channel must be carefully calculated. Otherwise, the flow could go in a wrong direction.

The basic function of those modules is to perform DNA hybridisation transfer from one channel to another using magnetic beads with immobilised DNA oligomers. Single-stranded DNA molecules, coming from the left-hand channel, hybridised to the DNA oligomers attached to the bead under a continuous flow when the beads were on the left-hand side of the chamber (see Figure 38). Then the beads were moved to the right-hand side of the chamber where the pH is strongly alkali, due to the NaOH solution delivered via the right-hand channel. As a result, the DNA hybridised to the beads is denatured and passed to the right-hand channel (see Figures 44 and 45). The denaturing solution with DNA should be neutralized before reaching the beads incorporated into the next selection module. That process could allow the performing of a multi-step DNA hybridisation transfer under isothermal conditions.

Choice of a buffering solution for the isothermal DNA hybridisation transfer was an important task. The Tris-acetate buffering solution could be replaced with the same concentration of HEPES or Tris-borate buffering solutions. The DNA/DNA hybridisation fidelity of all those buffers was demonstrated experimentally in section 3.2.1. The experimental realisation of both basic microfluidic architectures (see Figures 37 and 38) is presented in the next two chapters.

3.4.2 Efficiency of cascable hybridisation DNA transfer between micro-reactor selection modules by a pH neutralisation

In this chapter, I demonstrate experimentally the ability to select, restrain, transfer and pick up DNA between two modules. The procedure was described in the previous section. Both chambers were filled with beads and different buffer solutions were used at the inlets to the two chambers at various stages. Here the flows were switched in larger chambers to facilitate quantification of the transfer yields with constant bead locations. 5' amino-modified DNA (see Table 3, line 6), 35 in length, was immobilised on the beads as described in section 2.2.2.1_1. A perfectly matching 21 nt DNA oligomers was used (see Table 3, line 7) for the hybridisation experiments. The complementary strand in the solution was 5' R6G-labelled.

The series of events for a complete transfer round from one module to the next was⁴¹:

1. Hybridisation of perfectly matching DNA (see Figure 37_A) to beads in both chambers.

2. Washing of the beads in both chambers.

3. Releasing DNA from the beads in the second downstream chamber and washing of the beads in the first chamber (see Figure 37_B).

4. Simultaneous release of DNA from the beads in the first chamber and pickup of the same DNA in the second chamber (see Figure 37_C).

1 M Tris-acetate solution, pH 8.3, was used for a neutralisation the denaturing solution of 100 mM NaOH. 150 mM Tris – acetate solution was used as a washing buffer (for more details see section 2.2.3.4).

Previous to that 5' R6G-labelled DNA used in the hybridisation experiments was incubated in 500 mM Tris, pH 8.3, and in 100 mM NaOH for 3 hours at 40 °C. In both cases the values of measured fluorescence signal were identical (see Figure 27). 100 mM sodium hydroxide solution does not influence the fluorescence signal of R6G-labelled DNA under those conditions. Thus, the fluorescence intensity can be used for quantification of the hybridisation DNA transfer.

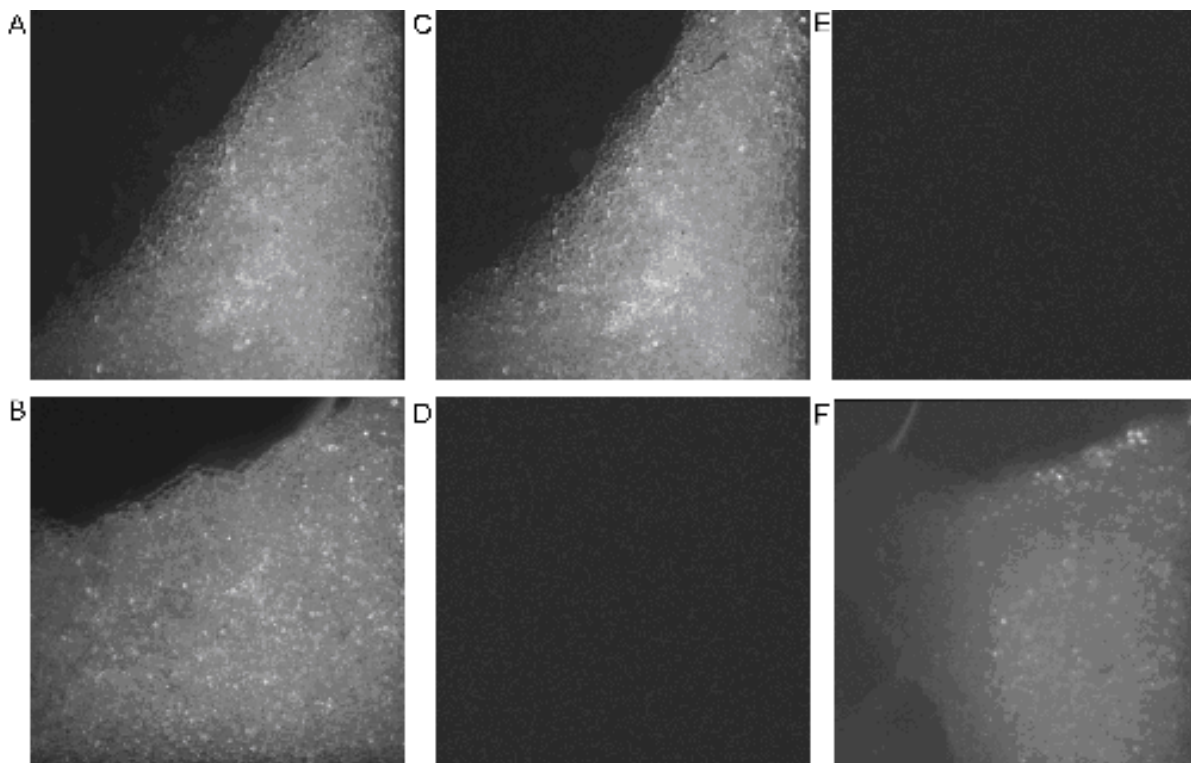


Figure 39 DNA hybridisation transfer between micro-reactors selection modules under isothermal conditions at a high flow rate (4 μ l/min). *Fluorescence images of DNA hybridisation on beads in a micro-flow reactor (see Figures 5 and 14) showing the course of transfer from one module to the next. DNA*

hybridisation on the beads placed in the first chamber (A) and second chamber (B); Washing of the beads in the first chamber (C) and DNA denaturation on the beads in the second chamber (D); DNA denaturation from the beads in the first chamber (E) and pick up of the same DNA on the beads placed in the second chamber (F). A CH250 camera was used (see Figure 11). The exposure time was one second.

Figure 39 shows images of the fluorescence from DNA hybridisation to the beads in the two chambers at various stages (see above 2, 3 and 4) of the above transfer procedure⁴¹. The results are summarized in Figure 40, showing the quantification of DNA on the beads in the two chambers at the four stages of the procedure. Moderately high flow rates were employed, so that diffusive mixing was not perfect as indicated by the slightly inhomogeneous pickup (Figure 39, image F). As seen in Figure 40, about half of the DNA bound in chamber 1 was successfully picked up in chamber 2 in the transfer step (see Figure 40).⁴¹

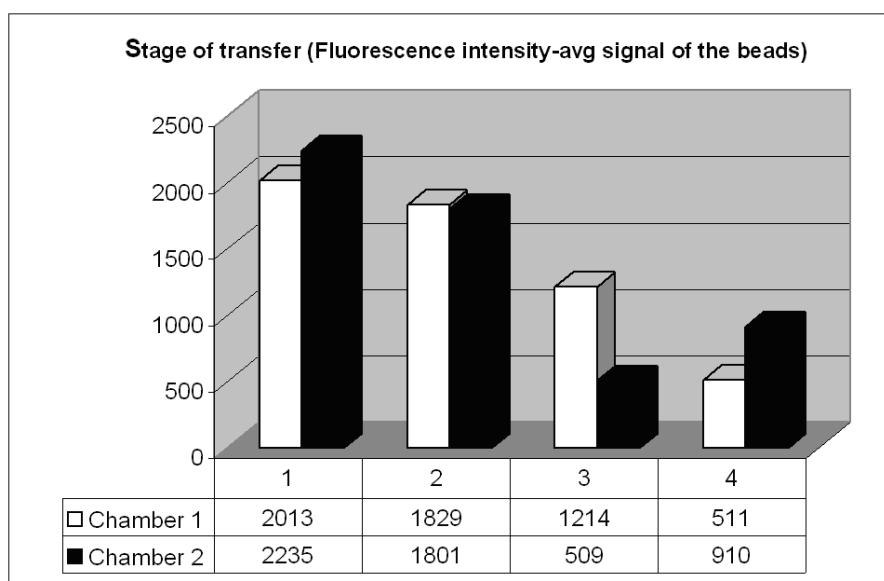


Figure 40 Quantitative analysis of DNA hybridisation transfer from beads in one module to those in a second module at a high flow rate. Average fluorescence intensity (including the bias signal of 490 units) images of two regions of the micro-reactor (see Figure 37) containing beads (see Figure 39) are shown under various flow conditions. White bars: fluorescence intensity from the first chamber of the micro-reactor. Black bars, fluorescence intensity from the second chamber. **1.** DNA hybridisation on the beads in the first and second chamber. **2.** Washing step of DNA hybridised on the beads in the both micro-reactor chambers. **3.** Continuous washing step on the beads in the first micro-reactor chamber and denaturation step on the beads in the second chamber. **4.** Denaturation of DNA from the beads in the first

chamber and pick up of the same DNA by hybridisation on the beads placed in the second micro-flow reactor chamber. For details, see text. The DNA pick up yield is about 55 %.

The DNA transfer yield was calculated as the average fluorescent signal on the beads from the second chamber after the pick up experiment (see Figure 40, column 4) being deviated to the average fluorescent signal on the beads from the first chamber immediately before the DNA pick up (see Figure 40, column 3). The background signal (510 units) was extracted in both values. The DNA pick yield was established to be about 55 %.

Mixing of buffers between crossing channels in micro-flow reactors is not a trivial task because of the low Reynolds number. Special mixing microstructures are developed to facilitate the mixing in micro-fluidic devices (see Figure 47). The micro-flow reactor applied by me for a DNA hybridisation transfer under isothermal conditions was designed for completely different goals so that the micro-reactor architecture was not the optimal one for the current experiments. It is obvious from Figure 39 that there is no complete mixing inside the second chamber between the solution coming from the first chamber and the one pumped through the first inlet. Different flow rates were to be applied to improve the mixing. The results, shown in Figure 41, were obtained at the lowest possible flow rate of the used pump. A 1 M Tris buffer solution, pH 8.3, containing 1 μ M rhodamine 6G, was pumped through inlet 1 (see Figure 37) at a flow rate of 0,01 μ l/min and 100 mM NaOH, rhodamine free solution was pumped through inlets 2 and 3 at a flow rate of 0,005 μ l/min.

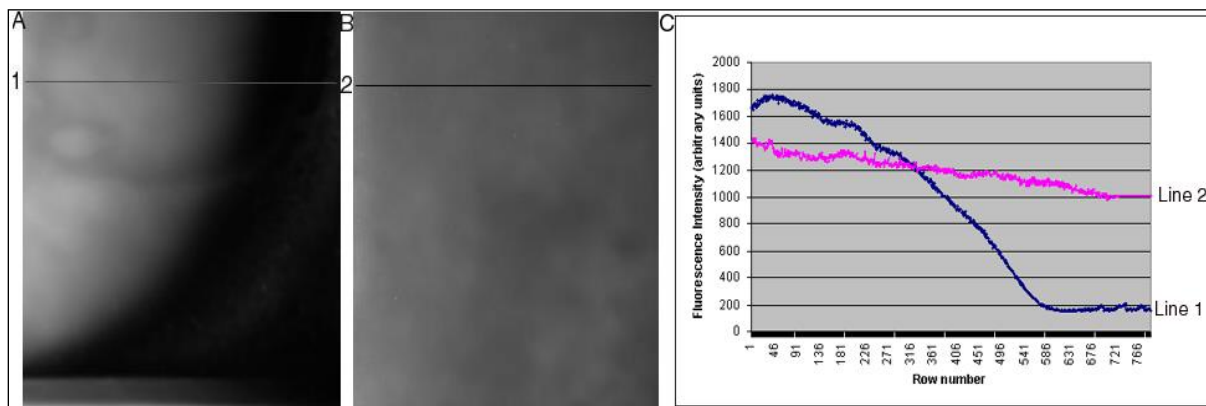


Figure 41 Mixing efficiency in the micro-flow reactor used for a DNA hybridisation transfer under isothermal conditions at a low flow rate. A 1 M Tris buffer solution, pH 8.3, containing 1 μ M rhodamine 6G was pumped through inlet 1 (see Figure 37) at a flow rate of 0,01 μ l/min and 100 mM NaOH, rhodamine

*free solution was pumped through inlets 2 and 3 at a flow rate of 0,005 $\mu\text{l}/\text{min}$. **A:** A fluorescence image from the top part of the second chamber. **B:** A fluorescence image from the middle part of the second chamber. **C:** A plot showing of the fluorescence intensity profiles from line 1 on a picture A and line 2 on a picture B. A CH250 camera was used (see Figure 11). The exposure time was a half of second.*

Fluorescence images from the top part of the second chamber (see Figure 41_A) and from its middle part (see Figure 41_B) were obtained. The intensity profile of both pictures is plotted in Figure 41_C. As obvious from the figures, there is a clear border between the two pumped solutions in the top part of the second chamber. The border, between the two fluids, disappears in the middle part of the chamber as a result of an almost complete mixing between the two solutions under the applied flow rate (see Figure 41_C, line 2). Let me make the same isothermal DNA hybridisation transfer experiment under the low flow rate conditions demonstrated above. The main question is, if that could increase the DNA hybridisation transfer yield. The obtained pictures are shown in Figure 42. The average fluorescence intensity signal of those images is plotted in Figure 43. As can be seen the fluorescence signal on the beads in Figure 42_F is much more homogeneous than the one in Figure 39_F. That is obviously a result of a more homogeneous mixing at the lower flow rate applied in the second DNA pick up experiment.

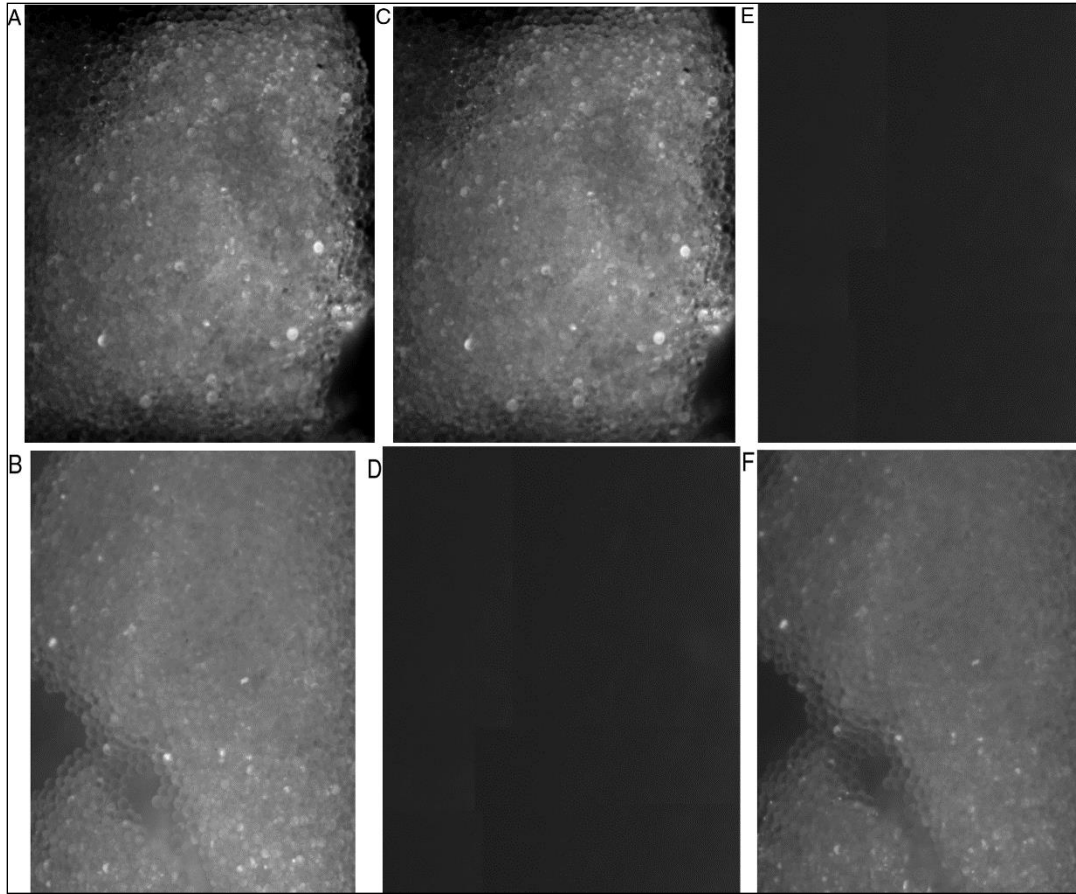


Figure 42 DNA hybridisation transfer between micro-reactors selection modules under isothermal conditions at a low flow rate (0.01 $\mu\text{l}/\text{min}$ as described in Figure 41). Fluorescence images of DNA hybridisation on beads in micro-flow reactor showing the course of transfer from one module to the next. DNA hybridisation on the beads placed in the first chamber (A) and second chamber (B); Washing of the beads in the first chamber (C) and DNA denaturation on the beads in the second chamber (D); DNA denaturation from the beads in the first chamber (E) and pick up of the same DNA on the beads placed in the second chamber (F). The DNA pick up yield is 59 %. A CH250 camera was used (see Figure 11). The exposure time was one second.

DNA hybridisation transfer yield was increased slightly with about 3-4 %. In both experiments the amount of beads placed in both chambers was aimed to be equal. However, in the first DNA transfer experiments presented in Figure 39 the amount of beads in the first chamber was about 80 % of that in the second chamber. The bead amounts in both chambers in the second pick up experiment were almost equal (see Figures 42 and 43). If one takes into account that factor, the pick up in the first experiment will be reduced to 50 %. That will increase the difference between

the DNA transfer yield in the two experiments to about 10 % in favour of the second one performed at the lower flow rate. One should take into account the fact that DNA/DNA hybridisation kinetics on beads under flow conditions is very much dependent on the low rate as demonstrated in section 3.3.1.

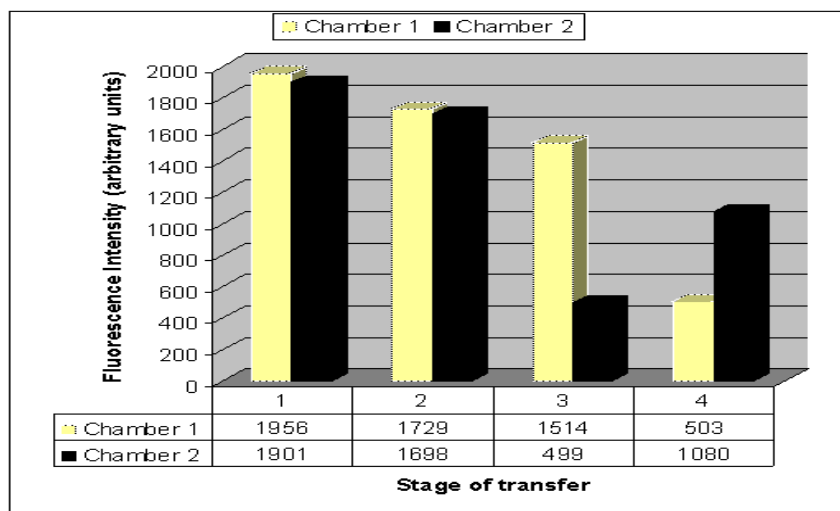


Figure 43 Quantitative analysis of DNA hybridisation transfer from beads in one module to those in a second module at a low flow rate. Average fluorescence intensity (including the bias signal of 490 units) images of two regions of the micro-reactor (see Figure 37) containing beads (see Figure 41) are shown under various flow conditions. White bars: fluorescence intensity from the first chamber of the micro-reactor. Black bars, fluorescence intensity from the second chamber. **1.** DNA hybridisation on the beads in the first and in the second chamber. **2.** Washing step of DNA hybridised on the beads in both micro-reactor chambers. **3.** Continuous washing step on the beads in the first micro-reactor chamber and denaturation step on the beads in the second chamber. **4.** Denaturation of DNA from the beads in the first chamber and pick up of the same DNA by hybridisation on the beads placed in the second micro-flow reactor chamber. For details, see the text.

3.4.3 DNA hybridisation transfer by moving beads in micro-chambers

The idea for implementation of a multi-step DNA hybridisation transfer in micro-flow reactors by moving magnetic beads between two spatially separated solutions with different pH under steady flow conditions was proposed by John McCaskill³⁷. The first practical implementation of that idea by using of one stand transfer module (STM) is presented here. The module consists of three inlet and three outlet channels and a chamber, with an etched bead barrier at the bottom (see Figure 3).

The hydrodynamic flow stability in the STM was tested using a fluorescence solution of rhodamine 6G.³⁹ The microflow reactor was illuminated with an argon-ion laser. The fluorescence images were obtained by using tandem optics with a combination of fluorescence filters and a nitrogen-cooled CCD camera and a quantix CCD camera with a combination of a microscope (see sections 2.2.6.2 and 2.2.7), controlled by PMIS software. Firstly, the fluorescent solution of 1 μM rhodamine 6G, solved in a 500 mM Tris-acetate buffer solution and 50 mM NaOH was pumped through all inlet channels (see Figure 44_A). Secondly, the fluorescence solution of 1 μM rhodamine 6G solved in 100 mM NaOH, was pumped through the right-hand channel, only, while non-fluorescence solutions of 1 M Tris were delivered via the middle channel and a 500 mM Tris-acetate buffer solution and 50 mM NaOH via the left-hand channel. As one can see from the image in Figure 44_B, there is a sharp border between the non-fluorescence solution coming from the middle channel and the fluorescence solution coming from the right-hand channel. The fluorescence intensity profile of that border is plotted in Figure 44_C.

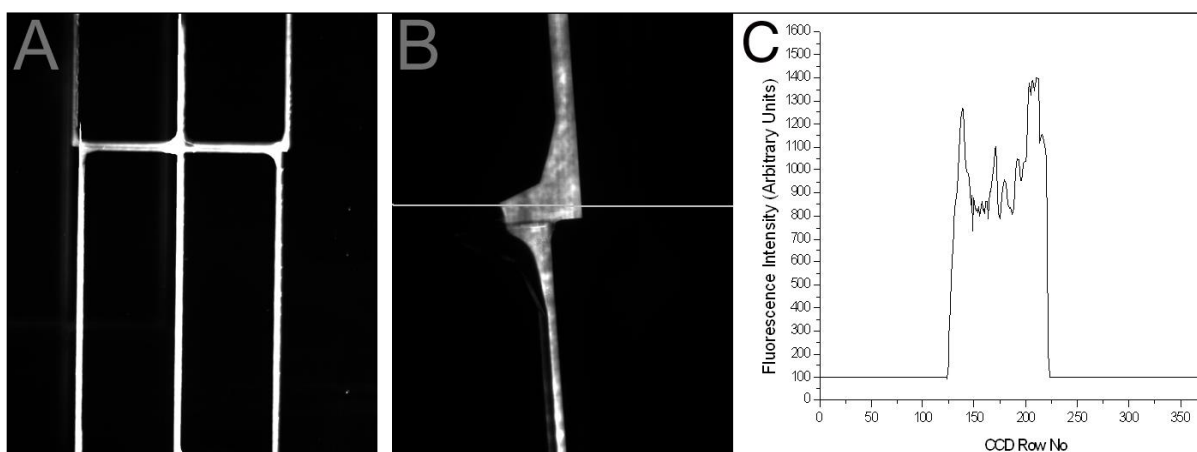


Figure 44 Fluorescence images of steady flow patterns in a strand transfer module. *A*: Tris solutions of rhodamine 6G were pumped through the three inlet channels on the top of the picture. The solution went out from the three outlet channels on the bottom of the picture. A LN camera was used. The exposure time was one second. *B*: Tris solutions free of rhodamine 6G were pumped through the left-hand and the middle channel, while a sodium hydroxide solution containing rhodamine 6G was pumped through the right-hand channel. The flow rate in all cannels was 0,5 $\mu\text{l}/\text{min}$. A quantix camera was used. The exposure time was a half of second. *C*: Fluorescence intensity profile of the line from a picture B is plotted.

The result shows that a significant part on the right-hand side of the bead chamber contains a solution, which is coming from the right-hand channel only. The micro-flow reactor`s design is

symmetric, which means that there is a similar part on the left-hand side of the chamber, through which only solution from the left-hand channel is passing.

I here present a single DNA hybridisation transfer using the same micro-flow reactor shown above. PVA magnetic beads (see Table 4, line 3) with a 50 % magnetic content were incorporated into the chamber using the inlet channels. 5' amino-modified DNA, capture probe 2.1, (see Table 1, line 3, column 4) were immobilised to the beads from the beads' manufacture. A buffer solution of 500 mM Tris, pH 8.3, and 50 mM NaOH containing 1 μ M, 5' end R6G labelled DNA library, assembled as described in section 3.5.2, was pumped through the left-hand channel. A 150 mM Tris solution through the middle channel was delivered simultaneously with a 100 mM NaOH solution through the right-hand channel. The micro-flow reactor images were obtained with an inverted microscope Axiovert 100 TV and a quantrix CCD camera (see Figure 11).

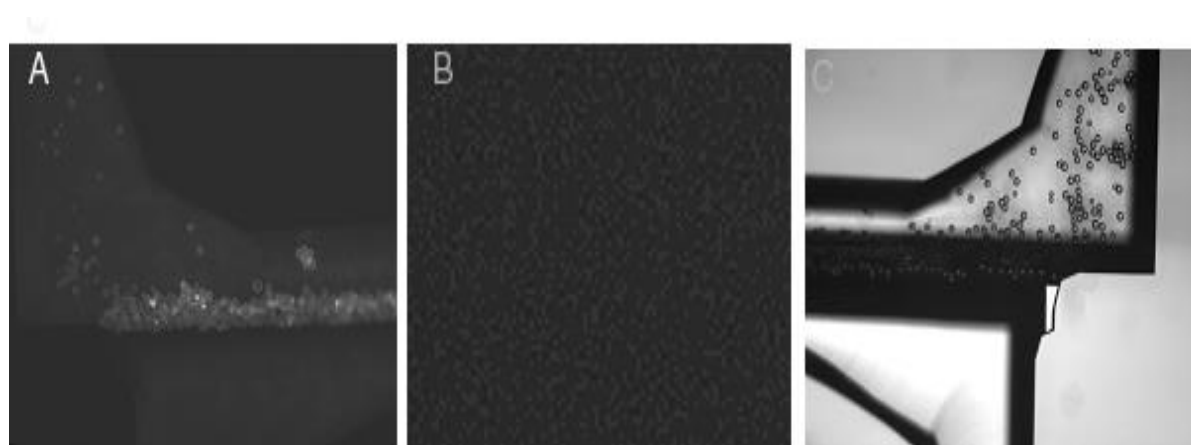


Figure 45 DNA hybridisation transfer in STM under steady flow conditions. The micro-flow reactor shown in Figure 3 was used. A solution including 500 mM Tris, pH 8.3, 50 mM NaOH and 1 μ M, 5' end R6G labelled DNA library was pumped through the left-hand channel. A 150 mM Tris pH 8.3 solution was pumped through the middle channel and 100 mM NaOH solution - through the right-hand channel. The flow rate in all channels was 0,5 μ l/min. **A:** Fluorescence image of DNA hybridisation on $12 \pm 3 \mu$ m PVA superparamagnetic beads, which was being fixed by a magnetic stand into the left-hand corner of the micro-flow reactor chamber. **B and C:** The beads were moved by the magnetic stand into the right-hand corner of the micro-reactor chamber. DNA hybridised to the beads was denatured with a 100 mM NaOH solution flowing through the right-hand channel. A fluorescence image obtained from the beads is shown on picture **B** and a white light image on picture **C**. A quantrix camera was used (see Figure 11). The exposure time was one second in **A** and **B**.

Firstly, the beads were moved to the left-hand side of the chamber by a magnetic stand put under the micro-reactor. DNA hybridisation took place at the left-hand position of the beads in the micro-chamber (see Figure 45_A). Then the beads were moved to the right-hand side of the chamber by the magnetic stand as described in section 2.2.7. The DNA denaturation took place at that position (see the fluorescence image in Figure 45_B and the white image in Figure 45_C). A single hybridisation transfer of DNA coming from the left-hand channel to the right-hand channel by moving beads between spatially separated hybridisation and denaturing solution in the micro-reactor chamber was demonstrated.

However, I should admit a lot of technical difficulties connected to that simple experiment. The beads had a 50% magnetic content (or even more, see Table 4, line 3). Despite of that, it was still a technical problem to move all of them in the single micro-flow reactor used. There are at least two reasons for that. Firstly, the beads had the ability to stack in certain parts of the micro-flow reactor such as the bead barrier, which has something to do with the way micro-flow reactor was produced. Secondly, the beads had to overcome a certain pressure in the microfluidic chamber. In the process of the bead movement the flow segregation (see Figure 44) in the bead chamber was disturbed. In this micro-fluidic design there was not good practical opportunity to wash the beads intensively with a low ionic strength buffer because it was difficult to fix simultaneously all of the beads into the middle part of the chamber. In addition, only 35 DNA pmol/mg beads hybridisation yield could be achieved on these beads according to the manufacture's report.

Van Noort et al did two implementations of the presented basic idea to several connected micro-modules^{59,60}. In the first case the micro-flow reactor applied the basic architecture shown on Figure 38_C.⁵⁹ In the second case the crossing channels were avoided (see Figure 38_B)⁶⁰.

3.4.4 An integrated and automated micro-fluidic chip for bio-molecular analyses

The bio-molecular chip arrays are playing an important role in many areas of contemporary molecular biology, pharmacology, and medicine and as we can see in DNA computing. A key advantage of bio-molecular chip arrays is the opportunity to analyse a large number of bio-molecules (DNA, RNA, proteins, or drug candidates) in parallel. A high level of automation, integration and programmability are required in the development of such devices. I here propose a novel microfluidic architecture for fully automated and integrated bio-molecular analyses of DNA, RNA, polypeptides, or drug candidates.

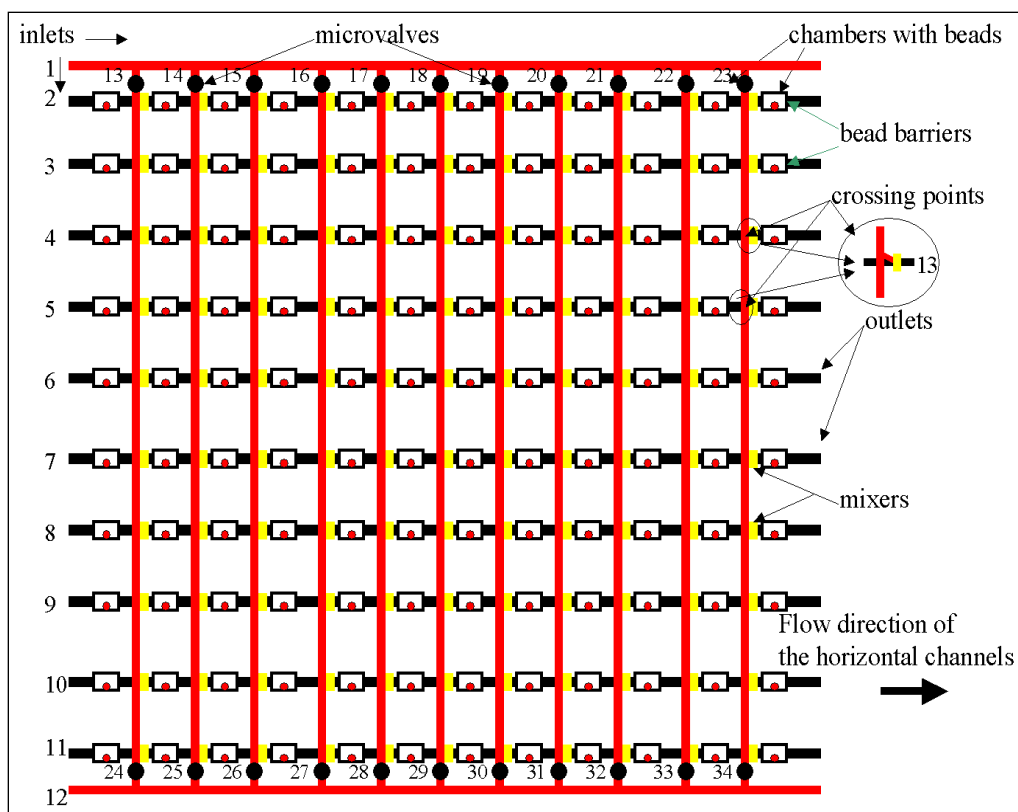


Figure 46 Scheme of an integrated, automated, programmable and reusable micro-fluidic device for a parallel, multi-step, sequence-specific DNA selection under isothermal conditions by using of valves. The same scheme as presented in Figure 20 but with a combination of valves. The use of valves reduces the number of inlets from the vertical channels to two only, regardless of the number of those channels. The principal immobilisation and transfer procedures could be described as follows. The first horizontal channel (number one) is applied to deliver the cross-linking reagent, in the case of immobilisation, or the neutralisation solution, in the case of transfer, and the horizontal channel is used to deliver the inhibitor of the immobilisation reaction or denaturing solution in the case of DNA hybridisation transfer. The other horizontal channels are used to deliver the bio-molecules to be immobilised or selected. For more details see the text.

The approach is based on the pH-reversible chemistry described in this thesis for an isothermal DNA hybridisation transfer between connected micro-chambers (see section 3.4.2) and the spatially defined bio-molecular immobilisation by separated delivery of the bio-molecules (DNA for instance) and the cross-linking reagent (EDAC for instance) in connected micro-chambers (see section 3.1.2). The already established inhibition of the immobilisation reaction guarantees an

absolute level of specific DNA attachment (see section 3.1.2). Both processes, the immobilisation and the transfer/selection, are fully integrated and automated, and take place in parallel.

The general scheme of the proposed microfluidic architecture contains $N+2$ in number horizontal channels crossed by M in number vertical channels by A in number ($A=N \times M$) small connecting channels (see point 13 in Figure 46 and Figure 47_C). There is a mixing structure X after each crossing point ($X=N \times M$), followed by a chamber, being a part of the horizontal channels (see Figure 46). The number of chambers is $C = N \times M + N$. Each chamber has a bead barrier at the bottom. Paramagnetic beads could be delivered to each chamber via the vertical channels (see Figure 46, 2-11). The micro-flow reactor has $I=N + 2$ in number inlets and an $O=N + 2$ in number outlets. The number of inlets (P) of the vertical channels is reduced to not more than two regardless of the number of vertical channels by using of valves $V=2 \times M$ as presented in Figure 46 in contrast to the microfluidic design presented in Figure 20. One could pay attention to the fact that the number of valves, inlets and outlets increases linearly while the number of chambers is in a square function. That makes the proposed design less complicated and easier to implement.

The microfluidic architecture could be used for creating DNA, RNA, polypeptides or cell microfluidic arrays. The presented approach is universal as every type of bio-molecule could be selectively immobilised to the beads placed in different chambers or to their surfaces by using of almost any cross-linking bio-conjugate chemistry. That makes the biochip's production chemistry independent. Different procedures for spatially defined immobilisation were employed such as light-directed DNA synthesis (Affimetrix)^{lx} and immobilisation⁴⁰, DNA spotting by electric field (Nanogen)^{lxi}, patterning in parallel laminar flow^{lxii, lxiii} or in crossing flows^{lxiv}. All of those processes are more or less dependent on the application of a particular chemistry and/or cannot guarantee an absolute level of specific bio-molecular immobilisation in contrast to the general immobilisation procedure proposed here employing the microfluidic architecture presented in Figure 46.

The general bio-molecular immobilisation procedure in the microfluidic device presented in Figure 46 can be described as follows: N in number different bio-molecules are delivered through the N number of horizontal channels with an exception of the first and the last channels. The molecules could be either modified or non-modified depending on the chemistry used. The employed cross-linking reagent is pumped through the first horizontal channel while an inhibitor of the

immobilisation reaction is pumped through the last one (see Figure 46). All micro-valves are closed. As a result the cross-linking reagent is not presented in any chamber and no bio-molecular immobilisation takes place. If the valve number 23 is opened the cross-linking reagent is presented into the chamber of the last column (a vertical row) as a result of the flow direction (see Figures 46 and 47). If no zero-cross linking reagent is used the delivery of the DNA will be next to the delivery (immobilisation) of the linking reagent to the chambers of an addressing column (vertical row).

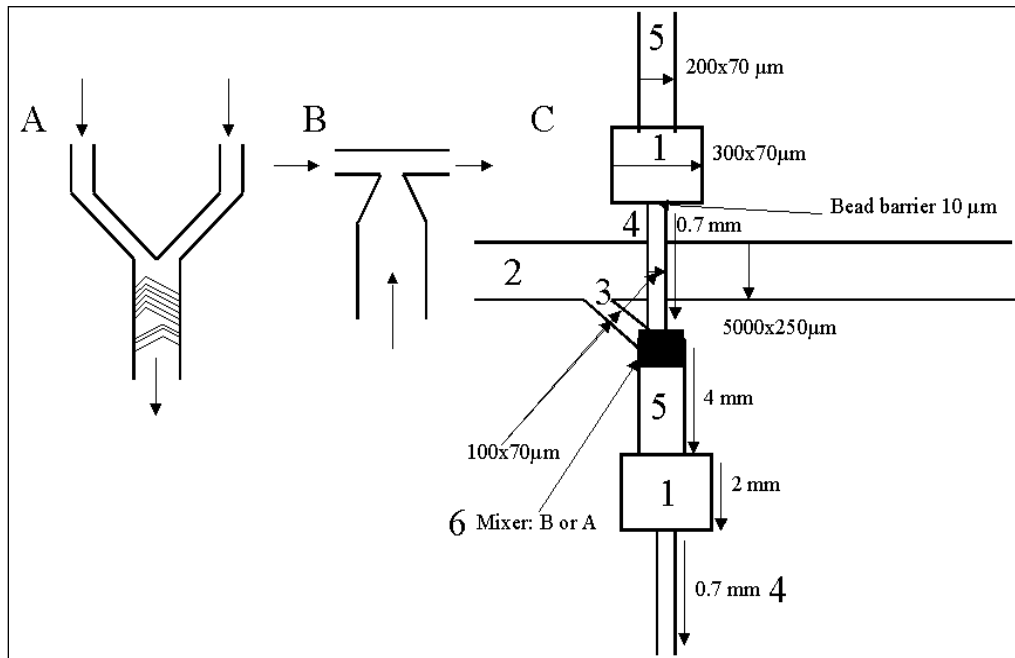


Figure 47 Micro-fluidic mixers and crossing channels. *A: chaotic horizontal mixer. B: vertical mixer. C: One point of crossing micro-channels with a combination of a micro-mixer (see Figures 20 and 46, points 13). The dimensions of the vertical channel (2) allows up to 100 crossing points in a row. 1: micro-chambers; 2: a vertical channel (see Figures 20 and 46). 3: small connecting channel; 4, 5: parts of a horizontal channel (see Figures 20 and 46); 6: a passive micro-mixer like A, B, or a combination of both. The velocity (pressure) between the crossing channels number 3 and 4 is equal as a result the flow direction in all vertical channels is down stream (from the top to the bottom).*

In the next step, N in number different bio-molecules are delivered through the N number horizontal channels (without the first and last one, see Figure 46). This time the valve number 23 is closed but valves number 22 and 34 are opened (all other valves are closed). That results in the presence of the cross-linking reagent in the chambers of the last two columns and simultaneously

in the presence of inhibitor in the chambers of the last column only. As a result, the immobilisation reaction takes place into the chambers of a column number 11. The use of an inhibitor avoids the need for reaching absolute saturation of the immobilisation reaction, which seems difficult to achieve simultaneously in many samples. The immobilisation scheme could be repeated $M+1$ times, guaranteeing specific immobilisation of unique bio-molecule to each micro-chamber ($N \times M+1$). The implementation of particular chemistry for DNA immobilisation to carboxyl-coated beads placed in cascably connected micro-chambers was already demonstrated (see section 3.1.2). It is indeed important to understand that the presented microfluidic architecture (see Figure 46) allows a fully automated implementation not only of programmable bio-molecule (DNA) immobilisation but also of cascable DNA hybridisation transfer under isothermal conditions, applying the chemistry demonstrated in section 3.4.2.

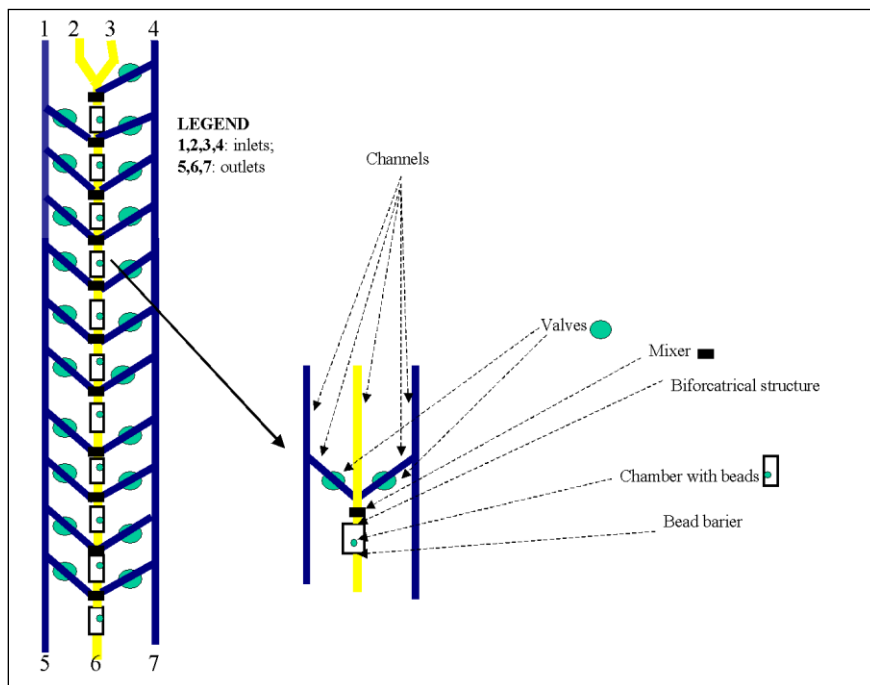


Figure 48 Scheme of an automated, programmable and reusable micro-fluidic device for a multi-step, sequence-specific DNA selection under isothermal conditions by using of valves. *The parallelism is not possible in that module in contrast to that presented in Figure 46. Inlets: 1: delivers the neutralisation buffer; 2: delivers ssDNA pool; 3: Washing solution, 4: denaturing solution. The same immobilisation and selection procedures could be applied as described for Figure 46 (see above) but not in parallel.*

Let all chambers (the beads' or chamber' surfaces) be addressed (immobilised) with different synthetic DNA sequences. An initial pool of ssDNA dissolved in a buffer solution of 500 mM Tris, pH 8.3, (or HEPES, pH 7.6,) and 50 mM NaOH is delivered through the N in number horizontal channels with an exception of the first and last channels (see Figure 46). All valves are closed. The first horizontal channel delivers the neutralisation buffer (1 M Tris-acetate, pH 8.3, or 1 M HEPES, pH 7.6) and the last channel delivers the denaturing solution of 100 mM NaOH.

Next to the hybridisation, the beads are washed with a 150 mM Tris buffer, pH 8.3, pumped through N in number horizontal channels. A valve number 24 is opened. As a result, the pH value in the chambers of all columns except the first one is more than 12. Thus a DNA denaturation takes place there. Next, a valve number 13 is opened only and simultaneously 100 mM NaOH (or 50 mM NaOH) is delivered through N in number horizontal channels (through all horizontal except the first and the last one). That means the hybridised DNA in the chambers of the first column is denatured and simultaneously picked up to the beads placed in the next chambers. That could be accomplished not only in parallel (see Figure 46) but also in a single run as shown in Figure 48. The proposed architectures (see Figures 46 and 48) requires simultaneously mixing between the crossing channels of two levels only, which is easy to achieve practically. That is a significant difference to the micro-flow design under steady flow conditions³⁷, which requires simultaneously mixing between crossing channels at all levels.

The concrete dimensions of the microfluidic design shown in Figure 46 depend on the number of chambers in one column and on the number of columns. One example shown in Figure 47_C allows up to 100 chambers to be supplied by one vertical channel. The pressure in both crossing channels (see Figure 47_C, points 3 and 4) should be similar, if not equal, to guarantee the flow in the right direction (downstream to the channels with micro-chambers). The use of special mixing structures (see Figure 47_A and B) allows complete mixing within 2-4 mm^{lxv}. A passive vertical mixer (see Figure 47_B) is in principal more efficient than a horizontal one (see Figure 47_A) due to the smaller mixing area between the crossing fluids. A turbulent flow in micro-channels is difficult to achieve due to a low Reynolds number. However applying special microstructures (see Figure 47_A, etching channel bottom) a turbulent flow can be achieved, which speeds up the mixing process. A complete mixing could also be achieved by actively moving beads in micro chambers by external magnetic stand (see Table 5). In addition, a bifurcation structure, as that

shown in Figures 5 and 14, could be applied at the top of each chamber being a part of the horizontal channels if there is a significant difference in the width of the channel number 5, presented in Figure 47, and the bead chamber. There are plenty of different micro-valves developed up to now. The practical implementation of hundreds of micro-valves on a single wafer is not yet achieved. The presented microfluidic designs (see Figures 46 and 48), however, requires a very limited number of valves, which is perfectly feasible by contemporary micro-valve technologies. The presented concrete microfluidic dimensions in Figure 47 could be optimised and reduced in order to achieve even higher level of integration.

3.4.5 Discussion

The presented an isothermal DNA hybridisation transfer between micro-fluidic chambers has been demonstrated for the first time by the author. The approach is novel and attractive because of its potential to integrate many selection modules in a row. The conventional approach is to use a high temperature (usually in a range of 85-93 °C) for DNA denaturation. However, maintaining of a temperature gradient in microfluidic structures seems to be more space demanding than mixing fluids between crossing micro-channels^{lxvi}. The DNA transfer efficiency, from one module to the next, of 60 % (see Figures 42 and 43, stage of transfer 3 and 4) may be optimised, with values greater than 90 % being sought. Nevertheless, let me base the calculations on 50 % transfer efficiency between two selection modules under conditions, in which the amount of DNA immobilised to the beads is equal to the amount of DNA in the free solution coming to the second selection module from the first one. What should be the conditions in which we will have guaranteed more than 95 % transfer efficiency? This will certainly be achieved if we will have an excess of five times of immobilised DNA to the beads in a comparison to the amount of DNA in the free solution (96.9 % pickup efficiency). If we need to achieve 99.9 % pick-up efficiency we should have an excess of 10 times of immobilised DNA to the beads than one in the passing solution.

The demonstrated chemistry for an isothermal DNA hybridisation transfer between micro-flow reactors raises the question for the most suitable microfluidic design, which makes use of it. There are two possible micro-reactor schemes, one with a bead movement (as demonstrated in Figures 38 and 45) and another with keeping of the beads at stationary conditions (as demonstrated in

Figures 37, 42 and 46). The demonstrated single DNA hybridisation transfer by moving of magnetic beads between spatially separated hybridisation and denaturation solutions in a micro-chamber (see Figure 45) opens the important question, whether that technology is scalable to a large number of cascadably connected reactors. There are at least three possible scenarios (see Figure 38) for employing of reversible chemistry for multi-step DNA hybridisation transfer by a bead movement. It seems quite a problem to have beads with a high magnetic content, a high DNA immobilisation yield, a low level of non-specific DNA attachment and a high chemical stability in sodium hydroxide solutions. Further improvement in the micro-flow reactor's architecture in terms of flow stability and beads movement must be achieved in order to have a successful integration of several micro-flow reactors in a row. The proposed micro-flow reactor designs (see Figures 20, 46 and 48) seems to be able to overcome the observed difficulties. There is no need to move beads at all; a simultaneous mixing between the crossing channels is required at two levels only in contrast to the steady flow design, where a simultaneous mixing between the crossing channels at all level is required. In addition, that micro-reactor design proposed by me is chemistry independent in terms of DNA programmability (immobilisation), which is embedded together with the selection procedure into the same microfluidic design. That means the same design /structure (see Figures 20 and 46) could implement two different functions (a programmable DNA immobilisation and a multi-step, sequence-specific selection of DNA in parallel).

3.5 DNA LIBRARY FOR MOLECULAR COMPUTATION IN MICRO-FLOW REACTORS

The fidelity of nucleic acid hybridisation in a large pool of different oligomer sequences is of essential importance to many methods of molecular biology such as expression analysis, single nucleotide polymorphism analysis, library screening, and different *in vitro* amplification reactions. In the DNA computing field, nucleic acid hybridisation was used as a basic computational operation. In this case the accuracy of the computation depends on the ability to discriminate between perfectly matching hybrids (the bits of the library and their complementary oligomers) and those with mismatches. In this respect the quality of the DNA code design is playing a crucial role in the fidelity of the computation. The problem of designing sets of modular RNA and DNA sequences, which hybridise in a predefined way, is fundamental not only to molecular computing but also to many applications in contemporary molecular biology and nanotechnology such as strand selection, PCR and isothermal amplification reactions, nucleic acid chip arrays, rational ribozyme design^{lxvii} and DNA self-assembly^{lxviii}.

Word design strategies for nucleic acid based computation have been already investigated experimentally^{lxix} and theoretically^{lxx, lxxi}. Sequence design methods implemented so far use discrimination between specific and non-specific hybridisation based on Hamming and related distances, ignoring the physical property of DNA to hybridise in more complex structures. The DNA library, presented here, is designed using discrimination between specific and non-specific hybridisation based on the thermodynamic stability of the DNA hybrids formed. The thermodynamic stability of certain DNA/DNA hybridisation is described by the free energy of the hybridisation reaction. In order to deal with the probability distribution of alternative DNA/DNA duplex structures, a partition function Q defined by John McCaskill^{lxxii} is computed for the formation of all possible secondary structures for a sequence, in which the first binding partner is connected via a spacer to the second binding partner. The spacer consists of artificial nucleotides ("N"), which are defined to have no binding properties so that no binding is possible to the spacer region (see Figures 49 and 50). To calculate the partition function Q and the free energy E_b

Equation 4

$$E_b = -kT \ln(Q)$$

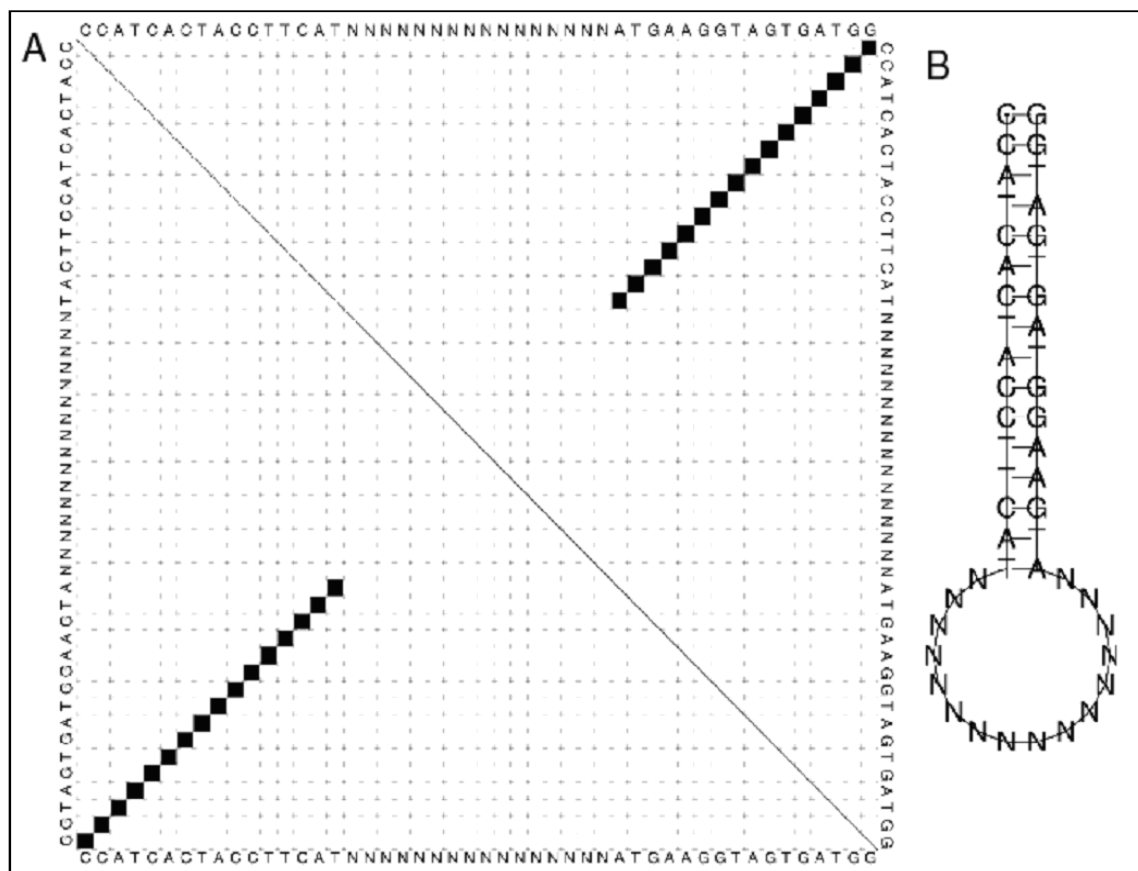


Figure 49 Schematic presentation of the partition function for perfectly matching DNA strands. *The Vienna RNA folding package was used to calculate the partition function with appropriate thermodynamic parameters (see Table 16) for the word 1_1 and its capture probe. A: The dot matrix represents base pairing probabilities. The example shows the hybridisation of a word to its complement. B: The dominant structure is plotted. The hybridisation thermodynamics is described by an ensemble of secondary structures for a sequence, which consists of the two binding partners connected via a spacer of sixteen artificial nucleotides “N” (see the text).*

to the ensemble of structures the Vienna RNA folding package^{lxxiii} was used (available via <http://www.tbi.univie.ac.at/~ivo/RNA>) and appropriate DNA parameters^{lxxiv, lxxv}.

The partition function (Q) is defined as the sum of the free energy contributions over the sum of all possible structures S:

Equation 5

$$Q = \sum_s e^{-[F(S)/kT]},$$

where F is the free energy of a secondary structure assumed in terms of its loops

Equation 6

$$F = \sum_{L \in s} F_L,$$

where F_L is the free energy of the various k and loop L (for $k \leq 2$).

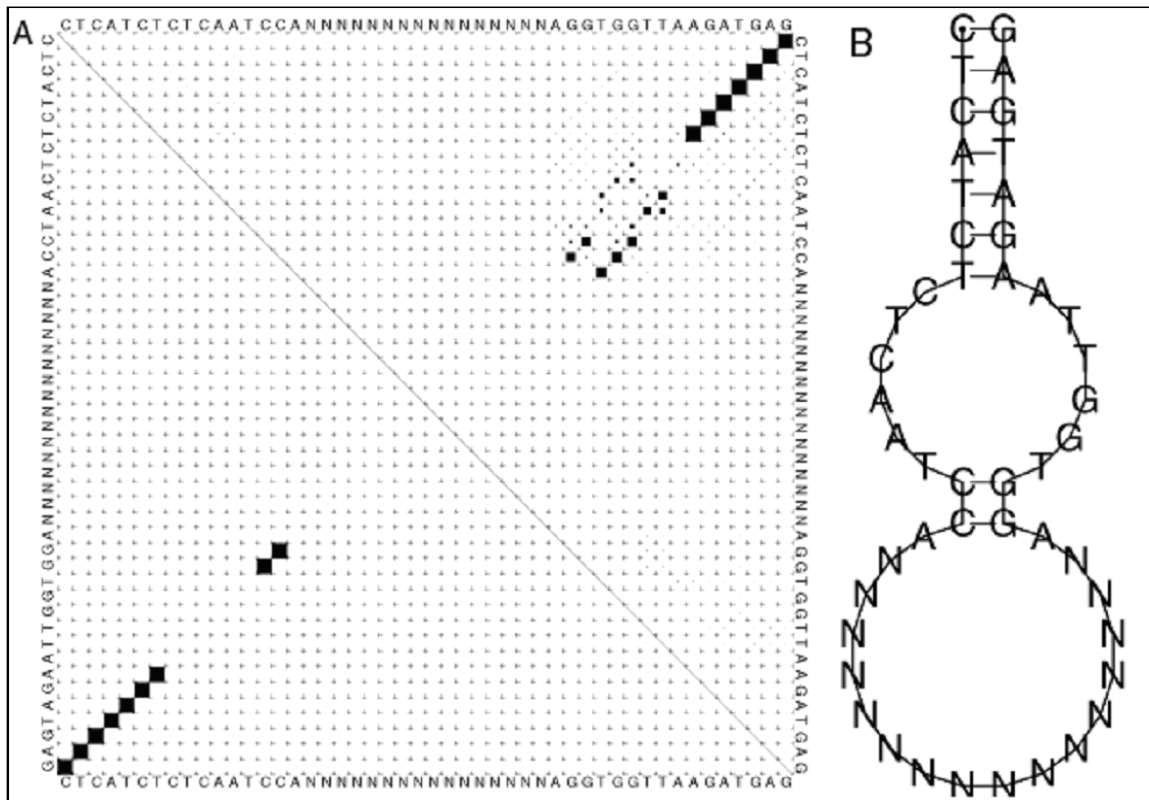


Figure 50 Schematic presentation of partition function for non-perfectly matching DNA strands. The Vienna RNA folding package was used to calculate the partition function with appropriate thermodynamic parameters (see Table 16) for the library sequence 010101010101 from 45 to 60 nt and the capture probe V_6^1 . The matching place was found by the software ADNA 4.1, which is one of the five places in entire DNA library with matching fragments of 7 nt at the 3' end of capture probes and the DNA library sequence. Two other places like that are shown in Figure 56. **A:** The dot matrix represents base pairing probabilities as on the left-hand side of the picture, the pairing probabilities for the dominant structure are shown. On the right-hand side of the picture the pairing probabilities for non-dominant structures are shown. **B:** The dominant structure is plotted. The hybridisation thermodynamics is described by an ensemble of secondary

structures for a sequence, which consists of the two binding partners connected via a spacer of sixteen artificial nucleotides "N" (see the text).

The probability (P) of a certain structure (S) is calculated on the basis of the partition function as follows:

Equation 7
$$P(S) = (1/Q) e^{-[F(S)/kT]}$$

The free energy E_b corresponds to the effective equilibrium constant for an ensemble of (probability weighted) duplex structures and has to be distinguished from the total minimal free energy ($\Delta G_{37}^{\circ}(\text{total})$, see equation 8), which describes the hybridisation of one particular structure (i.e. of the minimal free energy structure). To optimise the set of DNA words, a special algorithm was applied. The algorithm applied contains of two steps. In the first step, 24 words were optimised according to the thermodynamic stability of the hybrids formed using random search algorithm. In the second part of the algorithm, the obtain set of 24 words was ordered taking into account the thermodynamic stability of all possible hybridisation reaction between the capture probes to all sequence regions produced by the ligation of the words. The algorithm applied, implemented by Jörg Ackermann³⁸, is presented in section 2.2.8.

3.5.1 DNA library design criteria

The conditions to be fulfilled by the DNA library presented and tested in this work are given as follows³⁸:

1. It is a twelve-bit DNA library built from 24 different words (bits) representing a "one" or a "zero" at twelve different positions.
2. The library words contain A's, T's, C's but no G's^{lxxvi}. Avoiding the presence of G's in the sequences restricts their variability but simultaneously reduces significantly the stability of possible secondary structures and the hybridisation among the library sequences.
3. The words are 16 nt deoxyoligonucleotides. This length is a reasonable choice for primer binding sites and guarantees a large pool of $3^{16} \approx 4.3 \times 10^7$ different sequences.
4. The occurrences of 4 or more consecutive identical nucleotides in the words are avoided. The presence of long homopolymer tracts in the library sequences could be a reason for the

(kinetically favoured) formation of secondary structures. A similar constraint (not more than 5 consecutive identical nucleotides) is applied by Braich et al^{lxxvii}.

5. No word has a run of more than 7 consecutive nucleotides with all possible combinations of the other 23 words and their complementary sequences in order to avoid mispriming during the PCR amplification and formation of thermodynamically stable secondary structures among the library sequences.
6. Runs of three consecutive C's at either the 5' or the 3' ends are avoided because that could influence the hybridisation kinetics and produces mispriming during the PCR amplification.
7. The free energy gap between the weakest specific hybridisation and the strongest non-specific hybridisation within the word set should be as large as possible in order to reduce to a minimum any non-specific hybridisation reaction between the DNA library sequences and the capture probes.
8. The melting points (T_m) of the words have to be in a restricted range of ± 2.0 °C because I want to achieve uniform hybridisation yield for all capture probes under identical hybridisation conditions. To calculate the T_m values, the nearest neighbour approximation^{lxxviii} and the thermodynamic parameters of John SantaLucia (see below) were used.

In the thermodynamic approximation of nucleic acid hybridisation, the main energetic factor for hybridisation is not the energy of the hydrogen bonds formed between nucleotide bases, but is the nearest neighbour base stacking energies (see Table 16). The total minimal free energy of the hybridisation reaction based on nearest-neighbour thermodynamic approximation is given by the following equation:

Equation 8 $\Delta G_{37}^{\circ}(\text{total}) = \sum_i n_i \Delta G_{37}^{\circ}(i) + \Delta G_{37}^{\circ}(\text{sym}) + \Delta G_{37}^{\circ}(\text{init w/term G.C}) + \Delta G_{37}^{\circ}(\text{init w/term A.T}),$

where $\Delta G_{37}^{\circ}(i)$ are the standard free-energy parameters for the ten possible nearest-neighbour NN shown below, n is the number of occurrences of each neighbour, i , $\Delta G_{37}^{\circ}(\text{sym})$ equals to zero if the duplex is non-self-complementary and is +0.43 kcal/mol if the DNA strand is self-complementary. To take into account the differences between DNA hybrids with terminal pyrimidines vs terminal purine pairs, two different initiation parameters are introduced: initiation

with terminal pyrimidines ΔG_{37}° (init w/term AT) and initiation with terminal purines ΔG_{37}° (init w/term GC), see Table 16.

The enthalpy (ΔH°) and entropy (ΔS°) parameters given below are calculated of the free energy parameters thus the free energy could be computed by the ΔH° and ΔS° using the following equation:

Equation 9 $\Delta G^{\circ}_T = \Delta H^{\circ} - T\Delta S^{\circ}$.

Melting temperature (T_m) is defined as the temperature at which half of the strands are in double-helical state and half are in coil state (non-hybridised). ΔH° and ΔS° are used to compute the T_m as follows:

Equation 10 $T_m = (\Delta H^{\circ}/(\Delta S^{\circ} + R \ln (C/4))) - 273.15 + 12 \log_{10} (Na^+)$,

where R is the gas constant (1.987 cal/ K mol), Na^+ is salt concentration (M), C is DNA concentration (M) for hybridising of non-self complementary strands in equal concentrations and -273.15 is introduced for converting the T_m from Kelvin to Celsius. In order to estimate the free energy of non-perfectly matching DNA hybrids again Vienna RNA folding package was applied based on thermodynamic parameters by John SantaLucia.

Table 16 Unified nearest-neighbour thermodynamic parameters for DNA helix formation in 1 M NaCl by John SantaLucia⁷⁶.

Number	Sequence 5'-3'/3'-5'	ΔH° enthalpy kcal/mol	ΔG_{37}° free energy kcal/mol	ΔS° entropy cal/mol
1	AA/TT	-7.9	-1.00	-22.2
2	AT/TA	-7.2	-0.88	-20.4
3	TA/AT	-7.2	-0.58	-21.3
4	CA/GT	-8.5	-1.45	-22.7
5	GT/CA	-8.4	-1.44	-22.4
6	CT/GA	-7.8	-1.28	-21.0
7	GA/CT	-8.2	-1.30	-22.2
8	CG/GC	-10.6	-2.17	-27.2
9	GC/CG	-9.8	-2.24	-24.4
10	GG/CC	-8.0	-1.84	-19.9
11	Init. w/term. G.C	0.1	0.98	-2.8
12	Init. w/term. A.T	2.3	1.03	4.1

The difference in the free energy between specific and non-specific hybridisation in a random set of 24 different 16-oligomers is on the order of $\delta G = 2$ kcal/mol³⁸. δG decreases as the number of words increases and becomes zero for large set sizes (more than 100 random words). In that case it is not possible to distinguish between specific and non-specific DNA hybridisation. The free energy gap between the strongest non-specific hybridisation and weakest specific hybridisation in

the set of 24 words (see Table 1), generated by an algorithm presented in section 2.2.8, points 1_1-1_9, was found to be $\delta G = 8.9$ kcal/mol according to Jörg Ackermann³⁸. The melting temperatures of the words computed by equation 10 are in total range of 3.6 °C (see, Table 17, lines 5 and 17). The average number of C's is 6.7 (42 %), the average number of A's and T's is 4.5 (28 %) and 4.8 (30 %), respectively. It is an interesting result that the word set optimised according to the thermodynamic stability of all possible hybridisation reactions shows favourable mismatch properties as well (see Tables 18 and 19). In step B of the algorithm (see section 2.2.8; points 2_1-2_6), the order of the 16-oligomers in the library was determined³⁸. I tested the four sequences (111111111111, 000000000000, 101010101010, 010101010101), covering all word boundary sub-sequences in the library, against all words for slide complementary mismatches and complementary capture probe sequences for slide reverse mismatches (to do that an ADNA 4.1 programme was used).

Table 17 Thermodynamic properties of DNA word sequences (bits) and their capture probes used in the constriction of the presented DNA library. *The total minimal free energy (ΔG°_{37} , see equation number 8), enthalpy (ΔH°) and entropy (ΔS°) were calculated with an ADNA 4.1 computer programme based on the unified nearest-neighbour thermodynamic parameters by John SantaLucia (see Table 16). The melting points for all words were calculated thermodynamically for 1 M NaCl and 1 μ M oligomers. The difference between the highest and the lowest melting points (number 5 and number 17) is 3,60 °C. The free energy ($E_{b,37}$) based on partition function and SantaLucia's thermodynamic parameters was calculated by Vienna RNA folding package (<http://www.tbi.univie.ac.at/cgi-bin/RNAfold.cgi>) as -3 kcal/mol were added to each value due to the spacer (16N) influence.*

N	Bit	5'-3' Word sequences	5'- 3' Capture probe sequences	$E_{b,37}$, Free energy - partition function, kcal/mol	ΔG°_{37} ,	ΔH° ,	ΔS° ,	Melting points, in 0.05 M NaCl, °C	Melting points, in 0.1 M NaCl, °C
					Minimal free energy, kcal/mol	Enthalpy, kcal/mol	Entropy, cal/mol		
1	1,1	CCATCACTACCTTCAT	ATGAAGGTAGTGATGG	-17,67	-17,40	-117,40	-322,1	44,47	48,08
2	1,0	TCCTCTATCATCCTCA	TGAGGATGATAGAGGA	-17,69	-17,20	-114,40	-313,1	44,47	48,08
3	2,1	TCCCTATCACTCTCT	AGAGAGTGAATAGGGA	-17,71	-17,29	-114,60	-313,4	44,76	48,37
4	2,0	CACACCTCAACTTCTT	AAGAAGTTGAGGTGTG	-18,11	-17,94	-119,80	-327,9	45,78	49,39

5	3,1	ACTTCCCTTCTACACA	TGTGTAGAAGGGAAGT	-18,22	-17,86	-116,40	-317,3	46,20	49,81
6	3,0	CACCATCCTTATCTCA	TGAGATAAGGATGGTG	-17,48	-17,26	-117,20	-321,9	44,09	47,70
7	4,1	TCTCTCAATCCACTTC	GAAGTGGATTGAGAGA	-17,80	-17,39	-118,40	-325,2	44,38	47,99
8	4,0	TACAATCCACACTTT	AAAGTGTGGGATTGTA	-17,77	-17,33	-116,20	-318,4	44,57	48,18
9	5,1	TCTTCTCTTACCA	TGGTAAGAGGAAGAGA	-17,79	-17,41	-115,30	-315,2	45,05	48,66
10	5,0	TCATACCTAACTCCCT	AGGGAGTTAGGTATGA	-17,61	-17,27	-114,00	-311,6	44,76	48,37
11	6,1	CTCATCTTAACCACCT	AGGTGGTTAAGATGAG	-17,51	-17,35	-117,40	-322,2	44,38	47,99
12	6,0	ACCATTACTTCAACCA	TGGTTGAAGTAATGGT	-17,73	-17,33	-116,20	-318,4	44,57	48,18
13	7,1	TTCTACAACCTACCT	AGGGTAGGTTGTAGAA	-17,69	-17,53	-114,90	-313,6	45,44	49,05
14	7,0	TCCAACCTAACACTCC	GGAGTGTAAAGTTGGA	-17,88	-17,63	-118,70	-325,4	45,03	48,65
15	8,1	ACCTTTACCTATCCT	AGGATAGGGTAAAGGT	-17,65	-17,36	-113,20	-308,8	45,16	48,77
16	8,0	ACACCCTAACAATCAA	TTGATTGTTAGGGTGT	-17,77	-17,33	-116,20	-318,4	44,57	48,18
17	9,1	CACCCATTCTAATAC	GTATTAGGAATGGGTG	-16,90	-16,84	-118,20	-326,5	42,60	46,22
18	9,0	TCCTACACAAACATCA	TGATGTTTGTGTAGGA	-17,69	-17,24	-117,00	-321,2	44,19	47,80
19	10,1	ATTCTCACTCACAACC	GGTTGTGAGTGAGAAT	-18,09	-17,84	-119,50	-327,3	45,50	49,11
20	10,0	ACCACTCCAATAACTC	GAGTTATTGGAGTGGT	-17,85	-17,51	-118,00	-323,6	44,75	48,37
21	11,1	TCCTACTCTCCAATCA	TGATTGGAGAGTAGGA	-17,89	-17,46	-115,30	-315,1	45,14	48,76
22	11,0	TCTTTCACACATCCAT	ATGGATGTGTGAAAGA	-17,94	-17,40	-116,80	-320,1	44,66	48,27
23	12,1	ACACCATTTCACCTAA	TTAGGTGAAATGGTGT	-17,79	-17,33	-116,20	-318,4	44,57	48,18
24	12,0	ACACTAATCCTCCAAC	GTTGGAGGATTAGTGT	-17,84	-17,51	-118,00	-323,6	44,75	48,37
25	Standard Deviation $\sqrt{(n\Sigma x^2 - (\Sigma x)^2/n(n-1))}$			0,25	0,23	1,73	5,28	0,68	0,68

Table 18 Slide matches (S^C) and reverse complementary slide matches (S^R) for all 24 words to the library sequences 1111111111, 0000000000, 1010101010, and 0101010101. The four sequences represent all ligation subsequences in the whole DNA library. The four library sequences contain 48 (4×12) words and a capture probe hybridisation over 16 bp is possible for these 48 words ($S^C=48$ for 16 nt matches). Additional high number of matches could indicate either possible non-specific

hybridisations of capture probes to one (or several) of these library sequences (S^C) or a high probability of secondary structure formation (S^R). The presented data were obtained by an ADNA 4.1 computer programme.

Matches: nt	Homology: %	Total S^C	Total S^R	Total S^C+S^R
16	100	48	0	48
15	94	0	0	0
14	87	0	0	0
13	81	0	0	0
12	75	0	0	0
11	69	58	0	58
10	62	243	0	243
9	56	692	0	692
8	50	1498	5	1503
7	44	2517	31	2548

The result is listed in Table 18. Using this word order, the mismatch properties of the library are not worsened by the concatenations of the words. Every word and each capture probe had at least 5 mismatches with all possible concatenation of the words in the library. Neither a word nor a capture probe had a run of more than 7 consecutive nucleotides with all possible concatenation; see Table 19 (to verify this, custom software, an ADNA 4.1 programme, was used).³⁸

Table 19 Four sequences representing all ligation subsequences in the library (111111111111.000000000000, 101010101010, and 010101010101) used to find every fragment between them the bits and their complements with a length from 16 to 5 nt. There are not any additional fragments among all-possible words combinations bigger than 7 nt. There is not any indicial fragment between the library sequences and the capture probes in length as small as 5 nt. The presented data were obtained by an ADNA 4.1 computer programme.

Fragment length: nt	Minimum F^C	Total F^C	Additional F^C : Total F^C - Minimum F^C	Total F^R
16	48	48	0	0

15	96	96	0	0
14	144	144	0	0
13	192	192	0	0
12	240	240	0	0
11	288	288	0	0
10	336	336	0	0
9	384	384	0	0
Fragment length: nt	Minimum F ^C	Total F ^C	Additional F ^C : Total F ^C - Minimum F ^C	Total F ^R
6	528	738	210	0
5	576	1521	945	0

The free energy difference (δG) between the strongest non-specific hybridisation of all library sequences to all capture probes and the weakest specific binding was found to be in a total range of 6.8 kcal/mol according to Jörg Ackermann's calculations³⁸.

3.5.2 Assembly and amplification of the DNA library

The complete library was assembled by four ligation reactions³⁸ (see section 2.2.4) schematically shown in Figure 51:I. All four ligation experiments took place between two different oligomers,

one representing the first half of the library (oligomers number one or two) and another for the second half (oligomers number three or four), see section 2.2.1 and Figure 6.

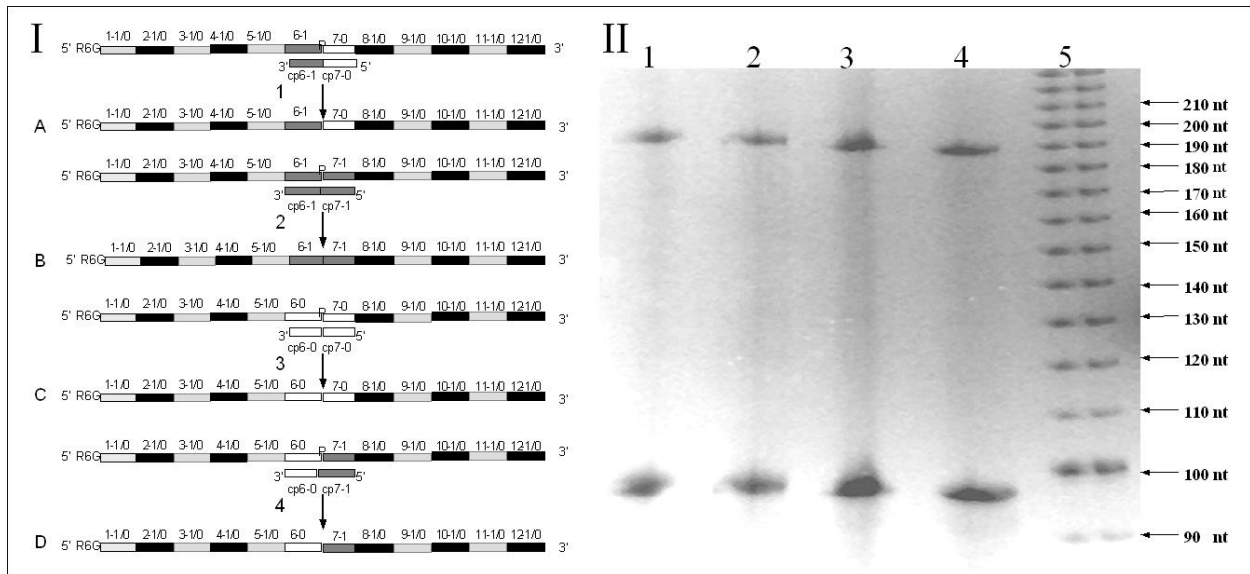


Figure 51 Assembly of the DNA library. *The library was assembled by four ligation reactions presented in scheme I. The products of the ligation reactions were analysed on a 12% denaturing polyacrylamide gel shown in the picture II - see lanes 1. 2. 3. 4. A denatured 10 bp ladder (Invitrogen GmbH, Karlsruhe, Germany) was run on the fifth lane. The ligated products are approximately 192 nt long as one can see from the gel picture. The gel was stained in SYBR Green Two.*

It was used one 32 nt oligomer complementary to the bits at sixth and seventh positions, which was different for each reaction. The results of the ligation reactions were analysed on a denaturing polyacrylamide gel shown in Figure 51:II. As one can see from the gel picture, the ligated products have the expected length.

The ligated products were analysed for the present of all bits by PCR amplifications as shown in Figures 54 and 55. The assemble DNA library was perfectly suitable for a direct use. However, for reasons of economy, I explored the opportunities for a PCR amplification of the assembled DNA library on a large scale. The four parts of the library were amplified by four different PCR experiments under conditions described in section 2.2.4.

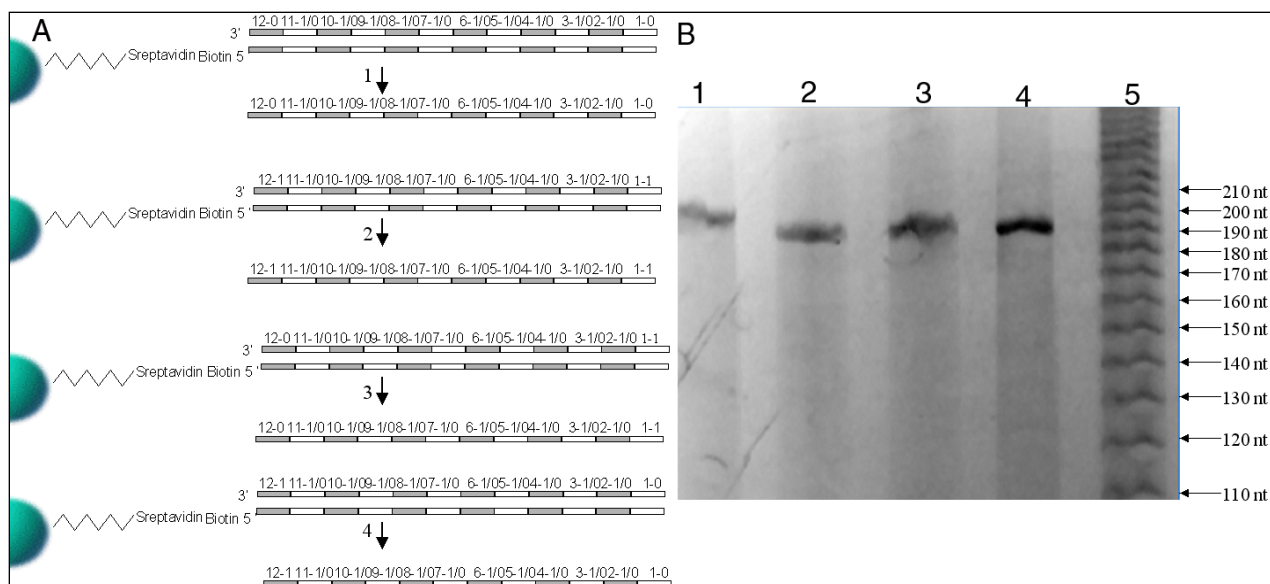


Figure 53 Single-strand purification of the DNA library. **A:** The amplified DNA oligomers from Figure 52 were attached to streptavidin-coated magnetic beads (see Table 4, line 4). The attached dsDNA oligomers to the beads were denaturised by heating at 95 °C for 4 min. **B:** The obtained single-stranded DNA oligomers were analysed on a 12 % denaturing gel, see lanes 1, 2, 3 and 4. On the 5th lane a denaturised 10 bp ladder was run. The gel was stained in SYBR Green Two.

3.5.3 Testing integrity and fidelity of the DNA library

In order to confirm the integrity of the assembled DNA library and to test its accuracy, twenty-two different PCR amplifications were performed (see Figures 54 and 55) ³⁸ under identical conditions (see section 2.2.4). In all PCR experiments, the assembled DNA library (see Figure 51) was used as a template and the word V_1^1 was used as a sense primer. The capture probes to the words from the second to the twelfth position were used as antisense primers in the twenty-two different PCR experiments (see Figures 54_I and 55_II). The amplified products with 'zero' capture probes were analysed on an 8 % non-denaturing polyacrylamide gel shown in Figure 54_II. As one can see from the gel picture, all eleven PCR products have the expected length (see Figure 54_I and II). No significant unexpected amplified products were observed.

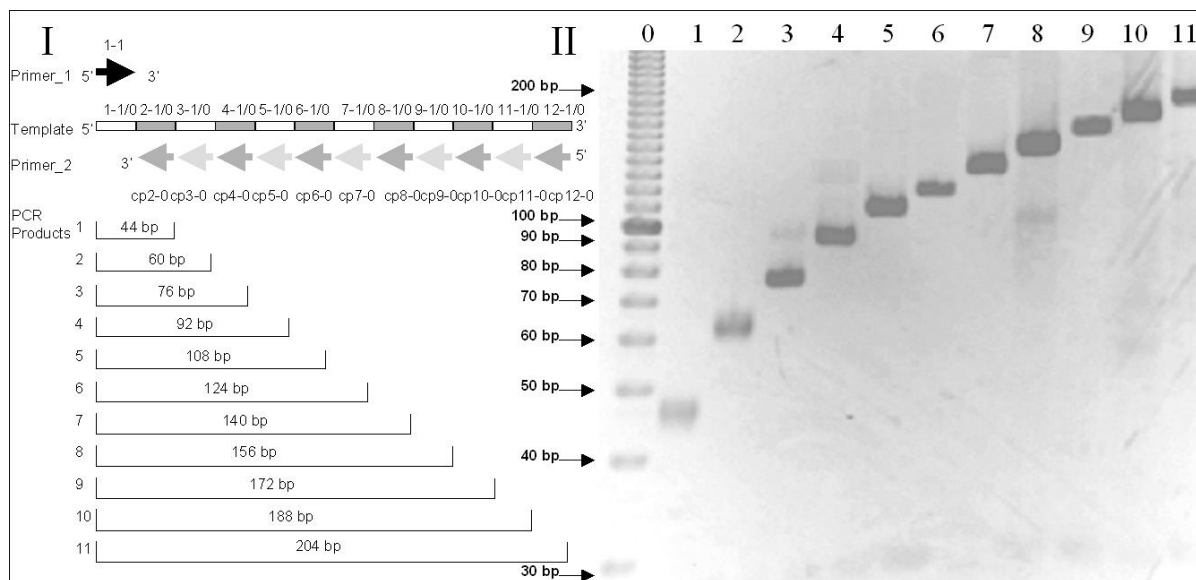


Figure 54 Testing the integrity and the fidelity of the DNA library by PCR amplifications with ‘zero’ capture probes. Eleven different PCR amplifications, with the DNA library are presented in scheme I. The word V_1^1 was used as a sense primer in all reactions. As an antisense primer, the capture probes to the bits with value ‘zero’ from second the twelve positions were used in all eleven reactions. All reactions were performed under identical conditions (see section 2.2.4). The PCR products were analysed on a 8% non-denaturing polyacrylamide gel shown in picture II – see lanes from 1 to 11. On lane 0, a 10 bp non-denatured ladder was run as a marker. The gel was stained in SYBR Green One. The picture was inverted

Similar results were obtained for the PCR experiments with the ‘one’ capture probes, as shown in Figure 55.³⁸ The PCR products also had the expected length with only one significant exception observed for the capture probe V_7^1 , see Figure 55. In order to localize the unexpected amplified product, four additional PCR experiments were performed. As a template, four sequences different for each reaction were employed (see Table 2). The capture probe V_7^1 was applied as an anti-sense primer in all reactions. In the first PCR experiment, the sequence 111111111111 was used as a template and the word V_1^1 as a sense primer. In the second reaction the sequence 101010101010 was employed as template together with the same sense primer as in the first reaction. The template sequences 000000000000 and 010101010101 were used in the third and fourth reactions respectively and the word V_0^1 was used as a sense primer in both reactions. The PCR products were analysed on a 8% non-denaturing polyacrylamide gel shown in Figure 56_I. As one can see from the gel picture, the longer amplified products with the templates 111111111111 and 101010101010 have the expected length of 124 bp. The unexpected PCR products have a length of about 70 bp in both cases.

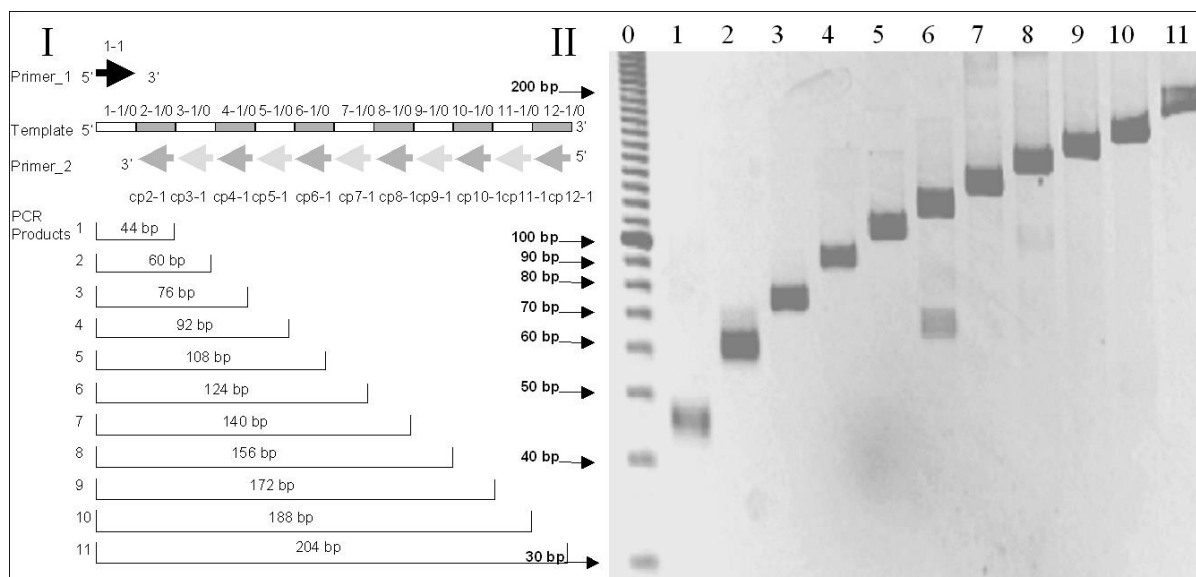


Figure 55 Testing the integrity and the fidelity of the library by PCR amplifications with ‘one’ capture probes. Eleven different PCR amplifications similar to those from Figure 54 are presented. In difference to Figure 54 the capture probes to the bits with value ‘one’ were used as antisense primers. The gel was stained in SYBR Green One.

In the other two PCR experiments, no amplified products were observed. Based on these results, I concluded that the unexpected PCR products in the first and the second reaction should involve a mispriming between a block of 7 nt on the 3’ end of the capture probe V_7^1 and the template region from 40 to 46 nt which is identical in the sequences 11111111111 and 101010101010 shown in Figure 56:II. If this explanation is correct, in both cases the unexpected product should be 68 bp long as found approximately in that gel analysis. The additional amplified product in the second reaction is more abundant than that in the first one due to four additional matches close to the 3’ end of the capture probe V_7^1 and the sequences 101010101010 (see Figure 56:II).³⁸

Two different DNA/DNA hybridisation analyses (section 2.2.3.2, but in 500 mM Tris-borate buffer and 50 mM NaOH) were made with the capture probe V_7^1 immobilised on paramagnetic beads as described in section 2.2.2.1_I.

I decided to focus on that capture probe because of the PCR results described above. In the first type of hybridisation reaction, the second half of the library containing ‘one’ at position seven was used. The second type of hybridisation analysis was made with the first half of the library. Beads

without immobilised DNA were used as a control for non-specific DNA attachment. The amount of denatured DNA from the beads was estimated by UV-spectroscopy.

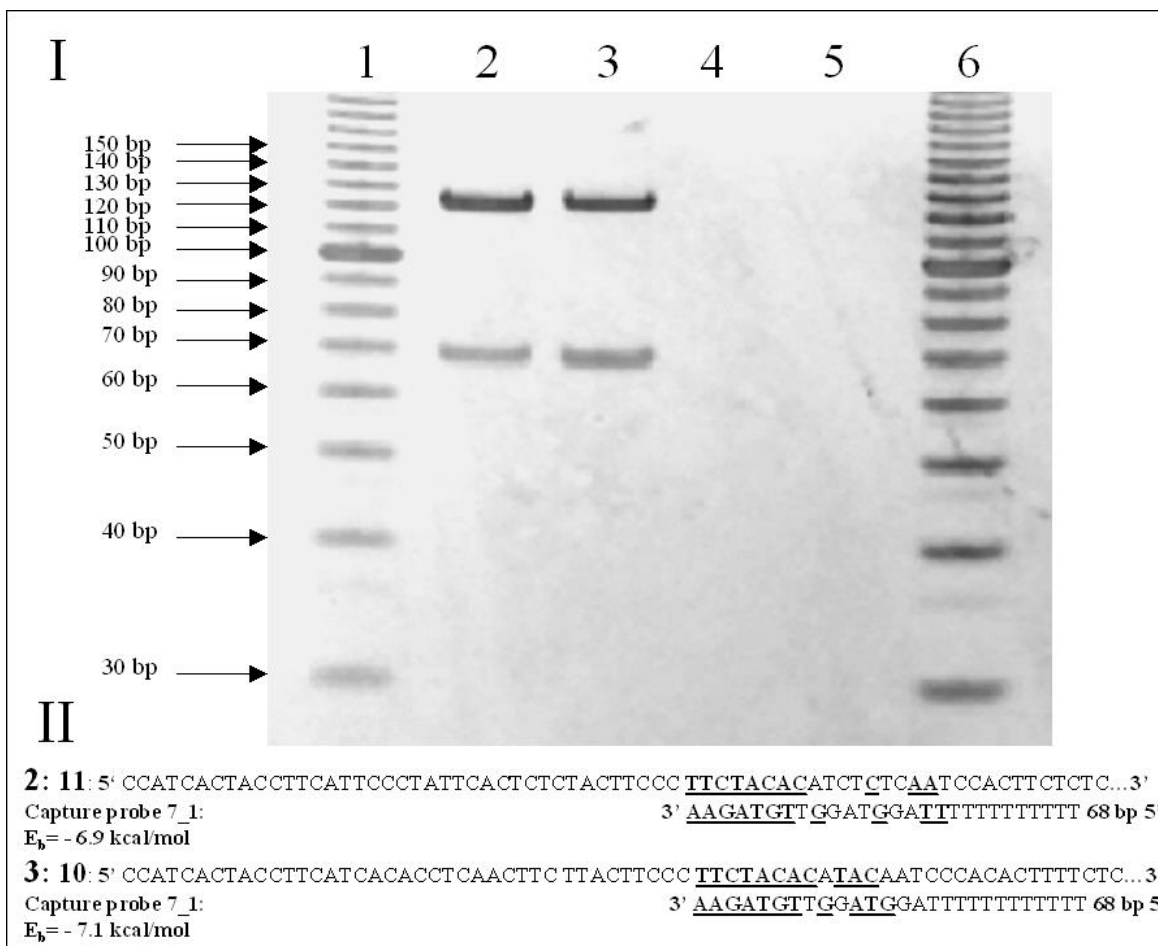


Figure 56 Finding the origin of the wrong library amplification signal with capture probe V_7^1 . Four PCR reactions were made with the capture probe V_7^1 . On lanes one and six a 10 bp ladder was run. On the lane 2 the sequence 111111111111 was used as a template. On the lane 3: 101010101010, lane 4: 000000000000, and lane 5: 010101010101. The wrong products in lanes 2 and 3 are a little bit shorter than 70 bp. There is only one place, which starts in the both sequences from the 40th nucleotide, has a free 3' end and produces amplification products of 68 bp. In the sequence 101010101010, the hybrid formed is a little bit more stable than that in the sequence 111111111111 because of additional matches. The gel was stained in SYBR Green One.

In the first case, the hybridisation yield was 33 ± 4 pmol DNA /mg beads. In the second hybridisation experiment, the hybridisation yield was 5 ± 2 pmol DNA /mg. The non-specific DNA

attachment to beads was 3 ± 1 pmol DNA/ mg beads. Those results indicate that the non-specifically amplified products with the capture probe V_7^1 do not provide a significant problem for the hybridisation experiments with the DNA library. In order to check the accuracy of the theoretically predicted margin between the highest and lowest melting point of the words, melting curves were obtained for each word for two different salt concentrations (50 mM and 100 mM NaCl) as described in section 2.2.4.

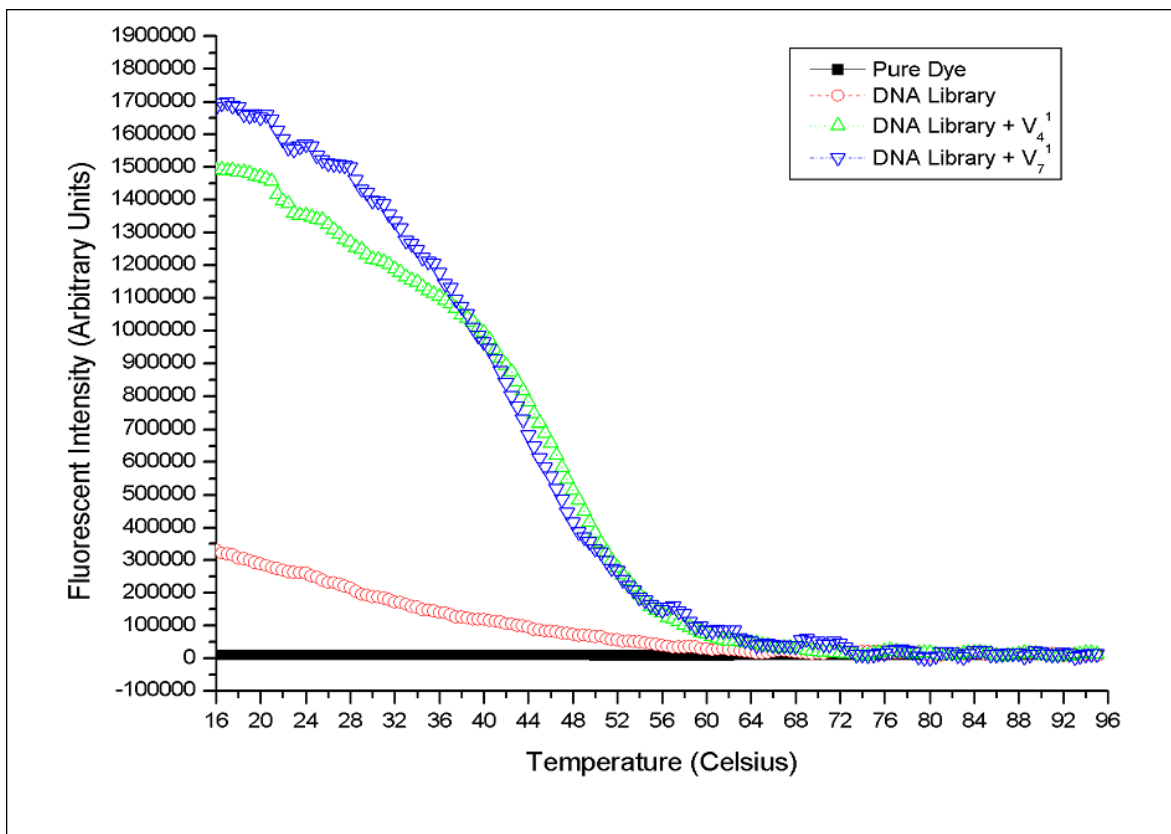


Figure 57 Testing the library sequences for a hybridisation and a secondary structure formation.

Melting curves of the whole DNA library ($2 \mu\text{M}$) were measured in the presence of a capture probe V_4^1 ($1 \mu\text{M}$) or a capture probe V_7^1 ($1 \mu\text{M}$) or in the absence of any capture probe in 50 mM NaCl and 10 mM sodium phosphate buffer solutions. The melting points of the capture probes V_4^1 and V_7^1 were found to be 46.3 and 43.7°C , respectively. The fluorescent signal for the DNA library without capture probe at that temperature is about seven times less than that with capture probes V_4^1 and V_7^1 , which suggest a low level of hybridisation among library sequences and an absence of secondary structures.

The sequence 111111111111 (see Table 2) was used as a template for obtaining the melting curves of the capture probes with value 'one' as described in section 2.2.4. The sequence 0000000000 (see Table 2) was

used with the 'zero' capture probes. The margin for both salt concentrations was found to be ± 2.5 °C, which is ± 0.7 °C more than the theoretically predicted one (see Table 17) but still close enough to guarantee identical hybridisation conditions for all capture probes.

Additional melting curves were obtained with the entire library in the presence of capture probes V_4^1 and V_7^1 or in the absence of a capture probe (see Figure 57). The relatively low fluorescent signal of the library-melting curve in the absence of a capture probe indicates a low level of hybridisation among library sequences and a low level of secondary structure formation.³⁸

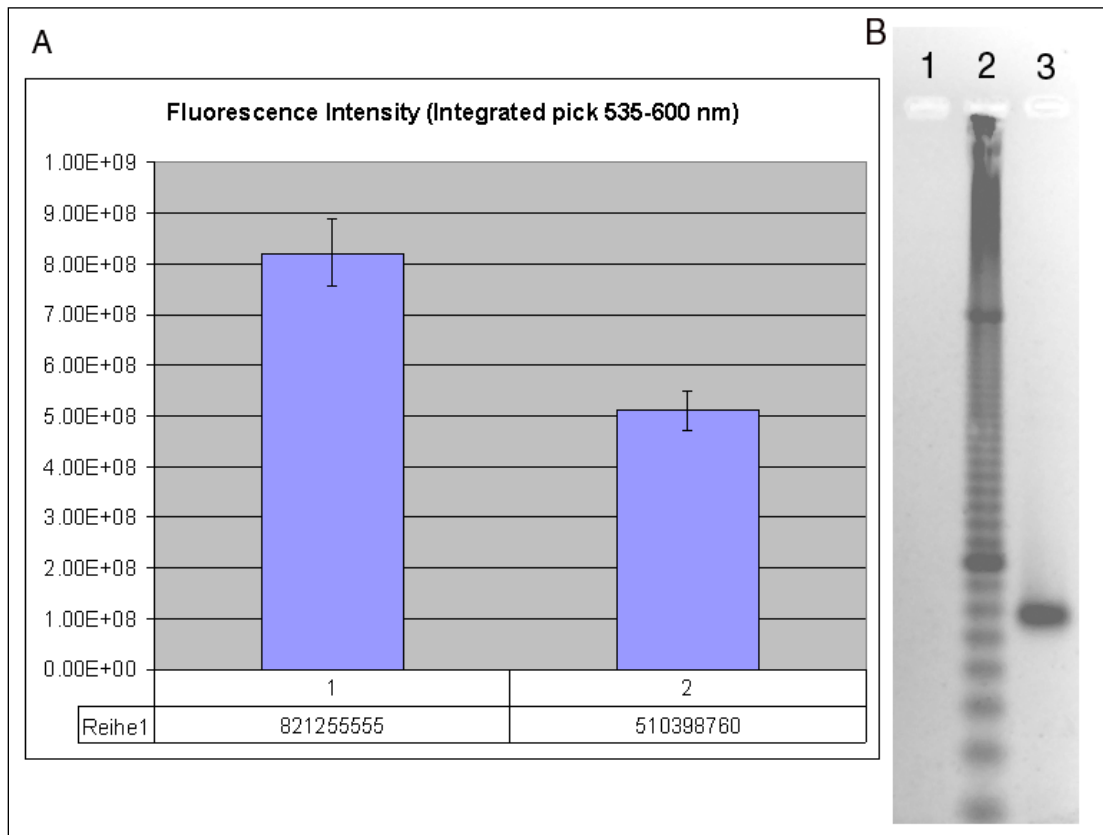


Figure 58 PCR readout of the DNA library on a 4% agarose gel after one selection step on beads with the capture probe V_4^1 . **A:** DNA hybridisation yield with the whole 5' R6G – labelled library, using beads immobilised with V_4^1 in 500 mM Tris-acetate buffer, pH 8.3, and 50 mM NaOH; **1:** incubation at 25 °C; **2:** incubation 42 °C. Every experiment was repeated three times (see Table 38); **B:** **1:** A PCR amplification of the library by using of words V_1^1 and V_0^1 as sense primers and capture probe V_4^0 as an antisense primer; **2:** 10 bp DNA ladder starting from 30 bp; **3:** A PCR amplification of the library by using of words V_1^1 and V_0^1 as sense primers and capture probe V_4^1 as an antisense primer. The gel was stained in SYBR Green One.

Finally, the hybridisation yield of the whole DNA library on beads was tested. Capture probe V_4^1 (see Table 1), 5' amino-labelled, was immobilised to carboxyl-coated beads (see Table 4, line 2). Hybridisation experiments, with the whole 5' end R6G labelled library on the beads immobilised with V_4^1 , were made in a 500 mM Tris-acetate, pH 8.3, and 50 mM NaOH buffering solution at two different temperatures 25°C and 42°C using temperature denaturing as described in section 2.2.3.2. The average results (for the complete experimental data see Table 38) are presented in Figure 58_A. As one can see the DNA hybridisation yield at 42°C is 62 % in a comparison to the hybridisation yield at 25°C. Two PCR amplifications using the DNA hybridisation products from the beads at 42°C were executed as described in section 2.2.4 but with fifteen amplification cycles. In the first experiment the words V_1^1 and V_0^1 as sense primers and capture probe V_4^0 as an antisense primer were used. Amplification products were not observed (see Figure 58_B, lane 1). In the second experiment the words V_1^1 and V_0^1 as sense primers and capture probe V_4^1 as an antisense primer were used. An amplification product with the expected length of 76 bp was observed (see Figure 58_B, lane 3). That experiments demonstrated that under conditions for ca 60 % hybridisation yield a high level of specific-hybridisation is achieved using the whole DNA library between 'one' and 'zero' of bit at position four, which has been randomly chosen. A similar DNA hybridisation yield was achieved in section 3.2.1 (see Figure 23).

3.5.4 Discussion

The presented DNA library design is novel because of the use of a thermodynamic discrimination between specific and non-specific DNA hybridisation. Up to now there is no other experimentally tested library for DNA computation design based primarily on thermodynamic criteria. The accuracy of the library design depends strongly on the quality of the experimental thermodynamic data available today. The general applicability of hybridisation thermodynamics was intensively demonstrated over the last decades of scientific research on nucleic acids.

It was shown by the PCR experiments that all bits are presented in the DNA library and identical conditions exist for all capture probes of the library, in which a rather uniform amplification of the expected PCR products is observed. No significant amplification of unexpected PCR products was observed with one exception involving capture probe V_7^1 . The PCR could be successfully used as a readout tool for the individual library sequences. I believe that the most accurate way for the library construction is by a

ligation. For a DNA library with that size there is not practical need for PCR amplification of the complete library. However, with increasing the library size, and increasing of the ligation steps needed, a consecutive PCR amplification of the assembled library may be needed.

DNA hybridisation analyses on beads suggested that these unexpected PCR products do not indicate significant problems for the selection procedure with the library. The DNA polymerase is very sensitive to mismatches at the 3' primer end. One mismatch in the last three nucleotides at the 3' end could prevent the elongation^{xxxx}. At the same time, it seems that rather unstable mispriming involving a formation of a short double-stranded 3' end could be responsible for unexpected PCR amplification even at high annealing temperatures. Such mispriming at the 3' end could be avoided in the future designs.

Table 20 Thermodynamic properties of DNA word sequences (bits) and their capture probes used in the construction of a DNA library designed on combinatorial constraints.^{xxxxi} *The library is constructed based on combinatorial constraints (number of slide mismatches and identical GC word content of 50%). The words are 16 nt long, containing G's. This DNA library is used here for a statistical analysis only. Despite the identical GC content of the words, the difference between the highest and the lowest melting points (number 2 and number 10) calculated thermodynamically is 8.50 °C as the standard deviation of the melting points and the minimal free energy (ΔG_{37}°) of the words are respectively 3.3 and 3.8 times bigger than those in the tested by me library (see Table 17).*

N	Bit	$E_{b\ 37}$, Free energy - partition function, kcal/mol	ΔG_{37}° , Minimal free energy, kcal/mol	ΔH° , Enthalpy, kcal/mol	ΔS° , Entropy, cal/mol	Melting points, in 0.05 M NaCl, °C	Melting points, in 0.1 M NaCl, °C
1	1.1	-19.49	-19.46	-120.30	-324.8	50.11	53.72
2	1.0	-20.90	-20.29	-127.50	-344.0	51.96	55.57
3	2.1	-18.59	-17.81	-119.50	-326.0	46.72	50.33
4	2.0	-19.97	-18.81	-118.80	-319.4	51.05	54.66
5	3.1	-19.83	-19.72	-118.50	-318.2	51.36	54.97
6	3.0	-19.37	-18.21	-118.50	-320.4	49.22	52.84
7	4.1	-18.86	-18.61	-125.60	-344.6	46.34	49.96

8	4.0	-19.97	-19.26	-121.30	-328.5	49.40	53.01
9	5.1	-19.17	-18.10	-120.60	-327.5	48.39	52.00
10	5.0	-17.21	-17.11	-118.50	-326.5	43.44	47.06
11	6.1	-19.54	-18.70	-126.60	-344.9	48.74	52.35
12	6.0	-19.55	-19.19	-125.80	-342.1	49.13	52.74
13	7.1	-19.40	-18.95	-122.30	-332.9	48.05	51.67
14	7.0	-19.43	-18.97	-121.80	-331.1	48.35	51.96
15	8.1	-19.67	-19.43	-123.00	-333.5	49.42	53.04
16	8.0	-19.88	-19.22	-122.20	-331.6	48.99	52.60
17	9.1	-17.38	-16.29	-118.10	-325.2	43.53	47.15
18	9.0	-19.10	-18.94	-119.50	-323.9	48.71	52.32
19	10.1	-17.52	-19.58	-121.60	-327.4	51.28	54.89
20	10.0	-19.45	-19.02	-121.60	-329.0	49.76	53.37
21	11.1	-17.84	-17.59	-119.30	-327.6	44.66	48.27
22	11.0	-19.07	-18.76	-122.10	-332.8	47.60	51.21
23	12.1	-19.05	-18.63	-121.60	-331.6	47.33	50.94
24	12.0	-19.84	-18.66	-119.70	-324.2	48.99	52.60
25	Standard Deviation $\sqrt{(n\sum x^2 - (\sum x)^2/n(n-1))}$	0.90	0.87	2.68	7.60	2.25	2.25

The melting curves obtained suggest one more time that identical hybridisation conditions exist for all capture probes, under which a pretty uniform hybridisation yield could be expected. The absence of G's in the library sequences, proved to be a successful strategy for avoiding the formation of secondary structures within the library sequences and hybridisation among them. It is important that the high level of specific DNA hybridisation was achieved under conditions, in which DNA/DNA hybridisation equilibrium is achieved below the melting points of the words allowing about 60 % hybridisation yield.

It is believed by some scientist that identical length and GC content of DNA oligomers result in very similar melting points. I do not absolutely agree with that assumption. A good example for that is the DNA library

published in⁸². The library words are 16-mers and all of them have a 50 % GC content. The difference between the highest and lowest melting point calculated thermodynamically is 8.5 °C (see Table 20), 3.3 times bigger standard deviation than that of the library tested by me (see Table 17).

I believe the discrimination between perfectly matching DNA hybrids and those with mismatches based on hybridisation thermodynamics is more accurate than using the Hamming distance or the numbers of slide mismatches. The application of partition function introduced by John McCaskill⁷³ takes into account the formation of hairpins, internal or bulge loops, increases the efficiency of the thermodynamic discrimination. The constraint for thermodynamically uniform melting points of the words is more accurate than that based on an identical CG content.

The high level of specific hybridisation achieved with the presented twelve-bit library opens the important question whether the method is scalable to large sets. Recently, a 20-variable 3-SAT problem was solved by the Adleman⁸ group applying multi-step DNA selection. Their 20-bit DNA library (40 words, each 15 nt long) was optimised based on combinatorial constraints. According to the same thermodynamic criteria their word set showed the following properties: a free energy gap of $\delta G = 4.6$ kcal/mol between specific and non-specific DNA hybridisation and a variation of the melting temperatures in a total range of $\Delta T_m = 8.4$ °C (according to the nearest neighbour approximation calculated by Ackermann³⁸). The design of bigger libraries needs an experimental verification. Further improvement may be possible by increasing the word size or introduction of spacers among the words (for instance 6 dT). However, the words (and eventually the spacers) should be kept as short as possible to maintain a high information density of the generated code. Introducing of G's into DNA library sequences will increase the diversity of DNA word sequences and the free energy gap between specific and non-specific DNA hybridisation between the library sequences and the capture probes. However, this will increase the possibility of formation of more stable secondary structures and hybridisation among the DNA library sequences. Computing of the thermodynamic stability of non-specific hybridisations between the DNA capture probe complements and the four library sequences (see Table 2) representing all ligation sites is one way to reduce the stability of the secondary structure formed.

The presented library design is very suitable for an integrated DNA computation in micro-flow reactors by multiple DNA selection under isothermal conditions because of the uniformity of melting points of the words.³⁸

4 CONCLUSIONS

*The road to wisdom?
Well. It's plain and simple to express:
Err and err and err again.
But less and less and less.*

*Piet Hein.
Crooks.*

*The best way to avoid many mistakes is to learn
not only from your own errors but also from the
mistakes made by others.*

Bulgarian folk wisdom.

4.1 SUMMARY OF THE ACHIEVED RESEARCH GOALS

The development of a new technology is not purely a theoretical exercise. It is to a great extent a matter of practical efficiency. A useful new technology should deliver new important capacities or/and a cheaper, more efficient way for delivering of the already existing goods. In these terms, let me go back to the research goals defined at the beginning of the PhD thesis research goals summarize their implementation.

1. A novel reversible chemical procedure, based on pH-alterations, for a multi-step DNA hybridisation transfer between micro-reactor selection modules under isothermal conditions has been established. The question is, if there are any advantages in the employing of reversible chemistry for an isothermal DNA hybridisation transfer between bead-based micro-fluidic selection modules compared to the use of temperature denaturation. The most important aspect of that question concerns the integration density. The key point is what is easier to achieve at the small distances: mixing of water solutions coming from two crossing micro-channels or keeping of a temperature gradient of at least 30 °C (the difference between the hybridisation and denaturation temperature for DNA oligomers). Both processes are not trivial for achieving at a micrometer scale. However, the PCR experiments in micro-reactors under flow conditions revealed that it is difficult to maintain such a temperature gradient on micrometer scale in microstructures. A lot of different mixing structures in micro-fluidic channels, which allow a complete mixing in micro-channels at a micrometer scale, are established. That means the use of

reversible chemistry for DNA hybridisation transfer under isothermal conditions has a real potential for an integration of more selection modules on a single wafer than using of a temperature gradient (see Figures 20, 46, 47 and 48).

The efficiency of the DNA hybridisation transfer between micro-reactor selection modules under isothermal conditions, applying the established reversible chemistry, has found to be ca 60 %. Farther improvements in micro-flow reactor designs are needed in order to achieve better mixing and higher pick up efficiency.

2. The suggested novel micro-fluidic architecture (see Figures 20 and 46) allows a parallel (or in a single run, see Figure 48) immobilisation of unique DNA, RNA or polypeptides to beads placed in cascably connected micro-chambers or to their surfaces, applying almost any type of cross-linking bio-conjugate chemistry. One particular chemical procedure, based on the zero cross-linking reagents EDAC has been tested for an immobilisation of amino-modified DNA to carboxyl-coated beads placed in cascably connected micro-reactor chambers. That approach for fabrication of micro-fluidic chip arrays, employing the proposed micro-fluidic architecture, is based on the separated delivery of DNA molecules, the cross-linking reagent, and the inhibitor of the immobilisation reaction. It guarantees an absolute specificity in the attachment of specific DNA molecules to a defined micro-chamber out of a huge number of cascably connected micro-chambers. The combination of all these features offers a cheap, robust, and scalable way for producing of DNA, RNA, or polypeptide micro-fluidic arrays with a huge number of chambers, suitable for many applications in the fields of molecular diagnostics, DNA computing, and *in vitro* evolutionary biotechnology.

3. The DNA/DNA hybridisation kinetics on beads under flow conditions seems to be non-diffusion limited reaction in a contrast to the DNA/DNA hybridisation on surface under stationary conditions. The DNA hybridisation reaction on beads under flow conditions could reach saturation within less than a minute. DNA/DNA denaturation kinetics under flow conditions using of sodium hydroxide has proven to be an almost simultaneous reaction, reaching completion within a few (2-3) seconds.

4. The fidelity of the DNA/DNA hybridisation on beads and in free solutions has been investigated extensively under hybridisation conditions of high concentration of Tris and HEPES (500 mM),

which allows the application of the established pH-reversible chemistry. It has been possible to reach equilibrium of the DNA hybridisation reaction in which there is no hybridisation between complementary DNA strands, which have two mismatches over a length of 21 nt. Under the same hybridisation conditions, DNA/DNA hybridisation yield for the perfectly matching hybrid has proven to be ca 60 %, having a free energy gap of -6.4 kcal/mol between the perfectly matching hybrid and that with two mismatches. In the case of DNA hybridisation analysis on beads, the non-specific DNA attachment to the beads' surface plays an important role. Carboxyl-coated polystyrene beads have proven to possess a less non-specific DNA attachment than amino-coated ones. The application of a washing step, with a low ionic strength buffers on beads incorporated in micro-chambers, offers an opportunity for increasing of fidelity of the picked up DNA.

5. The presented twelve-bit DNA library, designed mainly on thermodynamic constraints, has revealed a high level of specific DNA hybridisation for all library words under identical hybridisation conditions with ca 60 % hybridisation yield. The library sequences revealed a low level of secondary structure formation and hybridisations among themselves. The experimental results confirmed the suitability of the design criteria used. The thermodynamic criteria employed for discrimination between the specific and non-specific DNA hybridisation among DNA library sequences and the capture probes have proven to be more accurate than that based on the number of slide mismatches. A similar, thermodynamic based approach, could be employed for a capture probe design in DNA or RNA micro-arrays, primer design in PCR and many isothermal amplification reactions, rational ribozyme design, DNA self-assembly and others.

The achieved results make the introduction of a new approach, based on the proposed novel micro-fluidic architecture possible. This allows a spatially defined specific bio-molecule immobilisation in parallel applying almost any cross-linking bio-conjugate chemistry and a novel pH-reversible chemistry for multi-step DNA hybridisation transfer between cascadably connected microfluidic selection modules. That chemistry could allow an integration of many DNA selection modules on a single wafer. The approach takes advantages of the fast DNA hybridisation on beads under flow conditions, the fast DNA denaturation kinetics by sodium hydroxide, the small sample volume needed. The usage of beads, as a solid support for bio-molecular immobilisation, offers a high surface/volume ratio and makes the micro-fluidic chip completely reusable. I believe that the integration of all these features makes the proposed approach very suitable for creating of fully

automated, highly integrated and programmable micro-fluidic chips, with a broad range of applications in the fields of nucleic acid and protein based diagnostics, nucleic acid computing, and *in vitro* bio-molecular selection procedures.

However, I believe the best conclusions are to be made by the reader himself.

4.2 APPLICABILITY OF MICRO-FLUIDICS FOR MOLECULAR BASED COMPUTATION AND DIAGNOSTICS

The interaction among bio-molecular computing, molecular biology, DNA hybridisation thermodynamics, bio-conjugate chemistry, micro-fluidic and laser technologies has proven to be very productive for developing a novel 'computationally inspired' biotechnology. Based on my own research and on that done by others, I believe that micro-fluidics possess a significant potential for developing fully automated, highly programmable and integrated devices for multi-step bio-molecular processing.

It is still questionable whether nucleic acids are, for the moment being (due to undeveloped tools of molecular biology) or at all (due to the chemical properties of DNA), a very suitable computational medium. There are two dependent aspects in that question. On one hand, it is a matter of an applied algorithm. On the other hand, it is a matter of a practical implementation of the applied algorithm by the tools of molecular biology and biotechnology. It is clear, that general-purpose algorithms can be implemented by nucleic acid - based computers, potentially solving a large class of NP-complete search problems. In that approach, the required exponential time could be reduced in principal, so the algorithm could be 'time efficient'. At the same time, an exponential in number (depends on the problem's size) different solutions, in a form of different DNA or RNA sequences, have to be employed. Thus, the algorithm is space inefficient.

That inspired Adleman to learn and implement some molecular biological protocols in his famous paper⁵ that eventually provoked the recognition of DNA computing as a research field both theoretically and practically. The DNA library, presented and experimentally tested in this work, reveals that it is possible to design library sequences with a high specificity of the DNA hybridisation reaction. It may be possible to design forty-bit DNA library still maintaining a high specificity of the hybridisation reaction. However the construction of a working hundred-bit DNA library, containing all possible bit combinations (2^{100} different DNA sequences) seems to be a pretty difficult task from both theoretical and practical point of view. The avoiding of the need to generate all possible solutions of a NP-complete problem could reduce the size of the DNA library required. That may be achieved potentially by replacing of the 'brute force' approaches, implemented up to now, with some kind of probabilistic or even evolutionary algorithms. The

question, which kind of algorithm is the most suitable for nucleic acid based computation remains still open from my point of view. The scalability of the nucleic acid-based computation depends not only on the size of the problem but also on the number of selection steps required. The same size NP-complete problems could require different numbers of selection steps, depending on the specific problem instances. Apart from the idea of solving NP-complete problems on nucleic acid-based computers, there are certain ideas for implementing molecular circuits based on ribozymes used as molecular switchers¹⁹ where micro-fluidics could play an important role as well.

It is important to understand that contemporary molecular-based diagnostics have almost the same requirements for parallel multi-step bio-molecular processing as bio-molecular-based computations. The HGP generated a huge amount of DNA sequence data. The analytical methods of bioinformatics^{lxxxii} are becoming more accurate in finding functional DNA sequences. That increases continuously the number of available genome markers. In order to make genetic, RNA and polypeptide expression profiling not only research methods but also common and wide-spread approaches for molecular-based diagnostics, further progress in the development of fully programmable, reusable, automated and integrated bio-chips at low cost is needed.

Micro-fluidic devices are providing convenient platforms for fully programmable, reusable, automated and integrated bio-molecular processing in both fields of molecular based diagnostics and computation. Micro-fluidics allow the realization of complicated dataflow-like architectures for highly parallel, multi-step processing of nucleic acids or other bio- molecules. Such dataflow-like micro-flow devices could be used not only, and maybe not primary, for molecular computation but also for high throughput bio-molecular diagnostics and selections. RNA and protein expression, and genetic analysis require multi-step bio-molecular processing, which could be implemented on similar, if not the same, dataflow-like micro-fluidic architectures. In order to create a useful micro-fluidic device for bio-molecular processing, regardless of bio-molecular computation or diagnostics, one needs to achieve not only a big parallelism of analysis but also a high level of programmability, automation and integration of all essential steps.

Moving magnetic beads in STMs under steady flow conditions could be applied for automated multi-step DNA hybridisation transfer. However the synchronised movement of beads placed in many cascably connected STMs and simultaneously keeping of stable steady flow patterns in

all STMs seems to be a significant problem in terms of a micro-flow reactor design and implementation.

Programmability is of a significant importance in the production process of every biochip. The micro-fluidic architecture proposal by me, based on two-dimensional grid of crossing channels with a combination of micro-chambers, mixing structures and valves, allows a fully automated programmable immobilisation of unique bio-molecules to every chamber of the grid in parallel. The number of needed micro-valves is limited as it depends only on the number of vertical channels and does not depend on the number of chambers. The proposed architecture is not dependent on particular chemistry because any bio-conjugate cross-linking chemistry could be applied. That makes the programmability universal and potentially very cheap. The use of magnetic beads makes the micro-fluidic device re-programmable and re-useable as the already immobilised with DNA magnetic beads placed in the micro-chambers could be replaced with new ones by using of a magnetic stand. The multi-step DNA hybridisation transfer under isothermal conditions could be implemented in the proposed micro-fluidic architecture automatically as well. In both DNA immobilisation and selection processes a mixing must be achieved simultaneity only between the crossing points of two vertical and two horizontal channels, which allows a high level of flow stability. The performing of the hybridisation and denaturation processes at a constant temperature allows potentially integration of many selection steps (chambers) on a single wafer. The micro-fluidic design could produce of DNA, RNA, polypeptide, and cell chips, biosensors and bio-molecule circuits with applications in molecular based diagnostics and computing, drug discovery, and *in vitro* evolutionary biotechnology.

5 APPENDIX

5.1 STATISTICAL ANALYSIS OF EXPERIMENTAL DATA

Table 21 First half of the experimental data of 5' R6G labelled synthetic DNA titration curve presented in Figure 10. Fluorescence intensity, an integrated pick, 535-600 nm.

pmol DNA	0.2	0.4	0.8	1.6	3	6.2	12.5
1	3021060	5757591	9761899	18905156	28804865	47548711	82132549
2	2898745	5556544	11021214	18545454	26554545	45278645	86545114
3	3325544	5254545	9654544	21214210	29545444	50548754	89742484
average	3081783	5522893	10145886	19554940	28301618	47792037	86140049
stdev	179452.52	206741.54	620500.36	1182435.08	1271826.08	2158381.76	3119918.37
(stdev/aver)%	5.82%	3.74%	6.12%	6.05%	4.49%	4.52%	3.62%

Table 22 Second half of the experimental data of 5' R6G labelled synthetic DNA titration curve presented in Figure 10. Fluorescence intensity, an integrated pick, 535-600 nm.

pmol DNA	25	50	60	70	80	90
1	199748444	416601450	519678630	617544857	765243146	874374524
2	210212141	380995444	489851424	592147594	745244514	824150141
3	188585444	402517514	524545454	635454504	724854855	845045454
average	199515343	400038136	511358503	615048985	745114172	847856706
stdev	8830600.50	14641434.41	15337042.71	17767838.85	16488708.34	20600153.99
(stdev/aver)%	4.43%	3.66%	3.00%	2.89%	2.21%	2.43%

Table 23 Complete experimental data of DNA/DNA hybridisation experiments on beads presented in Figure 12. Fluorescence intensity, an integrated pick, 535-600 nm.

Number	1: Immobilisation	2: Immobilisation	Pure beads	Inhibition	without EDAC
1	383524543	393844696	52014557	50154450	53215219
2	401454542	385454545	53055458	51124142	52141413
3	402421414	421214517	53211420	50214513	50315414
4	422450486	384585458	54512140	52142144	52454225

stdev	15907896,0	17142671,2	1024369,6	934271,2	1229758,7
average	402462746,3	396274804,0	53198393,8	50908812,3	52031567,8
(stdev/aver)%	4,0%	4,3%	1,9%	1,8%	2,4%

Table 24 Complete experimental data of DNA/DNA hybridisation experiments on beads presented in Figure 13. Fluorescence intensity, an integrated pick, 535-600 nm.

Number	H-100	100 mM NaOH	Heating
1	816679182	213946901	135664420
2	809852443	209454852	130445451
3	789564554	200454540	129644453
average	805365393	207952098	131918108
stdev	11515235,59	5609792,29	2669149,63
(stdev/aver)%	1,43%	2,70%	2,02%

Table 25 Complete experimental data of DNA/DNA hybridisation experiments on beads presented in Figure 18. Fluorescence intensity, an integrated pick, 535-600 nm.

Number	Hybridisation	without EDAC	Without DNA
1	321442420	43642458	48454548
2	345444750	47545428	45475478
3	364548759	48754758	45475479
average	343811976	46647548	46468502
stdev	17635921,26	2181519,99	1404346,83
(stdev/aver)%	5,13%	4,68%	3,02%

Table 26 Complete experimental data of DNA/DNA hybridisation experiments in a solution by using of a quenching system presented in Figure 21. Fluorescence intensity, an integrated pick, 560-600 nm.

Number	1	2	3
1	231405917	114976576	5644040
2	225485874	129565454	5967466

3	209565464	109545444	5551121
4	255454545	115654549	5754548
5	243585485	105455454	5245145
average	233099457	115039495,4	5632464
stdev	15648580,08	8166078,29	238284,51
(stdev/aver)%	6,71%	7,10%	4,23%

Table 27 Complete experimental data of DNA/DNA hybridisation experiments with two mismatches in a solution by using of a quenching system presented in Figure 22 and Table 14. Fluorescence intensity, an integrated pick, 560-600 nm.

Number	TRIS-borate-2	TRIS-acetate-2	HEPES-2	6xSSPE-2
1	103639240	56066650	35003795	16316615
2	115465745	50754544	33321218	16564545
3	109873635	58454545	32254545	14545454
4	96754512	59545447	36545414	15215454
5	97852154	55454548	38545474	17545544
average	104717057.20	56055146.80	35134089.20	16037522.40
stdev	7124819.94	3046195.94	2246091.60	1051840.22
(stdev/aver)%	6.80%	5.43%	6.39%	6.56%

Table 28 Complete experimental data of DNA/DNA hybridisation experiments with three mismatches in a solution by using of a quenching system presented in Figure 22 and Table 14. Fluorescence intensity, an integrated pick, 560-600 nm.

Number	TRIS-borate-3	TRIS-acetate-3	HEPES-3	6xSSPE-3
1	202719580	158238760	102634420	38177553
2	215454854	168545457	115454540	41242544
3	195454545	149545454	95654454	36985454
4	189545454	148545449	108545428	40655465
5	203212740	156854554	98987454	37545454
average	201277434.60	156345934.80	104255259.20	38921294.00
stdev	8699078.38	7207828.25	7045284.67	1708163.55
(stdev/aver)%	4.32%	4.61%	6.76%	4.39%

Table 29 Complete experimental data of DNA/DNA hybridisation experiments with five mismatches in a solution by using of a quenching system presented in Figure 22 and Table 14. Fluorescence intensity, an integrated pick, 560-600 nm.

Number	TRIS-borate-5	TRIS-acetate-5	HEPES-5	6xSSPE-5
1	237017535	230948460	193110545	164818455
2	258454574	219535454	213212175	154845452
3	215458454	255155585	185465454	165454754
4	236548844	241385475	186545485	175454854
5	240221564	221585458	192454545	149545454
average	237540194.20	233722086.40	194157640.80	162023793.80
stdev	13663529.74	13224021.16	10005710.83	9024550.43
(stdev/aver)%	5.75%	5.66%	5.15%	5.57%

Table 30 Complete experimental data of DNA/DNA hybridisation experiments in a solution without any mismatches by using of a quenching system presented in Figure 22 and Table 14. Fluorescence intensity, an integrated pick, 560-600 nm.

Number	TRIS-borate-5	TRIS-acetate-5	HEPES-5	6xSSPE-5
1	22076165	14979875	11293120	8637930

2	20715456	15545454	11965454	7885424
3	20254545	13946542	10854524	7554545
4	23545847	16000954	10654545	8554454
5	23054584	13964544	11345444	8724554
average	21929319.4	14887473.8	11222617.4	8271381.4
stdev	1279005.8	826857.4423	453885.9344	465332.3366
(stdev/aver)%	5.83%	5.55%	4.04%	5.63%

Table 31 Complete experimental data of 5' TAMRA-labelled DNA in a solution presented in Figure 22 and Table 14. Fluorescence intensity, an integrated pick, 560-600 nm.

Number	TRIS-borate	TRIS-acetate	HEPES	6xSSPE
1	230058429	231138200	231745125	230894531
2	240547577	216565454	225454544	245454545
3	225454547	246545444	243451121	226456454
4	215454545	225654544	215754548	215454545
5	246585485	235455454	246545145	245854554
average	231620116.6	231071819.2	232590096.6	232822925.8
stdev	11004004.93	9984340.007	11382187.94	11621466.85
(stdev/aver)%	4.75%	4.32%	4.89%	4.99%

Table 32 Complete experimental data of DNA/DNA hybridisation experiments in HEPES solution by using of a quenching system, presented in Figure 23. Fluorescence intensity, an integrated pick, 560-600 nm.

Number	HEPES-1	HEPES-2	HEPES-3
1	70008780	207975335	230289070
2	73358498	220212454	245458758
3	69548321	221412911	225854447
4	72654740	195454254	215454774
5	66542870	199854541	239454424
average	70422641.8	208981899	231302294.6
stdev	2432688.29	10468757.70	10475803.04
(stdev/aver)%	3.45%	5.01%	4.53%

Table 33 Complete experimental data of DNA/DNA hybridisation experiments in a Tris solution by using of a quenching system, presented in Figure 23. Fluorescence intensity, an integrated pick, 560-600 nm.

Number	TRIS-1	TRIS-2	TRIS-3
1	93744010	228974335	231409170

2	98545445	204544744	228455447
3	90814754	229857474	240215474
4	89954442	226954445	215864475
5	94565444	233954117	240256854
average	93524819	224857023	231240284
stdev	3047283.21	10408667.01	9011680.33
(stdev/aver)%	3.26%	4.63%	3.90%

Table 34 Complete experimental data of 5' TAMRA DNA titration curve presented in Figure 24. Fluorescence intensity, an integrated pick, 560-600 nm.

DNA pmol	1.5	3.125	6.25	12.5	25	50	75	100
1	4092823	8055090	15966500	35450200	68385600	129907000	176662000	236662000
2	3854754	7854244	16575047	33554544	66545754	131227547	164724754	225475474
3	4099854	8154547	15675474	32545445	65504444	127544854	178548754	218349542
average	4015810	8021294	16072340	33850063	66811933	129559800	173311836	226829005
stdev	113920.19	124905.61	374797.30	1204131.50	1191190.80	1523366.37	6120645.02	7537044.73
(st/av)%	2.84%	1.56%	2.33%	3.56%	1.78%	1.18%	3.53%	3.32%

Table 35 Complete experimental data of DNA/DNA hybridisation experiments on beads presented in Figure 26. Fluorescence intensity, an integrated pick, 535-600 nm.

Number	Temperature	NaOH
1	376678003	44394605
2	186995030	17132650
3	365450030	16310850
4	8879173	5437995
5	94671704	17656705
6	6224270	753618

Table 36 Complete experimental data of DNA/DNA hybridisation experiments on beads presented in Figure 27. Fluorescence intensity, an integrated pick, 535-600 nm.

Number	500 mM Tris pH 8.3	100 mM NaOH
1	401897654	409877528
2	412055411	402142114
3	396554455	388975174
4	399854475	420145824
5	424575458	412475447
average	406987490,6	406723217,4
stdev	10204459,75	10575289,51

(stdev/aver)%	2,51%	2,60%
---------------	-------	-------

Table 37 Complete experimental data of DNA/DNA hybridisation experiments on beads presented in Figure 35. Fluorescence intensity, an integrated pick, 535-600 nm.

100 mM NaOH	50 mM NaOH	Temperature	100 mM NaOH
365456286	367121864	320039834	36327400
339031684	340733360	302977162	34510980
320343430	332777738	275191244	20779092
315149698	325706052	248840770	16144630
306588556	310635324	210708086	9035672
300159138	307769800	200357834	6204600
290819202	297859498	190446972	4677620
280796548	288938366	181840430	4246080
269315132	276481522	174266050	4044400
258017294	265717522	171318406	4246000
249511106	253462318	164077794	3806800
241089290	246109090	161892888	4028600
231089308	236303308	157093090	3806080

Table 38 Complete experimental data of DNA/DNA hybridisation experiments on beads presented in Figure 58. Fluorescence intensity, an integrated pick, 535-600 nm.

Number	1	2
1	891255555	510398760
2	790059545	555645561
3	784541567	474515544
average	821952222	513519955
stdev	49056606,48	33194641,22
(stdev/aver)%	5,97%	6,46%

5.2 ABBREVIATIONS USED

A	adenosin
ASO	allele-specific oligonucleotide
bp	base pair
C	cytidin
CAE	capillary array electrophoresis
CCD	charge coupled device
CE	capillary electrophoresis
CMC	chemical (or enzymatic) mismatch cleavage
cps	counts per second
DAPpNP	nitrophenyl 3-diazopyruvate
dATP	deoxyadenosine 5'-triphosphate
dCTP	deoxyguansin 5'-triphosphate
DGGE	denaturing gradient gel electrophoresis
DMSO	dimethyl sulphoxide
DNA	deoxyribonucleic acid
dNTP's	deoxyribonucleosidtriphosphates
dsDNA	double stranded deoxyribonucleic acid
DTT	dithiotheitol
dTTP	deoxythymidin 5'-triphosphate
EDAC	1-ethyl-3-(3-dimethyl-aminopropyl) carbodiimide
EDTA	ethylenediamine-tetraacetic acid
EXPTIME	exponential time

FITC	fluorescein isotioscyanate
G	guanosin
HEPES	(N-[2-Hydroxyethyl]piperazine-N'-[2-ethanesulfonic acid])
HPLC	high-performance liquid chromatography
MEMS	micro-electro-mechanical systems
MES	[2-(N-morpholino) ethane sulfonic acid]
mRNA	messenger ribonucleic acid
NP-complete	non-deterministic polynomial time complete problem
nt	nucleotide
P	polynomial
PA	polyacrylamide
PAGE	polyacylamide gel electrophoresis
PCR	polymerase chain reaction
PDPH	3-(2-pyridyldithio)propionyl hydrazide
PSPACE	polynomial space
R6G	rhodamine 6G
RFLP	restriction fragment length polymorphism
[R6G]dCTP	rhodamine 6G-labelled deoxycytidine 5'-triphosphate
RNA	ribonucleic acid
SAT	satisfiability problem
SELEX	systematic evolution of ligands by exponential enrichment
SDS	sodium dodecyl sulphate
SNP	single nucleotide polymorphisms

SSCP	single strand conformation polymorphism analysis
ssDNA	single stranded deoxyribonucleic acid
SSPE	standard saline-phosphate-EDTA buffer
STM	strand transfer module
T	thymidin
TAE	Tris-acetate-EDTA buffer
TAMRA	tetramethylrhodamine
Taq	thermus aquaticus
TBE	Tris-borate-EDTA buffer
TEMED	N, N, N', N'- tetramethylenediamine
T _m	melting point
TRIS	TRIZMA BASE (Tris [hydroxymethyl] aminoethane)
UV	ultraviolet
VLSI	very large scale integration

5.3 EQUIPMENT AND SOFTWARE USED

Equipment:

An emission filter (540 -580 nm)	Oriel Instruments, Stanford. CT
Argon-ion laser model 2080-155	Spectra-Physics Lasers, Inc., CA
Autoclave	Tuttnaner, Germany
Balance model	Sartorius, Göttingen, Germany
CCD camera, CH250	Photometrics, Tucson. AZ
CCD camera, LN/CCD-1024TK(B)	Princeton Instrument Inc., NJ
CCD camera, Quantrix	Photometrics, Tucson. AZ
C-Mount microscope adapter	Carl Zeiss, Jena, Germany
Electrophoresis power supply PAC 3000	BioRad, Hercules, CA
Gel-documentation system	Biozym, Hess. Oldendorf, Germany
Heating plate, Grant	Eppendorf, Hamburg, Germany
Inverted microscope model Axiovert 100 TV	Carl Zeiss, Jena, Germany
Mercury lamp, model UV-F400	Panacol-Elosol, Oberursel, Germany
MicroCentrifuge, model fresco	Heraeus, Hanau, Germany
MicroCentrifuge, model pico	Heraeus, Hanau, Germany
Objectives for Tandemoptics	Nikkor, Nikon, Tokyo, Japan
PCR gradient thermoblock	Biometra, Göttingen, Germany
pH-meter	Corning, model 450
Precision syringe pump Model 260	World Precision Instrum., Sarasota, FL
Quartz cuvette	Hellma, Mühlheim, Germany
Real time PCR detection system iCycler iQ	BioRad, Hercules, CA
Spectrofluorimeter, FluorMax-2	Instruments S.A. Inc., Edison, NJ
SpeedVac Concentrator, Model SC110	Savant Instrument. Inc., Holbrook, NY
Temperaturemeter Model	Ahlborn, Holzkirchen, Germany
Thermoelement NiCr-Ni	Philips, Kassel, Germany
Thermomixer, comfort	Eppendorf, Hamburg, Germany
UV spectrophotometer Cary 3E	Varian Inc., Walnut Creek, CA
Wave generator model 3312A	Hewlett-Packard, Palo Alto, CA

Software:

ADNA 4.1: The main part of the computer programme ADNA (Analysis of DNA), used in this thesis for a statistical analysis of the DNA library sequences, has written by the author in a connection to his work 'Computer analysis of genetic texts' in the Sofia University in 1995. The author has added a few additional functions facilitating the statistical analysis of the library sequences during his free time using free software. The programme belongs to the author but it is not a part of the current PhD thesis. However, a demonstration of the programme is available under request.

Microcal Origin 6.0 (Microcal Software, Inc., Northampton, MA) was used for plotting standard titration curves.

PMIS 4.0.2: The images from micro-flow reactors were obtained and analysed by PMIS image processing software (GKR Computer Consulting, Boulder, CO).

Vienna RNA folding package: <http://www.tbi.univie.ac.at/cgi-bin/RNAfold.cgi>

5.4 DEUTSCHE ZUSAMMENFASSUNG

Durch die Pionierarbeit von Adleman im Jahre 1994 wurde die Schleuse zum Rechnen mit DNS geöffnet. Seither arbeiten einsichtige (inspirierte/engagierte) Wissenschaftler daran die Lücke zwischen molekularer Biologie und Informatik zu überbrücken und geeignete auf DNS oder RNS basierende Rechner zu bauen. Die aktuelle Erforschung der Möglichkeit von DNS und RNS Rechnern erfordern eine kritische Bewertung der zur Zeit zur Verfügung stehenden, Werkzeuge der molekularen Biologie in Hinblick auf ihre potentielle Anwendung für das Rechnen mit biologischen Molekülen. Damit eröffnet sich die Chance für neue Einsichten in einige essentielle biomolekulare Prozesse wie die Selektion, die Ligatur, die Vervielfältigung und die Selbstkonstruktion von DNS.

Das Ergebnis der bisherigen Forschung hat bereits heute Einfluss auf die Entwicklung der neueren Biotechnologie. So wurde die Entwicklung der "on-Chip" Biotechnologie erwiesener Weise eine gemeinsame Grundlage für die DNA und RNA basierte Diagnostik und Informationsverarbeitung. Dies entsteht dadurch, dass beide Anwendungen einen hohen Grad an Automation und die Integration einer Vielzahl paralleler molekularer Prozesse benötigen. In dieser Dissertation werden die Ergebnisse eines neuen Ansatz für die automatisierte und integrierte mehrstufige Selektion von DNA durch die Anwendung von mikrofluidischen Modulen mit Mikrokugeln berichtet. Der vorgeschlagene Ansatz basiert auf einem neuartigen mikrofluidischen Design und einer neuen reversibel Chemie für die mehrstufige sequenzspezifische Hybridisierung und den aktiven Transport von DNS unter isothermalen Bedingungen. Das mikrofluidische Design erlaubt eine programmierte Bindung parallel von verschiedenen DNS Oligomeren (oder anderen Biomolekülen) an Mikrokugeln in kaskadierbar angeordneten Mikroreaktoren durch den getrennten Zufluss von DNA Oligomeren und den benutzten "cross-linking" Reagenzien. Durch die Anwendung einer Hemmung (durch eine pH Änderung) der DNA Immobilisierung nach der Mischung in sich kreuzenden Mikrokanälen wird ein hoher Grad an Spezifität erreicht. Die reversible Chemie für den sequenzspezifischen DNA Transport erlaubt eine mehrstufige Selektion aus einem komplexen Pool unterschiedlicher DNS Moleküle in kaskadierbar verbundenen Mikroflussreaktoren durch entweder die pH Änderung in dem Pumplösung oder unter Gleichgewichtsbedingungen durch die Bewegung von magnetischen Mikrokugeln zwischen Flüssigkeiten mit unterschiedlichen pH Wert. Die Durchführung der gesamten Selektionsprozedur

bei konstanter Temperatur erlaubt potentiell die einfache Integration einer Vielzahl von Selektionsmodulen auf einem einzigen Wafer. Die Methode profitiert von der schnellen Hybridisierung von DNS auf Mikrokugeln unter Flussbedingungen sowie vom geringen benötigten Probenvolumen. Die Effizienz und Präzision des Hybridisierungstransfer von DNA wird demonstriert. Die Methode ist geeignet für die integrierte Anwendung im Gebiet des Rechnens mit DNS und in der Diagnostik. Eine 12 bit Bibliothek, entworfen entsprechend thermodynamischer Bedingungen, wurde experimentell erzeugt und mit molekularbiologischen Werkzeugen getestet. Die Ergebnisse demonstrieren einen hohen Grad an spezifischer Hybridisierung, die für alle bits der Bibliothek unter identischen Bedingungen erreicht wird.

5.5 ERKLÄRUNG

Ich versichere, daß ich die von mir vorgelegte Dissertation selbständig angefertigt, die benutzten Quellen und Hilfsmittel vollständig angegeben und die Stellen der Arbeit – einschließlich Tabellen, Karten und Abbildungen –, die anderen Werken im Wortlaut oder dem Sinn nach entnommen sind, in jedem Einzelfall als Entlehnung kenntlich gemacht habe; daß diese Dissertation noch keiner anderen Fakultät oder Universität zur Prüfung vorgelegen hat; daß sie – abgesehen von unten angegebenen Teilpublikationen – noch nicht veröffentlicht worden ist sowie, daß ich eine solche Veröffentlichung vor Abschluß des Promotionsverfahrens nicht vornehmen werde. Die Bestimmungen dieser Promotionsorder sind mir bekannt. Die von mir vorgelegte Dissertation ist von Prof. Dr. Jonathan Howard betreut worden.

Teilpublikationen:

- Robert Penchovsky and Jörg Ackermann: **DNA Library Design for Molecular Computation**, Journal of Computational Biology, 2003, in press.
- Robert Penchovsky and John McCaskill: **Cascadable Hybridisation Transfer of Specific DNA between Microreactor Selection Modules**, LNCS, 2002, Vol. 2340, 46-56.
- Robert Penchovsky, Eckhard Birch-Hirschfeld and John McCaskill: **End-Specific Covalent Photo-Dependent Immobilisation of Synthetic DNA to Paramagnetic Beads**; Nucleic Acids Research, 2000, Vol. 28, No. 22, e98.
- John McCaskill, Robert Penchovsky, Marlies Gohlke, et al. **Steady Flow Micro-Reactor Module for Pipelined DNA Computations**, LNCS, 2001, Vol. 2054, 263-270.

Köln den Dezember 2002

5.6 LEBENSLAUF

von Robert Dimitrov Penchovsky

Geboren am 19. Juni 1971 in Sofia, Bulgarien

Nationalität: bulgarisch

Familienstand: ledig

Privatanschrift: Gielgenstr. 32, 53229 Bonn, Deutschland

Privattelefon:+49-178-2616422

E-mail: robert_penchovsky@web.de

Persönliche Web-Seite: <http://www.gmd.de/People/Robert.Penchovsky/index.html>

Schulbildung:

- 1978-1981 112. Schule in Sofia
- 1981-1983 97. Schule in Sofia
- 1983-1986 96. Schule in Sofia
- 1986-1989 30. Schule in Sofia (Abitur 1989)

Studium:

- 1989-1994 Biochemie und Genetik an der Universität zu Sofia (Diplom 1994, Master of Science in Biochemistry and Genetics)
- 1992-1995 Angewandte Informatik an der Universität zu Sofia (Diplom 1995)
- 2000- Doktorand, Promotionsfach Genetik an der Universität zu Köln

Themen der Diplomarbeiten:

- Analyse der Expression der Protooncogene *dfra* und *djra* in der antioncogen Mutation *l(2)gd* von *Drosophila melanogaster*: Universität zu Sofia, 1994.

- Computer Analyse von genetischen Texten: Universität zu Sofia, 1995.

Inaugural Dissertation:

- An Integrated DNA Selection in Microflow Reactors as an Approach for Molecular Computation and Diagnostics: eingerechnet an der Universität zu Köln, Dezember 2002.

Wehrdienst:

- 1995-1996 mit einer Ausbildung zum Reserveoffizier

Berufserfahrung:

- 05.1996 bis 12.1996 Institut für Molekulare Biologie, Bulgarische Akademie der Wissenschaften, Sofia, Bulgarien
- 01.1997 bis 11.1998 Software Entwickler, freiberuflich, Sofia, Bulgarien
- 12.1998 bis 03.1999 Institut für Molekulare Biotechnologie (IMB), Jena, Deutschland
- 04.1999 bis 12.2002 Fraunhofer Gesellschaft (FhG), Schloss Birlinghoven, Sankt Augustin, Deutschland

Köln den Dezember 2002

6 REFERENCES

* Spontaneous remarks made by the author.

ⁱConan Doyle, A., 1988, The sing of four in *The Complete Sherlock Holmes*, Barnes and Noble, Dayton, New Jersey.

ⁱⁱFeynman, R., in *Miniaturisation*, 1961, D.H. Gilbert, Ed. Reinhold, New York, 282-296.

ⁱⁱⁱTuring, A. M., 1936, On computable numbers, with an application to the Entscheidungsproblem, *Proc. London Math. Soc.*, 42, 230-265.

^{iv}Bennett, Ch. H., 1982, The thermodynamics of computation, *International Journal of Theoretical Physics*, 21, 905-940.

^vAdleman, L.M., 1994, Molecular computation of solutions to combinatorial problems, *Science*, 266, 1021-1024.

^{vi}Gifford, D. K., 1994, On the path to computation with DNA. *Science*, 266, 993-994.

^{vii}Lipton, R.J., 1995, DNA solution of hard computational problems. *Science*, 268, 542-545.

^{viii}Braich, R.S., Chevlyapov, N., Johnson, C., Rothmund, P.W.K., Adleman, L.M., 2002, Solution of a 20-Variable 3-SAT Problem on a DNA Computer, *Science*, 296, 499-502.

^{ix}Cox, J.C., Cohen D.S. and Ellington A.D., 1999, The complexities of DNA computation. *TIBTECH*, 17, 151-154.

^xFaulhammer, D., Cukras, A.R., Lipton, R.J. and Landweber, L.F., 2000, Molecular computation: RNA solution to chess problems. *Proc. Natl. Acad. Sci.*, 97, 1385-1389.

^{xi}Liu, Q., Wang, L., Frutos, A.G., Condon, A.E., Corn, R.M. and Smith, L.M., 2000, DNA computing on surfaces. *Nature*, 403, 175-179.

^{xii}Wang, L., Liu, Q., Corn, R.M., Condon, A.E. and Smith, L.M. 2000, Multiple Word DNA Computing on Surfaces, *J. Am. Chem. Soc.*, 122, 7435-7440.

^{xiii}Qiyang, Q., Kaplan, P.D., Liu, S. and Libchaber, A., 1997, DNA solution of the maximal clique problem. *Science*, 278, 446-449.

^{xiv}Head, T., 1987, Formal language theory and DNA: an analysis of the generative capacity of specific recombinant behaviours, *Bulletin of Mathematical Biology*, 48, 57-72.

^{xv}Sakamoto, K., Gouzu, H., Komiya, K., Kiga, D., Yokoyama, S., M., Yokomori, T. and Hagiya, M., 2000, Molecular computation by DNA hairpin formation, *Science*, 288, 1223-1226.

^{xvi}Winfrey, E., 1995, On the computational power of DNA annealing and ligation *DIMACS Workshop*, 27, 199-221.

^{xvii}Benenson, Y., Paz-Ellzur, T., Adar, R., Kelnan, E., Livneth, Z. and Shapiro, E., 2001, Programmable and autonomous computing machine made of biomolecules, *Nature*, 414, 430-434.

^{xviii}Breaker, R.R. and Joyce, G.F., 1994, A DNA enzyme that cleaves RNA, *Chemistry & Biology*, 1, 223-229.

^{xix}Wickiser, J. K., Chalamish-Cohen S., Narashimhan, S., Sawicki, B., Ward, D.C., Breaker, R. R., 2002, Oligonucleotide sensitive hammerhead ribozymes as logic gates, *Preliminary proceedings, DNA8, Hokkaido University, Japan*, 19.

-
- ^{xx}Khodor, J, and Gifford, D. K., 2002, Programmed mutagenesis is a universal model of computation. LNCS, 2340, 300-307.
- ^{xxi}Marth, G.T., Korf, I. et al., 1999, A general approach to single-nucleotide polymorphism discovery. *Nature*, 23, 452-456.
- ^{xxii}Group ISMW, 2001, A map of human genome sequence variation containing 1.42 million single nucleotide polymorphisms. *Nature*, 409, 928-933.
- ^{xxiii}Venter J.C., Adams, M.D., et al., 2001, The sequence of the human genome. *Science*, 291, 1304-1351.
- ^{xxiv}Peltonen L. McKusick VA., 2001, Dissecting human disease in the postgenomic era. *Science* 291, 1224-1229.
- ^{xxv}Watson, A., Mazumder, Stewart, M. and Balasubramanian, S., 1998, Technology for microarray analysis of gene expression. *Current Opinion in Biotechnology*, 9, 609-614.
- ^{xxvi}Kopp, M.U., de Mello, A. J., Manz, A., 1998, Chemical Amplification: Continuous-Flow PCR on a Chip, *Science*, 280, 1046-1048.
- ^{xxvii}Foquet, M., Korlach, J., Zipfel, W., Webb, W.W., Graighead, H.G., 2002, DNA Fragment Sizing by Single Molecule Detection in Submicrometer-Sized Closed Channels, *Anal. Chem.*, 74, 1415-1422.
- ^{xxviii}Cheek, B.J., Steel, A.B., Torres, M.P., Yu Y.Y., Yang, H., 2001, Chemiluminescence Detection for Hybridisation Assays on the Flow-Thru Chip, a Three-Dimensional Microchannel Biochip, *Anal. Chem.*, 73, 5777-5783.
- ^{xxix}Burns, M.A., Johnson, B.N., Brahmasandra, S.N., Handique, K., Webster, J.R., Krishnan, M.; Sammarco, T.S.; Man, P.M., Jones, D., Heldsinger, D., Mastragelo, C.H., Burke, D.T., 1998, An Integrated Nanoliter DNA Analysis Device, *Science*, 282, 484-487.
- ^{xxx}Han, J.; Craighead, H. G., 2000, Separation of Long DNA Molecules in a Microfabricated Entropic Trap Array, *Science*, 288, 1026-1029.
- ^{xxxi}Waters, L.C., Jacobson, S.C., Kroutchinina, N., Khandurina, J., Foote, R.S., Ramsey, J.M., 1998, Microchip Device for Cell Lysis, Multiplex PCR Amplification, and Electrophoretic Sizing, *Anal. Chem.*, 70, 158-162.
- ^{xxxii}Takayama, S., McDonald, J.C., Ostuni, E., Liang, M.N.; Kenis, P.J.L., Ismagilov, R.F., Whitesides, G.M., 1999, Patterning cells and their environments using multiple laminar fluid flows in capillary networks, *PNAS*, 96, 5545-5548.
- ^{xxxiii}Dodson, J.M., Feldstein, M.J., Leatzow, D.M., Flack L.K., Golden, J.P., Ligler, F.S., 2001, Fluidics Cube for Biosensor Minuturization, *Anal. Chem.*, 73, 3776-3780.
- ^{xxxiv}Service R. E., 1998, The Pocket DNA Sequencer, *Science*, 282, 399-401.
- ^{xxxv}Cheung, V.G. et al., 1999, Making and reading microarrays, *Nature*, 21, 15-19.
- ^{xxxvi}Gehani, A. and Reif, J., 1999, Micro flow bio-molecular computation. *BioSystems*, 57, 197-216.
- ^{xxxvii}McCaskill, J.S. 2001, Opticaly programming DNA computing in microflow reactors. *BioSystems*, 59, 125-138.
- ^{xxxviii}Penchovsky, R. and Ackermann J., 2003, DNA Library Design for Molecular Computation, *Journal of Computational Biol.*, in press.
- ^{xxxix}McCaskill, J.S., Penchovsky, R., Gohlke, M., et al., 2001, Steady Flow Micro-Reactor Module for Pipelined DNA Computations, LNCS, Vol. 2054, 263-270.

-
- ^{xi}Penchovsky, R., Birch-Hirschfeld, E., and McCaskill, J.S., 2000. End-specific covalent photo-dependent immobilisation of synthetic DNA to paramagnetic beads. *NAR*, 28, e98.
- ^{xli}Penchovsky, R. and McCaskill, J.S., 2002, Cascadable hybridisation transfer of specific DNA between microreactor selection modules. *LNCS*, 2340, 46-56.
- ^{xlii}Sambrook, J., Fritsch, E.F. and Maniatis, T., 1989, *Molecular Cloning: A Laboratory Manual*. Cold Spring Harbor Laboratory Press, Cold Spring Harbor, NY.
- ^{xliii}McGall, G.H., Barone, A.D., Diggelmann, M., Fodor S.P.A., Gentalen, E and Ngo, N., 1997 The efficiency of light-directed synthesis of DNA arrays on glass substrates *J. Amer. chem. Soc.*, 119, 5081-5090.
- ^{xliv}Beier, M. and Hoheisel, J.D., 2000, Production by quantitative photolithographic synthesis of individually quality checked DNA microarrays. *Nucleic Acids Res.*, 28, 4.
- ^{xlv}Goodfellow, V.S., Settineri, M. and Lawton, R. G., 1989, p-Nitrophenyl 3-Diazopyruvate and Diazopyruvamides, a new family of photoactivatable cross-linking bioprobes. *Biochemistry*, 28, 6346-6360.
- ^{xlvi}Zeller, K.P., Meir, H., Kolshorn und Müller, E., 1972, Zum Mechanismus der Wolff-Umlagerung. *Chem. Ber.*, 105, 1875-1886.
- ^{xlvii}Koch, M., Evans, A., Brunnschweiler, A., 2000, *Microfluidic Technology and Applications*, Research Studies Press.
- ^{xlviii}Lindahl, T. and Andersson, A., 1972, Rate of Chain Breakage at Apurinic Sites in Double-Stranded Deoxyribonucleic Acid. *Biochemistry*, 11, 3618-3626.
- ^{xlix}Shechepiniv, M.S., Case-Green, S.C. and Southern, E.M., 1997, Steric factors influencing hybridisation of nucleic acids to oligonucleotide arrays, *Nucleic Acids Res.*, 25, 1155-1161.
- ^lGhosh, S.S. and Musso, G.F., 1987, Covalent attachment of oligonucleotides to solid supports. *Nucleic Acids Res.*, 15, 5353-5372.
- ^{li}Lund, V., Schmid, R., 1988, Assessment of methods for covalent binding of nucleic acids, Dynabeads, and the characteristics of the bound nucleic acids in hybridization reactions. *Nucleic Acids Res.*, 16, 10861-10880.
- ^{lii}Fan, Z.H., Mangru, S., Granzow, R., Heaney, P., Ho, W., Dong, Q. and Kumar, P. 1999, Dynamic DNA hybridization on a chip using paramagnetic beads. *Anal. Chem.*, 71, 4851-4859.
- ^{liii}Seong, G.H., Zhan, W. and Crooks, R.M. 2002, Fabrication of microchambers defined by photopolymerized hydrogels and weirs within microfluidic systems: Application to DNA hybridisation. *Anal. Chem.*, 74, 3372-3377.
- ^{liv}Stevens, P.W., Henry, M.R. and Kelso, D.M. 1999, DNA hybridisation on microparticles: determining capture-probe density and equilibrium dissociation constants. *Nucleic Acids Res.*, 27, 1719-1727.
- ^{lv}Schwille, P., Oehlenschlänger, F. and Walter, N.G., 1996, Quantitative hybridisation kinetics of DNA probes to RNA in solution followed by diffusional fluorescence correlation analysis. *Biochemistry*, 35, 10182-10193.
- ^{lvi}Edman, C.F., Raymond, D.E., Wu, D.J., Tu, E., Sosnowski, R.G., Butler, W.F., Nerenberg, M. and Heller, M.J., 1997, Electric field directed nucleic acid hybridisation on microchips. *Nucleic Acids Res.*, 24, 4907-4914.
- ^{lvii}Sosnowski, R.G., Tu, E., 1997, Butler, W.F., O'Connell, J.P. and Heller, M.J. Rapid determination of single base mismatch mutations in DNA hybrids by direct electric field control. *Proc. Natl. Acad. Sci.*, 94, 1119-1123.

-
- ^{lviii}Vontel, S., Ramakrishnan, A. and Sadana, A., 2000, An evaluation of hybridisation kinetics in biosensors using a single-fractal analysis. *Biotechnol. Appl. Biochem.*, 31, 161-170.
- ^{lix}Van Noort, D., Gast, F.U. and McCaskill, J.S., 2002, DNA computing in micro-reactors, LNCS, 2340, 33-45.
- ^{lx}McGall, G.H., Barone, A.D., Diggelmann, M., Fodor, P.A. Gentalen, E., and Ngo, N., 1997, The efficiency of light-directed synthesis of DNA arrays on glass substrates. *J. Am. Chem. Soc.*, 119, 7863-7896.
- ^{lxi}Heller M.J. et al., 1998, An integrated microelectronic hybridisation system for genomic research and diagnostic applications. *Micro Total Analysis Systems'98*, Kluwer Academic Publishers, 221-224.
- ^{lxii}Kenis, P.J.A., Ismagilow, R.F., and Whitesides, G.M., 1999, Microfabrication inside capillaries using multiphase laminar flow patterning. *Science*, 285, 83-85.
- ^{lxiii}Delamerche, E., Bernard, A., Schmid, H., Michel, B. and Biebuyck, H., 1997, Patterned delivery of immunoglobulins to surfaces using microfluidic networks. *Science*, 276, 776-781.
- ^{lxiv}Chou, H., Unger, M.A., Scherer, A., and Quake, Integrated Elastomer Fluidic Lab-on-a-chip. *Surface Patterning and DNA Diagnostics*, Caltech, Pasadena, CA, USA.
- ^{lxv}Stroock, A.D., Dertinger, A.A., et al., 2002, Chaotic Mixer for Microchannels, *Science*, 295, 647-651.
- ^{lxvi}Koch, M., Evans, A., Brunnschweiler, A., 2000, *Microfluidic Technology and Applications*, Research Studies Press.
- ^{lxvii}Tang, J. and Breaker, R.R., 1998, Mechanism for allosteric inhibition of an ATP-sensitive ribozyme. *Nucleic Acids Res.*, 26, 4214-4221.
- ^{lxviii}Winfrey, E., Liu, F., Wenzler, L.A. and Seeman, N.C., 1998, Design and self-assembly of two-dimensional DNA crystals. *Nature*, 394, 539-544.
- ^{lix}Frutos, A.G., Liu, Q., Thiel, A.J., Sanner, A.M.W., Condon, A.E., Smith, L.M. and Corn, R.M., 1997, Demonstration of a word design strategy for DNA computing on surfaces, *Nucleic Acids Res.* 25, 4748-4757.
- ^{lxx}Marathe, A., Condon, A.E. and Corn, R.M., 2001, On combinatorial DNA word design, *J. Comp. Biol.*, 8, 201-219.
- ^{lxxi}Deaton, R., Garzon, M., Murphy, R.C., Rose, J.A., Franceschetti, D.R. and Stevens, Jr, S.E., 1998, Reliability and Efficiency of a DNA-based Computation, *Phys. Review Letters.*, 80, 417-420.
- ^{lxxii}McCaskill, J.S., 1990, The equilibrium partition function and base pair binding probabilities for RNA secondary structure. *Biopolymers*, 29, 1109-1119.
- ^{lxxiii}Hofacker, I.L., Fontana, W., Stadler, P.F., Bonhoeffer, S., Tacker, M. and Schuster, P., 1994, Fast folding and comparison of RNA secondary structures. (the Vienna RNA package), *Monatsh. Chem.*, 125, 167-188.
- ^{lxxiv}Allawi, H.T. and SantaLucia, Jr., J., 1997, Thermodynamics and NMR of internal GT mismatches in DNA. *Biochemistry*, 36, 10581-10594.
- ^{lxxv}SantaLucia, Jr., J., 1998, A unified view of polymer, dumbbell, and oligonucleotide DNA nearest-neighbor thermodynamics. *Proc. Natl. Acad. Sci.*, 95, 1460-1465.
- ^{lxxvi}Mir, K.U., 1999, A restricted genetic alphabet for DNA computing, *Proc. DNA Based Computers. DIAMACS Workshop, DIMACS Series in Discrete Mathematics and Theoretical Computer Science*, 44, 243-246.

^{lxxvii}Braich, R.S., Johnson, C., Rothmund, P.W.K., Hwang, D., Chevlyapov, N. and Adleman, L.M., 2001, Solution of a satisfiability problem on a gel-based DNA computer. LNCS, 2054, 27-42.

^{lxxviii}Wetmur, J.G., 1991, DNA probes: application of the principle of nucleic acid hybridisation. *Critical Reviews in Biochemistry and Molecular Biology*, 26, 227-259.

^{lxxix}McPherson, M.J., Hames, B.D. and Taylor, G.R. 1995. PCR 2, Oxford University Press, 71-87.

^{lxxx}Pirrung, M.C., Connors, R.V., Odenbaugh, A.L., Montague-Smith, M.P., Nathan, G.W. and Tollett, J.J., 2000, The Array Primer Extension Method for DNA Microchip Analysis. *Molecular Computation of Satisfaction Problems. J. Am. Chem. Soc.*, 122, 1873-1882.

^{lxxxi}Van Noort, D., Gast, F.U. and McCaskill, J.S, 2001, DNA computing in micro-reactors, DNA7, Preliminary proceedings, USF, FL, 128-137.

^{lxxxii}Baldi, P. and Brunak, S., 2001, Bioinformatics, the machine learning approach. The MIT Press.